Institute of Infection, Veterinary and Ecological Sciences

Department of Clinical Infection, Microbiology, and Immunology

EVALUATION OF HUMAN T AND B CELL IMMUNE RESPONSES TO ENTERIC VACCINES IN HUMAN NASOPHARYNX-ASSOCIATED LYMPHOID TISSUES

Thesis Submitted in Accordance with the Requirements of

The University of Liverpool for the Degree of Doctor in Philosophy

by

Miguel Angel Leon-Rios

June 2022

ABSTRACT

Evaluation of Human T and B Cell Immune Responses to Enteric Vaccines in Human Nasopharynx-Associated Lymphoid Tissues

Background: Human rotavirus (RV) and norovirus (NoV) are the most common agents for severe acute gastroenteritis (AGE) worldwide and a major public health burden in the human population. Group A rotavirus infection causes globally over 0.2 million deaths per year due to diarrhoeal diseases in children under five years of age, the majority of which occur in low-income countries, representing approximately 3.4% of annual child deaths worldwide. In parallel, noroviruses have become a critical seasonal cause of AGE in children and adults, with almost 4 million cases per year in the UK and an estimated 0.2 million annual deaths worldwide. Mucosal vaccination is an effective way of immunisation against enteric pathogens. Oral live-attenuated vaccines (LAV) have been shown to stimulate local production of antigen-specific antibodies and the development of memory B and T cells promoting both mucosal and systemic protective immune responses. While research efforts to develop a safe and effective NoV vaccine are still in progress, the lack of absolute correlates of protection for both NoV and RV and considerable variations in LAV efficacy among different socioeconomic settings remains a major concern to address.

Aims: Using human tonsillar tissues as an *ex vivo* cell culture system modelling nasopharynx-associated lymphoid tissue (NALT), we have evaluated the mucosal immunity activated by a live-attenuated rotavirus vaccine and a non-replicating NoV virus-like particle vaccine candidate and examined the effect of pre-existing immunity on vaccine-induced immune responses.

Methods: Ninety-four immunocompetent children and adults referred to adenotonsillectomy were included in this study. Serum levels of rotavirus-and-NoV-specific antibodies were measured by ELISA. Mononuclear cells (MNC) from tonsil tissues were isolated and stimulated either with a live-attenuated oral Rotavirus vaccine (RV1), or a GII.4 VLP-based NoV vaccine candidate (NoV1) alone or adjuvanted with α-Galcer. T cell immunity and virus-specific antibody responses were measured by flow cytometry and ELISA, respectively.

Results: A positive correlation was observed between patients' age and rotavirus-specific or NoV-specific serum antibodies. Significant rotavirus-specific antibody responses were detected in NALT of children and adults following RV1 stimulation. Increased production of NoV-specific IgG antibodies was also observed in NoV1-stimulated tonsillar MNCs, which was significantly enhanced by the addition of α-Galcer. A robust systemic and mucosal NoV1-specific antibody response in mice was shown after a three-dose oral immunization with α-GalCer-adjuvanted NoV1. Interestingly, both RV1 and NoV1 induced mucosal B cell antibody responses in tonsillar MNCs were positively correlated with patients' serum virus-specific antibody titres.

Although only a modest T cell response was observed in NoV1-stimulated tonsillar MNCs, the rotavirus vaccine elicited a marked T cell response in tonsillar MNCs of children and adults, with increased frequencies of both $CD4^+$ and $CD8^+$ IFN-γ-producing T cells and T cell proliferative responses. RV1 vaccine was also shown to activate a primary T cell response in naïve tonsillar MNC. No significant correlation was found between the mucosal T cell response and pre-existing antibody titres, although a trend of inverse correlation was observed particularly in those individuals who demonstrated low/no mucosal T cell response following RV1-stimulation. In contrast, NoV1-induced IFN-γ response in tonsillar T cells positively correlated with patients` pre-existing immunity to GII.4 NoV. Notably, an increased expression of the gut-homing receptor α4β7 was also detected in both RV1 and NoV1-stimulated human tonsillar T cells.

Conclusion: Our results suggest human NALT (e.g., tonsils) may be important induction sites for adaptive immune responses induced by rotavirus and norovirus vaccines, and suggest their role as an important reservoir of activated memory and effector T and B cells with gut-homing properties. This study also provides insights into the use of tonsils as an important source of human immune tissue to study both key vaccine-induced responses and underlying immune mechanisms of protection for mucosal vaccines and adjuvants.

DECLARATION

No part of this work has been submitted in support of an application for another degree or qualification at this or any other university or learning institution. All the work described in this thesis has been carried out by the author at the Institute of Infection, Veterinary and Ecological Science (IVES), at Department of Clinical Infection, Microbiology, and Immunology (CIMI) at the University of Liverpool.

Miguel A. Leon-Rios

June 2022

ACKNOWLEDGEMENTS

Firstly, I want to thank the Chilean National Agency for Research and Development (ANID) and its scholarship program "Doctorado BECAS CHILE 2017 – 72180437" for funding my PhD study and my stay in the UK and making possible this research work at the University of Liverpool.

I would also like thank to my PhD supervisors; Dr Qibo Zhang, Prof Miren Iturriza-Gomara and Prof Nigel Cunliffe, who made this project possible. Qibo, many thanks for these four years of supervision and for giving a chance to this young Chilean Researcher to be part of your group, I truly appreciate the opportunity. Special thanks to Prof Miren Iturriza-Gomara for their co-supervision and her always precise and valuable feedback. Thank you both for all the guidance and unconditional support throughout my PhD, for the trust and freedom to pursue additional challenges, and for your recommendations to continue my career as a researcher. Additional thanks to my panel assessors; Dr Neil Blake and Dr Lance Turtle, for their useful guidance and suggestions.

I would also like to thank the past members of QZ and MIG labs, including Dr Rong Xu, Dr Suttida Puksuriwong, Dr Shamsher Ahmed and Dr Daniel Kelly, for their mentoring, friendship, and relevant support to my research. Thanks also to my friends and members of the QZ group; Khalid Shrwani and Fadiyah Alrusayyis for taking this PhD path with me. Additional thanks to Yasmin Hilliam, John Newman, Jordan Thomas, Game and - of course to the Spanish speakers! - Noelia Carmona and Jocelyn Perez, for all the pints and support.

Big thanks to the people behind the scenes for their valuable help and support during my PhD; the technical team (Wes, Nahida, Debbie and Trevor) and public engagement team (Laura and Becky) at IVES; the staff in Alder Hey Children's Hospital, Royal Liverpool and Broadgreen University Hospitals and Aintree University Hospital for helping with samples collection, and of course to all the patients who took part of this study.

I want to thank my family and close ones. To Mom and Dad for gave me the tools and freedom of choice to pursue my dreams and for the massive effort you both made, which allowed me to be here. To my brother Sergio, for his advice and support and for (almost) being a role model. Thanks also to my Chilean/Mancunian family, Victor and Rodrigo for their company and friendship and to Francisco and Aldo for the long-distance support. – "you'll have to speak up, I'm wearing a towel".

And finally, but not less, a special thanks to my partner (and little one) Geraldyne, who made a huge sacrifice to follow this crazy scientist to pursue a PhD – Pequeña, este logro es de ambos y fue posible gracias a tu constante apoyo e incondicional amor –.

This work is dedicated to all the special ones who left us during these four years.

LIST OF ACHIEVEMENTS

CERTIFICATION

Associate Fellow of Higher Education Academy (AFHEA). Certified by UK Professional Standards Framework for teaching and learning support in higher education. 2021

CONFERENCES PAPERS

T and B cell responses by Live attenuated oral rotavirus vaccine in human nasopharynx-associated lymphoid tissues. **Leon-Rios, M.,** Sharma, R., Krishnan, M., Leong, S., Cunliffe, N., Iturriza-Gomara, M., & Zhang, Q. 6th European Congress of Immunology. Abstracts. Virtual. September 1-4, 2021. Eur. J. Immunol. 2021. 51, S1, 258. P-0443

Evaluation of human T and B cell immune responses in nasopharynx-associated lymphoid tissue (NALT) to live attenuated oral vaccine against rotavirus. **Leon-Rios, M**., Sharma, R., Krishnan, M., Leong, S., Cunliffe, N., Iturriza-Gomara, M., & Zhang, Q. 17th International Congress of Immunology. Abstracts. Beijing, China. October 19-23, 2019. Eur. J. Immunol. 2019. 49, S3, 1385-1386. P-2191.

MANUSCRIPT UNDER PREPARATION

Leon-Rios, M., Sharma, R., Krishnan, M., Leong, S., Cunliffe, N., Iturriza-Gomara, M., & Zhang, Q. Evaluation of human T and B cell immune responses in nasopharynx-associated lymphoid tissue (NALT) to live attenuated oral vaccine against rotavirus.

ACCEPTED ABSTRACTS

Leon-Rios M, Sharma R, Krishnan M, Leong S, Cunliffe N, Iturriza-Gomara M, Zhang Q. "T and B cell responses by Live attenuated oral rotavirus vaccine in human nasopharynx-associated lymphoid tissues". 6th European Congress of Immunology. Virtual. September 1-4, 2021. (E-Poster)

Leon-Rios M, Sharma R, Krishnan M, Leong S, Cunliffe N, Iturriza-Gomara M, Zhang Q. "Evaluation of human T and B cell immune responses in nasopharynx-associated lymphoid tissue (NALT) to live attenuated oral rotavirus vaccine". British Society for Immunology Congress 2019, December 2-5, 2019. Liverpool, UK. (Poster)

Leon-Rios M, Sharma R, Krishnan M, Leong S, Cunliffe N, Iturriza-Gomara M, Zhang Q. "Evaluation of human T and B cell immune responses in nasopharynx-associated lymphoid tissue (NALT) to live attenuated oral vaccine against rotavirus". 17th Congress of the International Union of Immunological Societies (IUIS) 2019. October 19-23, 2019. Beijing, China. (Poster)

Leon-Rios M, Sharma R, Krishnan M, Leong S, Cunliffe N, Iturriza-Gomara M, Zhang Q. "Evaluation of human T and B cell immune responses in nasopharynx-associated lymphoid tissue (NALT) to live attenuated oral vaccine against rotavirus". Faculty of Health and Life Sciences Poster Day. March 27, 2019. Liverpool, UK. (Poster)

Leon-Rios M, Sharma R, Krishnan M, Leong S, Cunliffe N, Iturriza-Gomara M, Zhang Q. "Evaluation of human T and B cell immune responses in nasopharynx-associated lymphoid tissue (NALT) to live attenuated oral vaccine against rotavirus". Centre for global vaccine research annual meeting. November 1, 2018. Liverpool, UK. (Oral presentation)

GRANTS AND AWARDS

British Society for Immunology Public engagement Grant scheme 2020 - Celebrate Vaccines.

British Society for Immunology International Congress Travel Award 2019.

Faculty of Health and Life Sciences Public Engagement Mentoring Grant Scheme 2017 – 2018.

OTHER ROLES

Medical Laboratory assistant. COVID LAMP Laboratory, LCL. Liverpool University Hospitals NHS Foundation Trust. Liverpool, UK.

Demonstrator in HLS modules. Faculty of Health and Life Sciences, University of Liverpool (from 2018 to 2020)

TABLE OF CONTENTS

LIST OF TABLES

LIST OF FIGURES

LIST OF ABBREVIATIONS

°C Degree Celsius

4PL 4-Parameter Logistic

α-GalCer α-Galactosylceramide

µg Microgram

µl Microliter

AGE Acute gastroenteritis

ANOVA One-way analysis of variance

APC Antigen presenting cells

ASC Antibody secreting cell

BFA Brefeldin A

bOPV Bivalent live-attenuated oral poliovirus

CCID50 Cell Culture Infective Dose 50%

CD Cluster of differentiation

CFSE Carboxyfluorescein succinimidyl ester

CoP Correlates of protection

CTL Cytotoxic T lymphocyte

DCs Dendritic cells

DLP Double-layered particle

DMEM Dulbecco's Modified Eagle Medium

DMSO Dimethyl sulphoxide

DPBS Dulbecco's Phosphate-Buffered Saline

ds Double-stranded

EBV Epstein-Barr Virus

ECs Epithelial cells

ELISA Enzyme-linked immunosorbent assays

ENS Enteric nervous system.

ER Endoplasmic reticulum

ETEC Enterotoxigenic Escherichia coli

EU Elisa Units

FDC Follicular dendritic cells

FFU Fluorescent focus units

FM2 Fluorescence minus two

FSC Forward scatter

g Gram (weight unit)

GALT Gut-associated lymphoid tissue

GC Germinal centres

GI Gastrointestinal

GMT Geometric mean titre

GPEI Global Polio Eradication Initiative

HBGAs Histo-blood groups antigens

HBSS Hank's Balanced Salt Solution

HEV High endothelial venules

HIE Human intestinal enteroid

HIV Human immunodeficiency virus

HPV Human papilloma virus

HRP Horseradish peroxidase

ICS Intracellular staining

IFN-γ Interferon-gamma

IgA Immunoglobulin A

IgA Immunoglobulin G

IL Interleukin

ILFs Isolated lymphoid follicles

iNKT Invariant Natural Killer T cells

IPV Inactivated poliovirus vaccine

IVIg Human intravenous immunoglobulin

LAIV Live attenuated influenza vaccine

LAV Live-attenuated vaccine

LMIC Low- and middle-income countries

M Molar

M cell Microfold cell

MACS Magnetic-activated cell separation

MAdCAM1 Mucosal addressin cell adhesion molecule 1

MALT Mucosal associated-lymphoid tissues

mg Milligram

MIS Mucosal immune system

mL Milliliter

MMR Measles, mumps and Rubeola vaccine

MNCs Mononuclear cells

MOI Multiplicity of infection

MPL A Monophosphoryl lipid A

NALT Nasopharynx-associated lymphoid tissue

NK Natural Killer cells

NoV Norovirus

NoV1 Norovirus GII-4 strain-derived Virus-like-particle-based vaccine candidate

NSP Non-structural proteins NSP

OPV Oral poliovirus vaccine

ORFs Open reading frames

p.i. post immunization

PAGE Polyacrylamide gel electrophoresis

PC Plasma B cells

pIgR polymeric immunoglobulin receptors

pNPP p-Nitrophenyl Phosphate

PP Peyer's patches

RCWG Rotavirus Classification Work Group

RdRp RNA-dependent RNA polymerase

RV1 Rotarix®

RV5 Rotateq®

RVA Group A rotavirus

SA Sialic acid

SD Standard deviation

SEM Standard error of the mean

Sf9 *Spodoptera frugiperda* insect cell line

sIgA Secretory IgA

sIgA Secretory immunoglobulin A

ss Single-stranded

SSC Side scatter

Tfh Follicular helper cells

TLP Triple-layered particle

tOPV Trivalent live-attenuated oral poliovirus

UT unstimulated control

VLP Virus-like particles

VP Viral protein

CHAPTER I

General Introduction

CHAPTER I

General Introduction

1.1 Acute gastroenteritis

Acute gastroenteritis (AGE) is one of the most common human diseases worldwide. This disease is characterized by vomiting and recurrent diarrhoea episodes as a result of acute inflammation and damage of the gastrointestinal mucosa (1). Most causes of AGE are foodborne or waterborne through pathogenic toxin and microorganism ingest and can lead to serious complications e.g., severe dehydration, due to electrolyte disturbance (1, 2). In 2016, diarrhoeal diseases were responsible for over 1.6 million deaths and estimated as the eight-leading cause of global mortality (2). Age and regional socioeconomics are two main factors that have significant impact on both prevalence and severity of AGE. Highest mortality rates have been observed among children under 5 years (71 deaths per 100 000) and adults over 70 years (172 deaths per 100 000) according to Global Burden of Disease Study in 2016 (2). Additionally, high numbers of diarrhoeal disease deaths are concentrated in low- and middle-income countries (LMIC), especially due to deprived access to safe water, sanitation, and oral rehydration (2). Although AGE can be caused by bacteria and non-infectious agents, viruses-associated episodes represent the major disease burden and a significant cause of morbidity and mortality across the globe (**Fig. 1.1**) (1, 2). Here we will particularly focus upon human rotavirus and norovirus, currently the two most important viral etiological agents of infectious intestinal diseases and associated-diarrhoeal episodes worldwide (2-7).

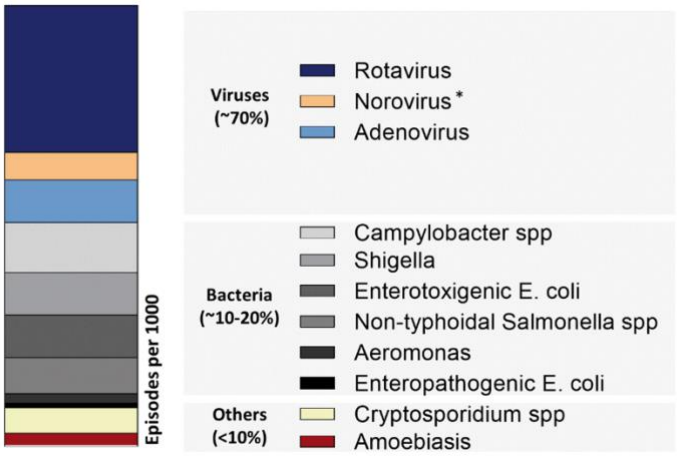

Figure 1.1. Diarrhoea episodes and aetiologies in children under 5 years. Global data from diarrhoea aetiologies and cases (episodes per 1000) from Children younger than 5 years in 2016. *Figure adapted from the 2016 Global Burden of Disease Study (2).* *An 18% of all AGE cases has been associated to NoV according to global estimates (4-7).

Human rotavirus is the leading infectious agent for severe AGE and diarrhoea mortality in children and adults. Group A rotavirus (RVA) is the main group in terms of epidemiological and clinical impact in human population causing globally over 0.2 million deaths per year due to diarrhoeal diseases among all ages, the majority of which occur in children under five years old and represent about 3-5% of child annual deaths worldwide (2-4). Specifically, about 29 per cent (95% CI: 25.2–32.4%) of all diarrhoeal deaths in children under 5 years are linked to rotavirus infection (Fig. 1.1), with the highest rates among sub-Saharan Africa and Southeast Asia regions (2, 3). Moreover, a high fraction of diarrhoea episodes and deaths among younger children has been attributable to rotavirus and documented in different geographical regions, evidencing the ubiquitousness of rotavirus infection (3, 4).

On the other hand, human norovirus (NoV) has now become another important seasonal cause of AGE in both children and adults especially due to global efforts and improvement in NoV diagnostics, and the widespread use and effectiveness of rotavirus vaccines in reducing rotavirus-associated AGE disease burden (3, 5). Currently, human NoV infection has been recognized as the most common cause of sporadic cases and outbreaks of AGE among all ages, associated with 18 per cent (95% CI: 17-20%) of diarrhoeal disease cases worldwide (5-7). However, there is still uncertainty about the accurate epidemiological and etiological figures of NoV diseases, especially from developing countries where highly sensitive diagnostics are not widely available. Recent reports have described about 4 million cases of NoV infections per year only in the UK and estimated over 0.2 million annual deaths by this virus constituting a major health and economic burden across all income settings (6-8). While NoV affects individuals from all ages and settings, a higher incidence has been described at earlier ages in lower income settings (5-8).

1.2 Enteric Viruses

Derived from the ancient Greek *enteron (*plural *entera*) which means intestine, the word “Enteric” (Greek*; enterikos)* refers to something Of, relating to, or within the intestines. The gastrointestinal (GI) tract conforms one of the largest mucosal surfaces in the body and a major interface with the luminal environment. Lined by millions of epithelial cells the GI tract, and predominantly the small intestinal mucosa, plays a key role for nutrients absorption and provide an optimal milieu for several

microorganisms, i.e., microbiota, while constantly interacting with potentially harmful antigens and infectious viral particles. Fifty-years ago most viral agents associated to gastroenteritis were unknown. Early 1970s studies using stool filtrates from "non-bacterial gastroenteritis" outbreaks together with advances in electron microscopy and antigen-detection techniques paved the field of what we currently know about enteric viruses and viral gastroenteritis (9-11). After decades of research, enteric viruses now represent a wide spectrum of viral families able to invade and replicate within the gastrointestinal mucosa (12). According to Bishop et al., enteric viruses can be grouped as follow: 1) Viruses that cause a local inflammation at any sites of the intestinal tract, resulting in AGE, e.g., rotaviruses, caliciviruses, adenoviruses; 2) viruses that replicates in the intestinal tract prior to generate distantly a clinical disease, e.g., measles, poliovirus or hepatitis A; 3) Viruses that spread to the intestinal tract at later stages of a systemic disease, e.g., human immunodeficiency virus (HIV) and cytomegalovirus (12). Here I have dedicated to study and detail the first category of enteric viruses; Rotavirus and Norovirus.

1.2.1 Rotavirus

Rotaviruses are 70 nm-diameter icosahedral viruses that belong to the Rotavirus genus in the *Reoviridae* family. Rotaviruses are non-enveloped triple-layered viruses with an 11-segment-organized, double-stranded (ds) RNA genome. Each segment encodes for a single protein, except for the 11th segment coding for two, comprising a total of 12 proteins: 6 structural viral proteins (VPs; VP1-VP3, VP4, VP6, VP7) and 6 non-structural proteins (NSPs; NSP1-NSP6) (13). Structurally, the rotavirus genome is protected by a core-shell of 120 dimers of VP2 protein, including an RNA-dependant RNA polymerase (VP1) and the RNA capping enzyme, VP3 (Fig. 1.2). The rotavirus core is also enclosed by a "middle" layer, i.e., intermediate capsid, formed by VP6 (260 trimers), which in turn is surrounded by an outer third protein layer conformed by 260 trimers of VP7 and 60 spike-shaped VP4 trimers[1] (13, 14). All together forms a wheel-shaped virion better known as triple-layered particle (TLP) (Fig. 1.2).

[1] During rotavirus replication, the VP4 spike protein is cleaved by proteases into VP8* and VP5* subunits. Products remain associated in the virion and mediates the virus binding and entry into host cells (13).

Rotaviruses capsid layers possess a wide antigenic and genetic diversity. As part of the Rotavirus genus, rotaviruses are classified into at least eight groups, also named species (referred to as A to H) based on the serological reactivity of the inner capsid protein, VP6 (14-17). Most human and mammalian infections associated to AGE are caused by Group A rotaviruses (RVA). This group is further classified into G types (G for glycoprotein) and P types (P for protease-sensitive) binary nomenclature based on the molecular properties of the outer capsid proteins VP7 and VP4, respectively. While serotype and genotype for G designations largely coincide, a dual nomenclature has been introduced for VP4-based classification, e.g., P1A[8]; where the P serotype 1A is assigned first, followed by the P genotype 8 in brackets (14). Currently, the Rotavirus Classification Work Group (RCWG) has defined a full-genome based classification system for RVA, with a total of 41 G-genotypes and 57 different P-genotypes. This system assigns a specific genotype to each structural and non-structural protein-encoding gene of a particular rotavirus strain, highlighting the role of all 11 rotavirus gene segments reassortment in the vast diversity among co-circulating rotaviruses known so far (Fig. 1.3) (15, 16).

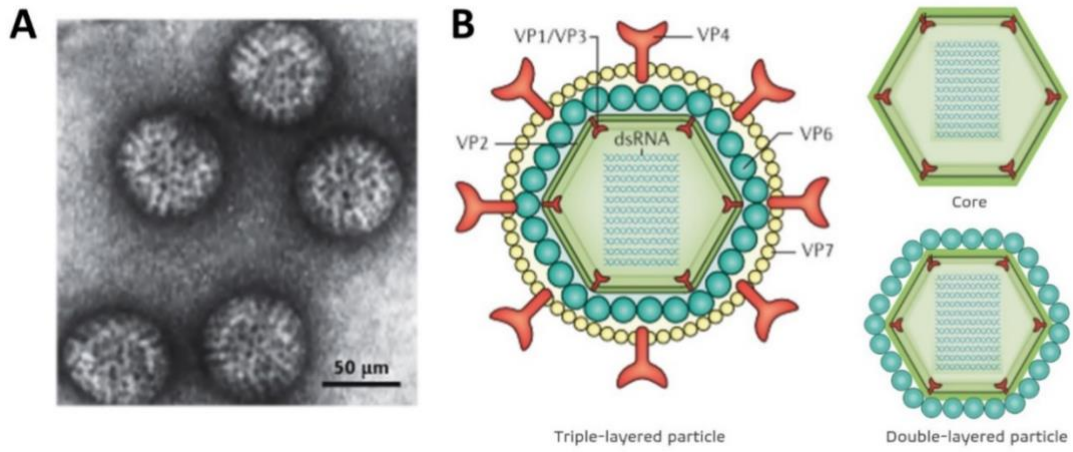

Figure 1.2. Structure of Rotavirus. Rotavirus 70 nm-diameter icosahedral particle resembles a wheel (Latin; rota) as seen by Electron micrograph (A) and consists of 3 layers: the inner capsid layer formed by viral protein (VP) 2, which together with VP1 and VP3 enzyme and the 11-segment dsRNA genome compose the virion core; the VP6 middle capsid layer, which determines the viral species and subgroups; and the outer capsid layer formed by VP7 and the spike protein VP4, which elicit an immune response in infected hosts. Figure adapted from (15).

Several RVA strains, from nearly a dozen of both G types and P types, have been isolated in humans. Group A rotavirus G/P genotypes; G1P[8], G2P[4], G3P[8], G4P[8], G9P[8], and G12P[8], have been the most common causes of AGE disease globally in humans for the past 40 years (Fig. 1.3) (12, 15).

Host	Strain	Viral structural proteins						Non-structural proteins				
		VP[7]	VP4	VP6	VP1	VP2	VP3	NSP1	NSP2	NSP3	NSP4	NSP5
Human	Wa	G1	P[8]	I1	R1	C1	M1	A1	N1	T1	E1	H1
	KU	G1	P[8]	I1	R1	C1	M1	A1	N1	T1	E1	H1
	Dhaka 16-03	G1	P[8]	I1	R1	C1	M1	A1	N1	T1	E1	H1
	D	G1	P[8]	I1	R1	C1	M1	A1	N1	T1	E1	H1
	P(rice)	G3	P[8]	I1	R1	C1	M1	A1	N1	T1	E1	H1
	ST3	G4	P[6]	I1	R1	C1	M1	A1	N1	T1	E1	H1
	IAL28	G5	P[8]	I1	R1	C1	M1	A1	N1	T1	E1	H1
	WI61	G9	P[8]	I1	R1	C1	M1	A1	N1	T1	E1	H1
	B3458	G9	P[8]	I1	R1	C1	M1	A1	N1	T1	E1	H1
	RMC321	G9	P[19]	I5	R1	C1	M1	A1	N1	T1	E1	H1
	Dhaka 12-03	G12	P[6]	I1	R1	C1	M1	A1	N1	T1	E1	H1
	Matlab 13-03	G12	P[6]	I1	R1	C1	M1	A1	N1	T2	E1	H1
	B4633-03	G12	P[8]	I1	R1	C1	M1	A1	N1	T1	E1	H1
	Dhaka25-02	G12	P[8]	I1	R1	C1	M1	A1	N1	T1	E1	H1
	DS-1	G2	P[4]	I2	R2	C2	M2	A2	N2	T2	E2	H2
	TB-Chen	G2	P[4]	I2	R2	C2	M2	A2	N2	T2	E2	H2
	B1711	G6	P[6]	I2	R2	C2	M2	A2	N2	T2	E2	H2
	DRC86	G8	P[6]	I2	R2	C2	M2	A2	N2	T2	E2	H2
	DRC88	G8	P[8]	I2	R2	C2	M2	A2	N2	T2	E2	H2
	69M	G8	P[10]	I2	R2	C2	M2	A2	N2	T2	E2	H2
	L26[a]	G12	P[4]	I2	R2	C2	M1/M2	A2	N1	T2	E2	H1
	N26-02	G12	P[6]	I2	R2	C2	M2	A2	N1	T2	E6	H2
	RV176-00	G12	P[6]	I2	R2	C2	M2	A2	N2	T2	E6	H2
	RV161-00	G12	P[6]	I2	R2	C2	M2	A2	N2	T2	E1	H2
	Au-1	G3	P[9]	I3	R3	C3	M3	A3	N3	T3	E3	H3
	T152	G12	P[9]	I3	R3	C3	M3	A12	N3	T3	E3	H6
Bovine	NCDV-Lincoln	G6	P[1]	I2	R2	C2	M2		N2	T6	E2	
	BRV033	G6	P[1]	I2	R2	C2	M2	A3	N2	T6	E2	H3
	RF	G6	P[1]	I2	R2	C2	M2	A3	N2	T6	E2	H3
	Uk	G6	P[5]	I2	R2	C2	M2	A3	N2	T7	E2	H3
	WC3	G6	P[5]	I2	R2	C2	M2	A3	N2	T6	E2	H3
	KJ44	G5	P[1]	I1	R1	C1	M2	A1	N1	T1	E1	H1
	KJ75	G5	P[5]	I1	R1	C1	M2	A1	N1	T1	E1	H1
Porcine	A131	G3	P[7]	I5	R1	C2	M1	A1	N1	T1	E1	H1
	Gottfried	G4	P[6]	I1	R1	C1	M1	A8	N1	T1	E1	H1
	OSU	G5	P[7]	I5	R1	C1	M1	A1	N1	T1	E1	H1
	A253	G11	P[7]	I5	R1	C2	M1	A1	N1	T1	E1	H1
	YM	G11	P[7]	I5	R1	C1	M1	A8	N1	T1	E1	H1
Avian	PO-13	G18	P[17]	I4	R4	C4	M4	A4	N4	T4	E4	H4
Simian	SA11g4"O" (5N)	G3	P[1]	I2	R2	C5	M5	A5	N5	T5	E2	H5
	SA11-5S	G3	P[1]	I2	R2	C5	M5	A5	N5	T5	E2	H5
	SA11-30/19	G3	P[1]	I2	R2	C5	M5	A5	N5	T5	E2	H5
	SA11-30/1A	G3	P[1]	I2	R2	C5	M5	A5	N5	T5	E2	H5
	SA11-H96	G3	P[2]	I2	R2	C5	M5	A5	N5	T5	E2	H5
	SA11-Both	G3	P[2]	I2	R2	C5	M5	A5	N2	T5	E2	H5

Figure 1.3. Genome-Based classification and nomenclature of group A rotavirus. Structural and non-structural protein-encoding gene classification as per recommendations of the Rotavirus Classification Work Group (RCWG) and genotype distribution patterns for group A rotavirus strains; Wa-like (green), DS-1-like (red), and AU-like (orange), and avian PO-13-like (Yellow), Porcine (blue; VP4, VP7, and VP6 genotypes) and Simian SA-11-like (purple) rotavirus gene segments, respectively**.** *Table adapted from Matthijnssens et al (16).*

Particularly, G1P[8] strains have been consistently circulating globally and constitutes most of the human RVA infections worldwide, accounting for over 70% of rotavirus infections in North America, Europe, Australia (18). However, geographical differences in the distribution of rotavirus strains and AGE incidence have been noted with more RVA-associated disease in children from low-and middle-income countries than developed countries (2-4). For example, although G1P[8] and G2P[8] strains represent approximately 29% and 25% of all the circulating RVA strains in Africa, there is also a higher prevalence of G12P[8] and regional important strains (particularly P[6] genotypes) as compared developed countries (19). Similar findings have been reported previously for G5P[8] strains in South America (20) and G8P[6] in Africa (21) suggesting a high genotype diversity in LMIC.

1.2.1.1 Rotavirus transmission and life cycle

Rotaviruses are transmitted by faecal-oral route mainly by close person-to-person contact or through contaminated fomites. On reaching the GI mucosa, rotaviruses infects and replicates in mature enterocytes lining the small intestinal villi and resident enteroendocrine cells (12). This process causes a non-bloody watery diarrhoea, one of the hallmarks of rotavirus disease, as a result of two proposed mechanism: 1) Osmotic diarrhoea due to malabsorption caused by damage or lysis of enterocytes; 2) Secretory diarrhoea induced by NSP4 and activation of the enteric nervous system (ENS). Other associated symptoms include vomiting, malaise, and fever. Although asymptomatic rotavirus disease is frequently common, diarrhoea symptoms last for a short period (up to 3-7 days). Thus, after initial incubation period (24 – 48 h) viral particles can be shed in stools two days before and one month after symptoms onset, especially during the first week where large quantities are excreted (Reviewed in (15)). Rotavirus replication cycle is primarily initiated by the spike protein VP4. This protein has been implicated on cell attachment and entry through subunits VP8 and VP5, respectively (13). Followed VP4 cleavage by gut proteases, the subunit VP8 recognize and attach to different glycan receptors containing sialic acid (SA) residues. Rotavirus strains can also bind to host genetically determined non-

Box 1. Histo-blood group antigens (HBGAs) are oligosaccharides-based antigens including blood group antigens (ABH), Lewis antigens and FUT2-dependent HBGAs. The latter are formed by fucosylated-oligosaccharides (by FUT2 glycosyltransferases) and can be found in secretions and at mucosal surfaces, i.e. intestinal mucosal epithelial cells, serving as receptors for norovirus and rotavirus. Individuals with functional *FUT2* genes are classified as *secretors* and therefore are susceptible to NoV and RV infection, whereas non-secretors ($FUT2^{-/-}$) have less diverse NoV and RV infections, including a genotype-dependent resistance to NoV GI.1, GII.4 and partially to RVs P[8] strains, respectively.

sialylated oligosaccharides named Histo-blood groups antigens (HBGAs) (Box 1). Subsequently, interactions of VP5 subunit and VP7 with host cell co-receptors facilitates rotavirus entry via endocytosis. At this stage, low calcium levels within endosomes facilitates the removal of the outer capsid layer and expose the DLP into the cytoplasm. Thus, the 11 different segments of positive-sense single-stranded (ss) RNA are released from the DLP functioning either as mRNAs for translation or as pre-genomic RNA templates for viral progeny. The resulting transcripts are later assorted and packaged into viral cores in specialized replication factories named viroplasm, accompanied by RNA replication for (-) ssRNA synthesis and new DLPs formation by addition of the VP6 middle layer (Fig. 1.4).

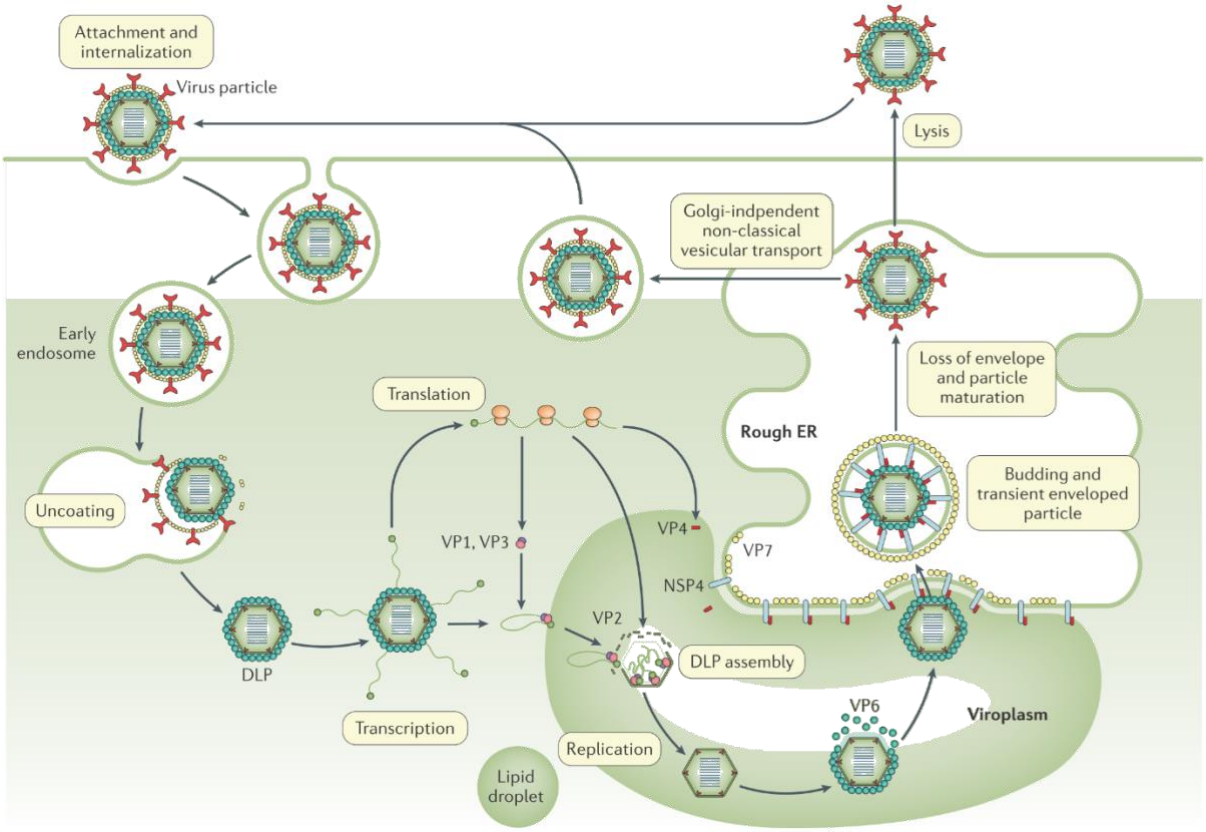

Figure 1.4. Rotavirus replication cycle. Rotavirus attach to host cell sialylated glycan receptors, e.g., the gangliosides GM1 and GD1a, through VP8 domain of viral spike protein 4 (VP4). Additionally, fucosylated-oligosaccharides, known as histo-blood groups antigens (HBGA), serves as nonsialylated receptors for VP8 and genetically determines the host susceptibility to some rotavirus strains. Interaction with host cell co-receptors by VP5 subunit and VP7 mediates viral entry and endosomes formation. Double-layered particles (DLP) are released into cytoplasm where transcription and translation of each of the 11 ssRNA segments occur. Formed transcripts are packed and assembled into new DLPs within viral replication structures known as viroplasms composed by non-structural protein 5 (NSP5) and NSP2 along with cellular proteins and VP1-VP3 complex. After VP6-

addition, NSP4 mediates DLPs budding into endoplasmic reticulum (ER) and consequently the formation of triple-layered particles following VP7 and VP4 addition. Finally, the partially ER-formed enveloped is lost and mature virions are released by cell lysis or by Golgi-independent non-classical vesicular transport by host epithelial cells. *Figure extracted from Crawford et al. (15).*

Finally, NSP4 protein mediates DLPs budding within the endoplasmic reticulum (ER) and vesicular transportation for the assembly of triple-layered particles and consequently the virion release (14, 15).

1.2.2 Norovirus

Human noroviruses derive their name from the "Norwalk agent"; the infectious agent of a 1968 outbreak of acute non-bacterial gastroenteritis (as named on that time) in the city of Norwalk, Ohio, USA. Since their identification in 1972 by Kapikian et al (22), major progress has been made to date overcoming nearly 50 years of historical difficulties due the lack of proper study models associated to the inability of *in vitro* propagation of NoVs (Reviewed in (23)). Currently, noroviruses are classified as part of the Norovirus genus within the *Caliciviridae* family. Noroviruses consist of non-enveloped, 27–30 nm-diameter icosahedral particles (T3 symmetry) with a linear, positive-sense, single-stranded RNA genome of approximately 7.5 kb in length (Fig. 1.5). Human norovirus genome is organized in three main sections known as open reading frames (ORFs). ORF1 encodes a large non-structural (NS) polyprotein which is post-translationally cleaved by a 3C-like virus-encoded protease, named Pro or NS6, into 6 non-structural proteins involved in viral genome replication steps: p48 (or NS1/2), NTPase (NS3), p22 (NS4), VPg, RNA-dependent RNA polymerase (RdRp) and the mentioned protease Pro. Additionally, the ORF2 and ORF3 encodes for the major (VP1) and minor (VP2) structural protein, respectively. Differently from rotavirus and the *Reoviridae* family, noroviruses (and the *Caliciviridae* family) are structurally organized in a single viral capsid particle formed by 90 dimers of VP1, which comprises of a shell (S) and a protruding (P) domain. While the S domain face the capsid interior surrounding the RNA genome, the P domain is exposed and responsible for HBGAs binding in host cells (Box 1) and interaction with neutralizing antibodies (22, 23). Additionally, only a few VP2 units conform each viral particle and are associated to the inner side of VP1 S domain capsid (Fig. 1.5). Noroviruses, as members of the norovirus genus, are both genetically and antigenically diverse and

infects a wide spectrum of mammalians host such as humans, rodents, cattle, pigs, and felines. Recent advances in viral genome genotyping and sequencing have currently classified noroviruses into at least 10 major genogroups: GI-GX, and further divided into 48 or 60 genotypes, based on full VP1 sequences and the nucleotide diversity of the RNA-dependent RNA polymerase (RdRp) region of ORF1 (24).

Further norovirus organization will consider the complete viral genome sequence similar to the classification system described for rotavirus (16). Over the past two decades, strains of the genotype GII.4 have caused the majority (70-80%) of AGE cases in humans. Additional GII.4 classification consider strains that has become an epidemic in at least two geographically distant regions. Since 1995, six antigenically GII.4 variant have resulted in major outbreaks worldwide, where GII.4 Sydney-2012 (GII.4-SYD), has been the most recent pandemic strain circulated and the dominant genotype so far. Currently, a new potentially high-transmissible norovirus lineage containing a polymerase substitution (GII.P16) and GII.4 capsid structure, has been detected in Asia and Germany and confirmed in the UK and USA (26).

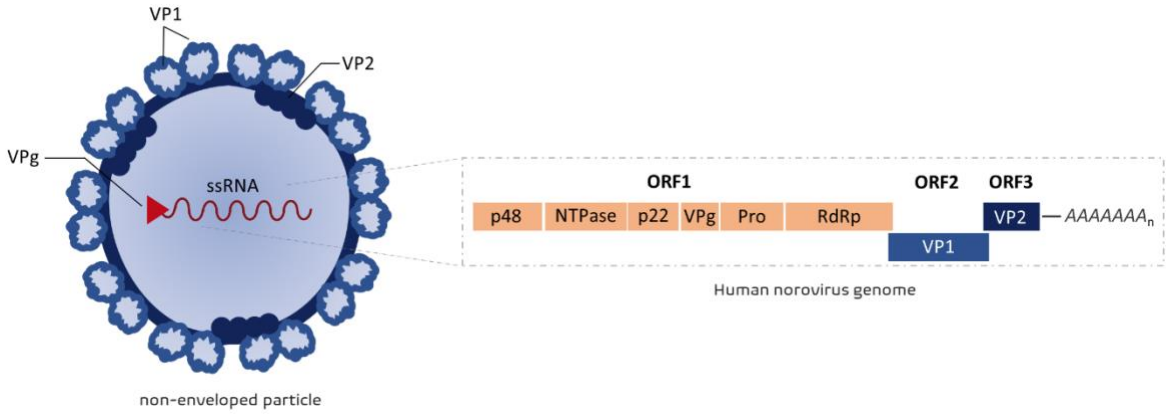

Fig. 1.5. Structure and genome of human norovirus. Human norovirus non-enveloped icosahedral particle (~30 nm-diameter) consists of a capsid formed by viral protein 1 (VP1) dimers. The inner capsid side is formed by a few units of VP2 and VPg, which is linked to the 5`end of the linear, single-stranded, RNA (positive sense) genome. As shown on the right-hand side, human norovirus ssRNA genome is organized in three open reading frames (ORF): ORF1, encodes a large polyprotein, which is post-translationally cleaved into six non-structural proteins (p48, NTPase, VPg, RNA-dependent RNA polymerase (RdRp) and Pro) by the viral-encoded protease Pro. ORF2 and ORF3 encodes for the major (VP1) and minor (VP2) structural proteins, respectively. Additionally, a 3`end polyadenylated tail (A_n) protects the genome templates and mature RNA transcripts (25).

1.2.2.1 Norovirus transmission and life cycle

Human noroviruses are mainly transmitted by faecal to oral route and foodborne outbreaks, following a seasonal infection pattern causing sporadic and epidemic AGE episodes during the coldest months (October to March in the northern hemisphere). Noroviruses are highly contagious and resistant to common disinfecting agents, e.g., alcohol-based hand sanitizers. Thus, the direct contact with infected persons, contaminated food or water and objects (fomites), are important transmission routes associated to NoV outbreaks, especially in communal or enclosed living spaces such as restaurants, hospitals, care homes, schools, cruise ships among others. In terms of clinical symptomatology, human NoV infection triggers an acute, non-bloody and watery diarrhoea in conjunction with recurrent vomit, being generally referred as the "winter vomiting bug". Additional symptoms include abdominal pain, nausea, and fever, which together with the hallmark clinical symptoms can last up to three days, followed by post-clinical viral shedding via the faeces or vomit ranging from 7 days to 4-6 weeks (Reviewed in (23)).

Human noroviruses cell tropism and pathogenesis is not completely understood, primarily due to the inability of cell culture adaptation of these viruses and the lack of small animal models. Evidence from different studies to date suggest that human NoV replicates in human intestinal enterocytes (Reviewed in (27) and human B cells (28). Thus, recent effort has currently established two human norovirus replication system using a transformed B cell line (BJAB) (28, 29) or non-transformed stem cell-derived human intestinal enteroids (30). Similar to rotavirus entry mechanism, human NoV attaches to fucosylated-HBGAs present in secretor-positive individuals, i.e., persons with a functional FUT2 enzyme (Box1). Thus, norovirus capsid protein VP1 interacts with fucosylated glycans present at human enterocytes surfaces facilitating the virus binding to host co-receptors (currently unknown) and subsequent viral particle internalization. After viral entry and capsid removal, the (+) ssRNA genome is exposed into the cytoplasm, where the 5'end genome-linked protein VPg mediates the interaction with host translation factors (23, 25). Then, ORF1-encoded polyprotein is cleaved into functional six non-structural proteins including the RNA-dependent RNA polymerase (RdRp), p48 (NS1/NS2) and p22 (NS4) crucial for replication complex formation (Fig. 1.6).

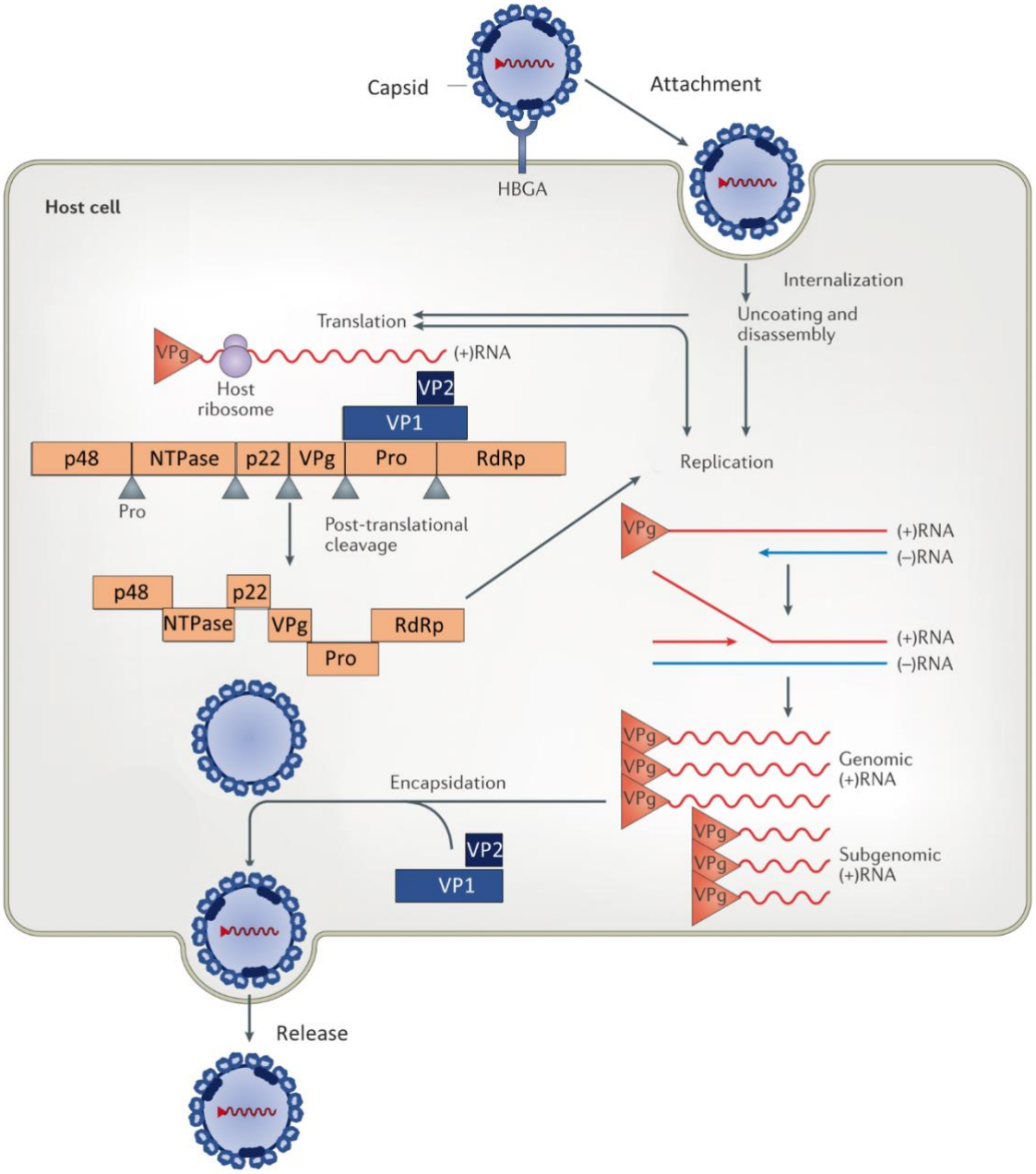

Figure 1.6. Norovirus replication cycle. Human noroviruses attach to host cell fucosylated glycan receptors, i.e., HBGAs, through VP1 protruding domain. Virion is internalized by an unknown mechanism after interaction with host cell co-receptors and then uncoated, releasing the genome into the cytoplasm. Translation starts by VPg interaction with host ribosome (left). The ORF1-derived polyprotein (orange rectangles) is post-translationally cleaved into six non-structural proteins: p48, NTPase, VPg, Pro and the RNA-dependent RNA polymerase (RdRp). This last one commands the formation of both (-) RNA intermediates and subsequent new viral genome copies (right) during replication. In parallel, the major (VP1) and minor (VP2) structural proteins are translated, allowing the final virion assembly, encapsidation and mature particle release from the host cell. *Figure adapted from de Graaf M. et al (25).*

Additionally, negative sense RNA intermediates are formed and used as templates during genome replication, while sub-genomic positive sense RNA comprised by ORF2 and ORF3 are used for VP1 and VP2 production and new capsid formation. Finally, genome copies are packaged into new virions for the final particle assembly and release from host cell by an unknown mechanism (23, 25, 27). Current progress using human stem cell-derived enteroids, as an active 3D intestinal epithelium system for human NoV cultivation, will provide valuable insights about noroviruses life cycle requirements and unveil host-pathogen interactions (27).

1.3 The mucosal immune system: MALT

The human mucosal immune system (MIS) comprises both anatomically and physiologically different compartments, covering a substantial surface area of over 300m^2. This vast surface includes the ocular, oral nasopharyngeal, respiratory, gastrointestinal, and genitourinary mucosa – and is primarily lined by a monolayer of epithelial cells (ECs) – forming an environmental-exposed barrier responsible for protecting our body against microbial colonization and pathogens entrance (31). The MIS is divided in two functional compartments: the inductive sites and effector sites (Fig. 1.7). The former is closely interconnected with lymphoid tissues, where naïve T and B cells are primed or stimulated following exogenous antigen uptake from mucosal surfaces by antigen presenting cells, whereas effector sites is where activated (or effector) cells migrates to perform their respective immunological action, e.g., production of antigen-specific IgA antibodies (32). Inductive sites are constituted by organized lymphoid structures commonly referred as mucosal associated-lymphoid tissues (MALT), a major compartment of the mucosal immune system (MIS) for the induction of protective immune responses.

The structure of MALT resembles to lymph nodes (LN) and are divided according to anatomical regions, where different cell composition and distribution among species are found (Fig. 1.7) (31). MALTs are covered by a subset microfold (M) cells, ECs, and underlying lymphoid cells that play central roles in antigen uptake and the initiation of mucosal immune responses. Human MALTs are also constituted by B cell-enriched areas, i.e., B-cell follicles, and T cell zones, forming a complex and dynamic network between mucosal inductive sites, including the gut-associated lymphoid tissues (GALT) and nasopharynx-associated lymphoid tissues (NALT), and the effector sites within MIS (31-

33). The human MALT provides an important source of memory B cells and T cells, including both central memory and effector memory T cells, which are restricted by cell expression of homing receptors (site-specific integrins) to specific mucosal effector compartments (expressing cognate addressins), such as the lamina propria (LP) of the gastrointestinal or upper respiratory tract, and surface epithelia. Thus, the migration and homing properties of these immune cells from mucosal inductive to effector tissues is crucial for the initiation of mucosal-specific immune responses (31-33) (Fig. 1.7). Protection at regional mucosal tissues is mediated mainly by secretory IgA (sIgA) – dimeric IgA molecules joined by a J chain – which are produced by mucosal plasma B cells (PC) and actively exported by secretory epithelia preventing pathogens from direct mucosal epithelial attachment by immune exclusion (32). Although similar activities have been described for each type of MALT, the immune mechanism associated are often different and organ-specific, depending on the mucosal location and the types of antigens that are encountered.

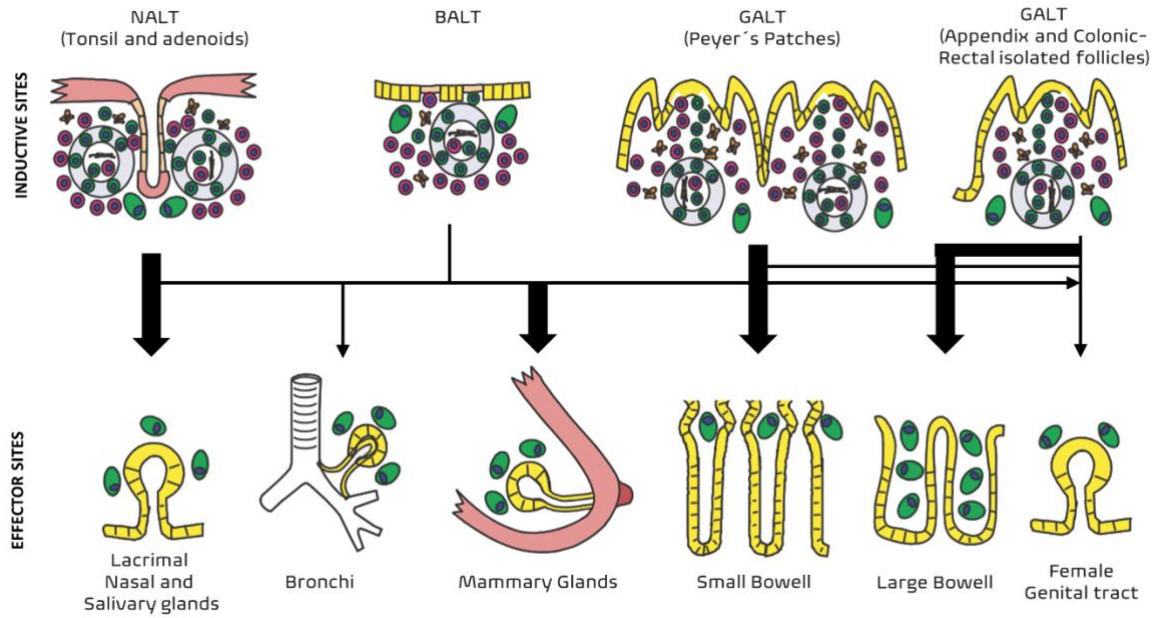

Figure. 1.7. The mucosal immune system. The mucosal immune system relies on migration of memory B and T cells from inductive (top) to effector (bottom) sites. Graded arrows represent the more or less preferred pathways followed cell activation in nasopharynx-associated lymphoid tissue (NALT) - tonsils and adenoids - , bronchus-associated lymphoid tissue (BALT), and gut-associated lymphoid tissue (GALT) - Peyer's patches, appendix, and colonic-rectal isolated lymphoid follicles -. *Figure adapted from Brandtzaeg et al (32).*

1.3.1 Mucosal Immune system in the intestinal tract: Gut-associated lymphoid tissues

The human gut-associated lymphoid tissues, or GALT, are the body's largest inductive sites mediating the adaptive immune responses to gut-derived antigens from food, the microbiota and foreign pathogens. Human GALT comprises of Peyer's patches (PP), the appendix and isolated lymphoid follicles (ILFs), where induction and regulation of mucosal immunity takes place. The GALT structures lack of afferent lymphatics differing from gut-draining mesenteric lymph nodes. Instead, human GALT contain specialized follicle-associated epithelium portions with fewer mucus-producing goblet cells, which gives them the faculty to sample antigens directly from the intestinal lumen through specialized M cells and transport them to underlying antigen presenting cells (32). Subepithelial regions include a network of follicular dendritic cells (DCs) and interfollicular T cell areas, which mediates the generation of IgA-committed (IgA+) B cells in germinal centres (GC) containing B cell follicles (Fig. 1.8). Activated B cells along with primed T cells migrate via efferent lymph to mesenteric lymph nodes, and finally to effector sites at the gut lamina propria via bloodstream. This process is directed by the expression of gut-homing receptors, $\alpha 4\beta 7$ and CCR9, on IgA+ B cells, as well as CD4+ and CD8+ T cells, which specifically attach to mucosal addressin cell adhesion molecule 1 (MADCAM1), a tissue-specific adhesion molecule, and chemokines expressed by endothelial cells. Once reached the inductive site, activated lymphocytes become effector or memory cells, where antigen-specific T cells and primarily IgA-producing plasma cells (differentiated from IgA+ B cells) mediates mucosal immune response (Fig. 1.8) (34, 35). Secretory IgA antibodies are further produced and/or released through epithelial polymeric immunoglobulin receptors (pIgR) by intestinal epithelial cells, being the predominant immunoglobulin class in human gut secretions for pathogen neutralization (34-36).

1.3.2 Mucosal Immune system in the oropharynx: nasopharyngeal-associated lymphoid tissues

The human oropharynx tissue is part of the mucosal-associated compartments that mediates immunity in humans. The human oropharynx is comprised by nasopharyngeal (adenoids), tubal, lingual, and palatine tonsils, which are arranged in a lymphoepithelial architecture named Waldeyer´s ring (Fig. 1.8) (37). These organized lymphoid structures are functionally similar to the nasopharynx-associated lymphoid tissue (NALT) in rodents, which are constitutively developed as a lymphoid organ present on

both sides of the nasopharyngeal duct (37). Waldeyer's ring, referred as human NALT, are constantly exposed to airborne and alimentary antigens, functioning as MALT inductive sites and also as an effector organ for both local and systemic immunity.

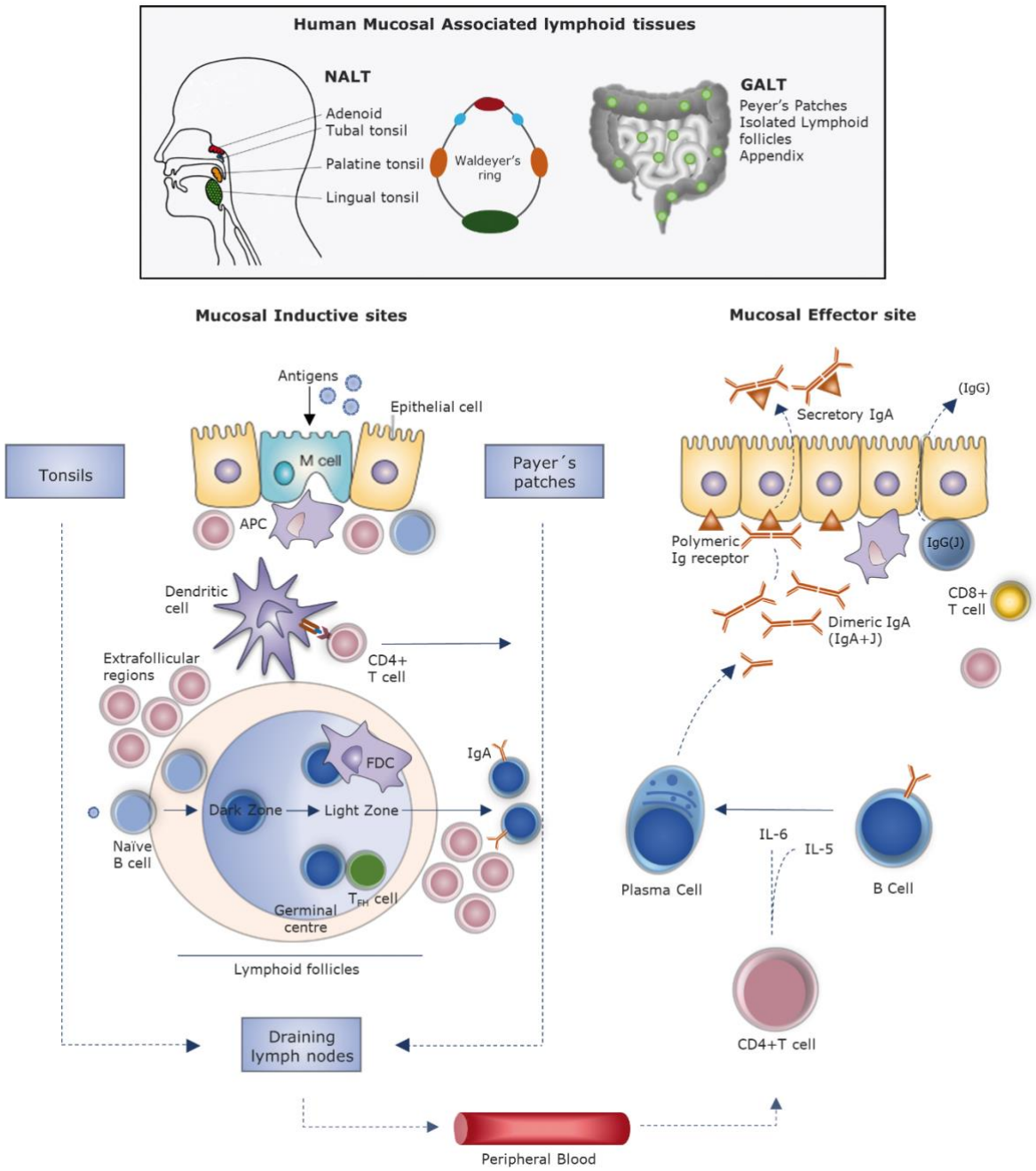

Figure 1.8. Human Mucosal Associated Lymphoid Tissues. The nasopharynx-and-gut-associated lymphoid tissues (NALT and GALT, respectively) are two main compartments of the mucosal immune system sharing similar structural features. Human tonsils (NALT) or Peyer's patches (GALT) receive antigens from lumen through microfold (M) cells located in the epithelial surface overlying mucosal lymphoid tissues. Professional antigen presenting cells (APC), such as dendritic cells, process and present antigens to T cells in these lymphoid-

tissues. Antigen-stimulated cells induce IgA-committed B-cell development at germinal centres (GC) in lymphoid follicles with help of Follicular dendritic cells (FDC) and T follicular helper cells (Tfh). After IgA class switching and affinity maturation in GC light zones, B cells migrate from MALTs to regional lymph nodes via the efferent-lymphatics. Antigen-specific CD4+ T cells and IgA+ B cells finally migrate to mucosal effector sites (such as the nasal passage and intestinal lamina propria) through the thoracic duct and blood circulation. Here, IgA+ B cells differentiate into IgA-producing plasma cells, in the presence of cytokines (IL-5 and IL-6) produced by Th2 cells. and produce dimeric IgA, which then become (secretory) sIgA by binding to polymeric Ig receptors displayed on mucosal epithelial cells. Finally, both IgG and sIgA are released into effector sites to mediate an immune response. *Figure modified and adapted from (33, 35).*

Human tonsils are the largest components of Waldeyer's ring and are at the first line of immune defence against pathogens. Like human Peyer's patches, the cellular architecture of tonsils consists of three main sections: reticulated crypt epithelium, lymphoid follicles and extrafollicular regions (Fig. 1.8). The first section represents the external lymphoepithelial layer, integrated by ECs, M cells and APCs organized into crypts near the surface epithelium and exposed to environmental antigens (37, 38). Furthermore, the subepithelial area is composed by extrafollicular regions with T cell-enriched zones (25-35% of T cells) and GC in B cell follicles (up to 75% of B cells). These compartments are crucial for T cell activation and B cell differentiation into memory or effector antibody-secreting plasma cells, respectively (37-39). Specifically, GCs are formed after the stimulation of naïve B cells and subdivided into different zones. The dark zone is where B cells, or centroblast, proliferates after antigen recognition. After clonal expansion, B cells migrates to the light zone, where are selected by antigen affinity i.e., affinity maturation, with help of Follicular dendritic cells (FDC). Additionally, FDC stimulates T follicular helper cells (Tfh) within this zone, which promotes B cell class switching and differentiation to plasma cells (PCs) producing high-affinity antibody (Fig. 1.8) (38). Consequently, pIgA-producing PCs mediates the effector response following plasmablast homing from GCs to both distant and local secretory effector sites (38). Moreover, human adenoids and tonsils contain more IgG secreting cells than IgA in both the epithelial and the subepithelial compartments, which differentiates them from GI tract lamina propria and support a systemic role of this compartment (37, 39). Thus, human tonsils are recognized as secondary lymphoid tissues and have shown to be induction sites for polio and influenza

vaccine-induced immunity and for natural immunity against several nasopharyngeal pathogens (38, 39). Particularly, human tonsils organization parallels with enteric primary poliovirus replication sites, i.e. intestinal epithelial cells and Peyer's patches, where tonsils crypts and APC in the tonsil follicles can both work as poliovirus replication sites and at the same time promote a mucosal antibody production which is critical for the control of poliovirus (40, 41). Therefore, tonsil tissues, as a human NALT model, can be a useful system to evaluate the immune response against enteric viruses and for testing both new and available vaccines again them.

1.4 Mucosal Vaccines

Mucosal vaccines have been recognized as an important method of immunization against enteric pathogens. These vaccines - including oral, nasal, sublingual, and genital tract vaccines - can stimulate a local production of antigen-specific antibodies and the development of long-term B and T memory cells, promoting both a mucosal and systemic protective immune response (42). Given the mucosal immune system compartmentalization in MALT and effector sites, vaccination route is crucial for an effective mucosal immune response at the desired sites (36). Oral delivered vaccines, such as rotavirus and poliovirus vaccines, have been widely used in the population and associated to a protective immunity in the gastrointestinal tract, salivary and mammary glands (42, 43). These types of vaccines have shown a great potential in the prevention of diseases by promoting the production of antigen-specific secretory immunoglobulin A (sIgA), a key immune mechanism against pathogens at mucosal sites, together with a systemic immunoglobulin G (IgG) response (42-44).

1.4.1 Oral Polio vaccines and mucosal response

Almost sixty years have passed since the development and implementation of the oral poliovirus vaccine (OPV). This led to the creation of the Global Polio Eradication Initiative (GPEI) in 1988, which involved a massive public health campaign for the widespread use of OPV in conjunction with an inactivated poliovirus vaccine (IPV), leading to a 99% reduction of the global incidence of wild poliovirus cases worldwide (45). Since then, OPV has become one of the classical oral mucosal vaccines and a cornerstone for elucidating fundamental aspects of human mucosal immune responses.

Poliovirus is a human enterovirus within the *Picornaviridae* family and the causing agent of polio (or poliomyelitis). This virus spread by faecal-oral route and multiplies in the intestine, where can also reach the central nervous system inducing a minor illness with mild symptoms to a severe paralytic disease, respectively. Three serotypes of wild poliovirus (type 1, type 2, and type 3) have been described according to differences in their capsid protein (45). Thanks to global immunization campaigns both type 2, and type 3 wild poliovirus has been declared eradicated in 2015 and 2019, respectively (46).

The OPV has been an essential part of the joints efforts to eradicate wild-type poliovirus. This vaccine was originally formulated as a trivalent live-attenuated oral poliovirus (tOPV), which mimicked the immune response to natural exposure of the three poliovirus serotypes. Currently, there are three global formulations of OPVs in use: tOPV, bivalent or bOPV (types 1 and 3 WPV); and monovalent OPV or mOPV), which (two subtypes for serotypes 1 and 3; mOPV1 and mOPV3, respectively (45). After oral administration, OPVs replicates in the gastrointestinal tract producing a robust sIgA immune response in the intestinal mucosa (47). This local virus-specific antibody response has demonstrated to be crucial to decrease virus shedding after subsequent WPV exposures. Moreover, additional induction sites, including human tonsils and adenoids, have been described following oral OPV administration, as observed by reduction of poliovirus-specific IgA antibody titres in nasopharyngeal secretions after adenotonsillectomy procedures in OPV immunized children (41), supporting the role of human NALTs as key induction sites for oral vaccines and efficacy. In parallel, OPV promotes a mild systemic antibody production that will partially protect against myelitis by preventing the spread of poliovirus to the nervous system (47). However, the injectable IPV alone induced a stronger systemic response that protects from paralytic disease but failed to provide adequate protection from poliovirus shedding (47). Thus, a combined regimen of OPV with IPV was introduced in 1988 by the GPEI to provide a broaden immunity, including a strong seroconversion and robust intestinal immunity (48).

1.4.2 Rotavirus Vaccines

Four oral, live-attenuated rotavirus vaccines: a monovalent human rotavirus vaccine, RV1 (Rotarix®, GSK 2-dose series); a pentavalent bovine-human rotavirus reassortant, RV5, (Rotateq®, MERCK; 3-dose series); a monovalent natural bovine-human G9P rotavirus reassortant (Rotavac®, Bharat

Biotech);and a pentavalent bovine-human reassortant with human G1, G2, G3 and G4 and bovine G6P[5] backbone (RotaSiil®, Serum Institute of India, 3-dose series) are available internationally and WHO prequalified. Particularly, RV1 and RV5 have been widely included into routine immunization programs worldwide and both followed the OPVs approach, as though that an orally administered live-attenuated tissue-culture grown rotavirus would mimic the natural immunity by wild-type rotavirus within the GI tract (49).

Rotarix (RV1) vaccine derived, after several passages in Vero cells, from a rotavirus candidate vaccine based on a clinical G1P[8] rotavirus isolate from Cincinnati, USA (human 89-12 strain) (50). The G1P[8] strain is the most common cause of AGE by human rotaviruses and was therefore chosen by the manufacturer to provide a serotype-specific immunity against rotavirus disease (50). On the other hand, Rotateq (RV5) is a pentavalent vaccine formed by a mixture of five live rotavirus strains, i.e., reassortants, using a bovine WC3 strain backbone (G6P[5]). Each genetically distinct human-bovine rotavirus reassortant contains a human gene encoding 1 of the outer capsid proteins: the VP7 capsid protein of four human rotaviruses (G1, G2, G3 and G4), and the human VP4 (type P8) commonly referred as P1 (49). Although these oral vaccines are less efficacious against rotavirus infection or mild disease, both have shown clear signs of protection against severe AGE and significantly decreased rotavirus disease burden worldwide. The introduction of rotavirus vaccines has globally contributed to 22%-45% reduction in mortality from all-cause AGE in children younger than 5 years (51). Additionally, these vaccines have effectively prevented hospital admissions due to rotavirus AGE, with vaccine effectiveness ranging from 57% to 85% for RV1 and from 45% to 90% for RV5 according to countries' mortality distribution. However, a considerable variation has been noted among different regions as evidenced by higher efficacies in high-income countries (85-100%) compared to LMIC (< 50%) (44, 49, 51). Same patterns have been observed in low socioeconomic settings for the live-attenuated oral polio vaccine (52) and oral cholera vaccines (reviewed in (53), where impaired immunogenicity was described. Although the immunological basis of this phenomenon is currently not understood, several factors could be associated to poor oral vaccine responses against enteric pathogens, such as host nutritional status, genetic, gut microbiota, and pre-existing immunity (44, 53).

1.4.2.1 Immune correlates of protection against Rotavirus vaccines

The nature of the immune response generated by wildtype rotavirus infection and current licensed vaccines has been mainly studied using animal model, however absolute correlates of protection (CoP) and the underlying cellular responses against rotavirus in humans remains uncertain. A variable, not sterilizing, immune protection against subsequent symptomatic disease has been described in young children after natural rotavirus infection (reviewed in (44). Particularly, rotavirus-specific IgA and IgG antibody titres in sera have been significantly associated to provide protection against natural infection (both symptomatic and asymptomatic), which increase following rotavirus vaccination (54, 55). Thus, as rotavirus-specific antibody levels in sera increase, the lower is the risk of rotavirus-associated AGE, especially in regions with low mortality (55). This type of immune response has been mainly described as homotypic, i.e., against an initial circulating genotype, and may also vary depending on several host factors such as the number of infection episodes, the level of immunity, genetic predisposition, and individual settings. Apart from seroconversion, several studies have also examined rotavirus-specific IgA in stools as an indicator for local immunity (44). However, no absolute correlates have been found due to inconsistences between asymptomatic and symptomatic copro-IgA levels and the development of rotavirus disease.

On the other hand, a heterotypic response is developed against other serotypes not present in the immunizing strain (or the initial natural infection strain). Thus, and despite the lack of an established correlate of protection induced by natural infection, widely licensed live-attenuated oral rotavirus vaccines as the monovalent RV1 and pentavalent RV5 have provided efficient protection against severe AGE. Although both vaccines are antigenically different, comparable efficacies (56) with similar levels of protection have been described including the induction of rotavirus-specific serum IgA and virus-specific neutralizing antibodies against VP7 or VP4 epitopes (44, 55, 57, 58). Interestingly, a cross-reactive IgA and IgG protection (independent of G and P-types) has been observed against the main immunogenic middle-capsid protein VP6 of rotavirus, supporting the generation of heterotypic responses after rotavirus vaccination (49, 57, 59) and the role of antibody-mediated intracellular neutralization (60). Moreover, the presence of mucosal immune mediator such as rotavirus-specific

sIgA has been also detected in sera and correlated with protection against rotavirus disease in children following RV1 vaccination (61). In terms of cellular immune response, a lower frequency of rotavirus specific CD4+ or CD8+ T cells in children has been described as compared with adults (62). However, an expansion of rotavirus specific CD4+T cells expressing gut homing receptors, has been detected in children PBMCs following monovalent RV1 vaccination (63). Nevertheless, further studies evaluating mucosal immune response in humans are necessary to provide humoral and cellular mechanistic correlates of protection associated to rotavirus vaccines.

1.4.3 Novel norovirus vaccine candidates

The development of a norovirus vaccine has confronted many obstacles, including the highly genetic and antigenic diversity of NoVs and the lack of a suitable cell line or animal models to further characterize the immunological determinants of NoV-associated disease. Although no absolute immune correlates of protection have been described against natural NoV infection to date, human challenge and vaccination studies have identified and correlated the presence of antibodies that block NoV-HBGA binding with protection against NoV-associated gastroenteritis and infection (64, 65). Moreover, HBGA-blocking antibodies has been recently described as a surrogate for human NoV neutralization using human intestinal enteroids (66). Additionally, a recent study in care homes settings highlight the role of mucosal antibodies as a correlate of protection, as observed by an increase of mucosal IgA levels (from saliva) in both symptomatic and asymptomatic (shedders) patients after GII.4 outbreak onset (67). This response remained up to 3 months later and correlated with systemic NoV-specific IgA levels and HBGA blockade antibodies titres (67). Moreover, both a genotype-specific and cross-reactive systemic immune response mediated by serum IgG has been described in children following exposure to GII.4 NoV (68). Thus, a vaccine could be effective as primary homotypic NoV infection seems to protect against subsequent new symptomatic reinfections (68, 69). Currently clinical and pre-clinical studies with parenteral non-live vaccines mainly based on NoV virus-like particles (VLPs) have been performed, yet established correlates of protection and human mucosal immune responses remain undefined (70, 71).

1.4.3.1 Virus-Like particles-based vaccines

Norovirus candidate vaccine strategies have focused on the outer capsid protein VP1, which spontaneously self-assemble into non-infectious, yet immunogenic virus-like particles (VLPs) when expressed in eukaryotic cells (71). Overall, VLPs are classified as a type of subunit vaccine, which morphologically and antigenically resembles to native virions and can be produced in large quantities. Three prophylactic VLP-based vaccines against human papilloma virus (HPV) have been approved and incorporated in national immunization programs, which have proven to be highly effective in the prevention of cervical HPV infection (72). These vaccines consist of major capsid protein (L1) VLPs, intramuscularly administered in 3-doses, providing a strong sterilizing immunity mediated by HPV-specific antibodies (72). In case of NoV, both monovalent and multivalent VLP-based vaccines candidates from common human NoV genotypes (GI and GII) are currently being tested in pre-clinical and clinical trials. Additionally, subunit vaccine candidates based on viral particles formed exclusively by the P domain of VP1 have been also developed (all recently reviewed in (71, 73).

1.4.3.2 Immune correlates of protection against Norovirus vaccines candidates

Clinical (and preclinical) studies on NoV vaccine candidates have started to clarify some inconsistencies about correlates of protection against natural NoV infection.

Monovalent GI.1 VLP-based vaccine. As an initial formulation, this vaccine candidate was adjuvanted with monophosphoryl lipid A (MPL), a detoxified bacterial lipopolysaccharide and TLR-4 agonist, and intranasally administered, inducing NoV-specific antibodies in sera from vaccinated subjects and homotypic protection against subsequent GI.1 challenges (65, 74). This initial phase 1 studies provided a proof of concept for safety and immunogenicity for mucosal NoV GI.1-derived VLP vaccine candidates (65, 74).

Bivalent NoV vaccine. Further research has concentrated in the use of bivalent vaccine combinations of GI.1 and GII.4 VLPs as a way to improve NoV vaccine cross reactogenicity and considering the epidemiological impact of these genotypes. A dry powder formulation of a bivalent NoV GI and GII.4 VLPs-based vaccine candidate, evaluated in guinea pigs, have shown a dose-dependent increase in systemic and mucosal antibody response against each of the VLPs after two intranasal doses (75).

Additionally, an intramuscular bivalent VLP-based vaccine based on GI.1 and 3 consensus sequences from GII.4 strains (2006a, Yerseke; 2006b, Den Haag; and 2002, Houston) have progressed into advanced stage of development (*Takeda Nov Vaccine candidate: TAK-214*) (76). These studies (reviewed in (73)) have evidenced the production of NoV-specific antibodies and HBGA-blocking antibody titres in sera. Moreover, antibody secreting cells (ASC) and memory B cells have been observed following vaccination, with presence of antigen-specific IgG memory B cells after 180 days postvaccination for both GI.1 and GII.4 VLPs (76, 77).

1.4.3.3 Vaccine Adjuvants for VLP-based vaccines

The utilization of adjuvants as immunomodulatory molecules may improve vaccine safety and immunogenicity and promote long-term protection in subunit vaccines. Moreover, adjuvants can help to reduce vaccine dosage and promote a stronger response among low-responders individuals, such as neonates and the elderly (78). Although VLP-based vaccines alone have been shown to be more efficacious than common subunit vaccines, adjuvants have been included in most VLP-based vaccine formulations, including several vaccine candidates for NoV infection (73, 77, 78). To date, most licensed VLP-based vaccines are mainly adjuvanted with aluminium salts, including Gardasil (HPV) (72), Engerix-B (HBV vaccine), and HEV (reviewed in (78)). In case of Norovirus, Takeda's bivalent norovirus vaccine candidate (TAK-214) has also included aluminium ($AlOH_3$; commonly referred as alum) in their first single-dose in-human efficacy trial, with significant efficacy against moderate to severe norovirus AGE (76).

In other hand, the chitin polysaccharide-derivate Chitosan, have been reported as an effective mucosal adjuvant and delivery system promoting both systemic and mucosal immune responses by stimulating local phagocytes (78). Intranasal immunization with a VLP-based monovalent norovirus vaccine formulated with chitosan and MPL has demonstrated an effective protection against G1.1 NoV infection with virus-specific IgA serological response in vaccinees (74). However, to date no adjuvants have been included in licensed oral vaccines for enteric pathogens. Experimental studies in mice using α-Galactosylceramide (α-GalCer), a sponge-derived sphingolipid and invariant Natural Killer T (iNKT) cell activator, have shown to increase mucosal immunogenicity of experimental oral-delivered vaccines

against enterotoxigenic Escherichia coli (ETEC) and Cholera (79). Further research is needed to better characterize the mucosal immune responses (and immune CoP) of NoV vaccine candidates along with mucosal adjuvant formulations.

1.5 Host factors on enteric vaccine effectiveness

From the nine current licensed mucosal vaccines, eight correspond to oral vaccines against cholera, salmonella, poliovirus, and rotavirus; the majority of which are live-attenuated formulations (all reviewed in (80). As described by Parker et al (53) relevant measures of oral vaccine responses can be grouped into immunogenicity, seroconversion, and post-vaccination shedding. This also includes vaccine efficacies and effectiveness parameters, defined as the percentage of disease reduction in vaccinees compared to unvaccinated under optimal conditions (e.g., clinical trials) and routinary use, respectively (53). Unfortunately, a considerable variation of protection levels (immunogenicity and efficacy) induced by oral-delivered vaccines - including enteric vaccines, such as rotavirus, OPV, and cholera - have been observed among different income settings, with lower efficacies in LMIC (44, 49, 51-53). Although this poor immunogenicity has often documented for oral live-attenuated vaccines, inactivated vaccines, e.g., oral-killed cholera vaccine, have also shown similar variation among children in Nicaragua compared with Sweden (81). However, efficacies of new vaccines such as VLP-based vaccines have not been evaluated in low income-settings (82).

Different environmental and host factors can contribute to poor oral vaccine responses, such as genetic, host nutritional status, gut microbiota, and pre-existing immunity, although the immunological mechanisms of this phenomenon are still incompletely understood (44, 53) (Fig. 1.9).

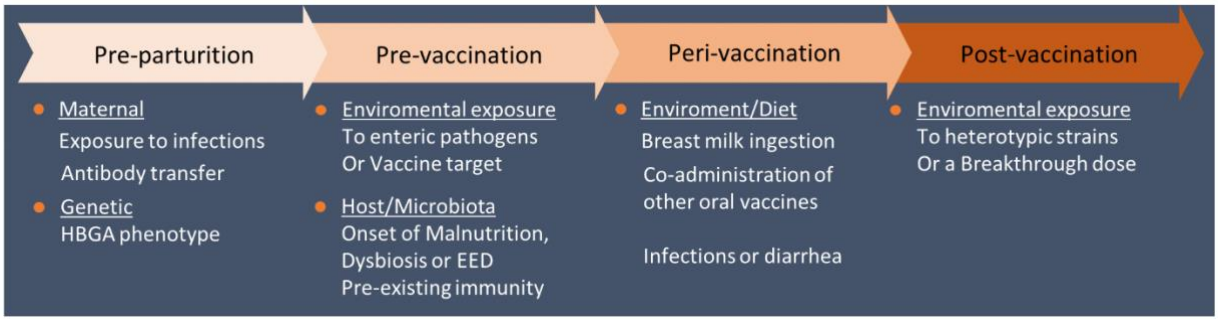

Figure 1.9. Risk Factors associated to oral vaccines failure. EED: Environmental enteric dysfunction; HBGA: Histo-blood group antigen. *Figure modified from* (53).

1.5.1 Genetic

As we previously mentioned, host genetic predisposition to enteric pathogens, such as rotavirus and noroviruses, has been associated with the expression of Histo-blood group antigens (HBGAs) as a main factor for disease susceptibility (Box 1). In addition, strong strain-specific differences have been found in secretors (i.e., individuals with functional *FUT2* gene), being significantly more susceptible to NoV GII.4 genotype and P[8]-type rotaviruses infection (83, 84). These findings opened the possibility that genotype-specific HBGA binding patterns may contribute to vaccine efficacy differences among countries, as norovirus GII.4 strains and P[8]-types rotaviruses are main components of candidates and licensed vaccines for NoV and rotavirus, respectively. Nevertheless, a recent study from Malawi found no differences in virus faecal shedding nor seroconversion between HBGA phenotypes after rotavirus vaccination (RV1) and a reduced risk of vaccine failure among non-secretors (85). However, further investigation is required to evaluate maternal secretor status as a possible explanation for these results and to also examine the role of HBGA phenotypes on the efficacy of NoV vaccine candidates.

1.5.2 Gut Microbiota

The diversity of the gut microbiota is highly variable and unstable during early life until reaching an adult-like composition (by age 2-3 years), which subsequently decline with ageing (86). Significant differences in the composition of microbiota have been observed between industrialized or high-income countries and those with lower incomes, which in turn correlates with reduced vaccines immunogenicity (74). Most differences in the gut microbiota between these populations seem to be determined by environmental factors and diet rather than genetics, and for example, associated with a less diverse microbiota in industrialized countries (86). In terms of oral vaccines performance, studies from Pakistan and Ghana have reported significant differences in the gut microbiota from RV1 responders and non-responders infants based on serological rotavirus-specific IgA response, where responders shared common microbiota signatures with healthy Dutch infants (RV1-associated conversion rates are >90% in infants from Northern Europe) (87, 88).

1.5.3 Pre-existing immunity

The baseline immune status of an individual prior to vaccination can shape the way they respond to a vaccine. This status is better known as pre-existing immunity, which is commonly associated to the baseline presence of antigen-specific antibodies due to maternal–foetal transmission, natural infection, or vaccination. As appropriate levels of protection against severe disease following subsequent natural infection have been associated with the baseline presence of specific antibodies to NoV and rotavirus (69, 89, 90), pre-existing humoral immunity appears as a main factor associated with vaccines underperformance in low-and middle-income settings, where high NoV and Rotavirus infection rates are present (53). Thus, while the presence of pre-existing antibodies can diminish the infectivity of rotaviruses and NoV, it may also interfere with the normal uptake and presentation pathways to oral vaccines. For example, high titres of rotavirus neutralizing antibodies (predominantly IgA) have been observed in breast milk from mothers in low-income countries (91). These virus-specific antibodies found in breast milk have the capacity to neutralize rotavirus vaccine strains and may affect the vaccine immunogenicity in infants (91, 92). Additionally, passively acquired serum IgG antibodies have also been associated with a reduction in the immunogenicity of OPV and oral rotavirus vaccines, such as Rotarix (53, 93). Similar outcomes have been documented in early natural infections, i.e., when pathogen exposure precedes the host vaccination phase (53, 92). Thus, a prior exposure to a pathogen may induce either a local IgA response or systemic specific immunity with a subsequent impairment of oral vaccine immunogenicity (53). Global Rotarix vaccination schedule has been applied in two-doses, 4 weeks apart, starting at 8-weeks (2 months) and 12-to-16-weeks (3-4 months) respectively. A relevant factor considering that human rotavirus infection frequently occurs during the first 3 months of life in developing countries (44). Although the precise mechanisms of interference remain uncertain, overall, these factors may be also relevant for VLP-based vaccine investigations, as inactivated antigens could be masked by host pre-existing immunity (94) and the presence of pre-existing anti-VLP antibodies may decrease the efficacy of some VLP vaccines (95). A recent study using sequential immunizations with multiple NoV VLP candidate vaccine, suggest that such interference may be given by the *original antigenic sin*, where the immune response to a priming antigen/vaccine (first exposure) shapes/interfere with the immunity of a closely related booster antigen (96).

1.6 HYPOTHESIS

Using an *ex vivo* mucosal cell culture model with human tonsillar tissues (NALT), this project will focus on the evaluation of immunogenicity of enteric vaccines: 1) a live-attenuated oral rotavirus vaccine (RV1) and 2) a VLP-based GII.4 norovirus potential vaccine candidate, to comprehend the immunological mechanism associated with mucosal vaccine-mediated protection. Specifically, this project aimed to study the capacity and functional properties of T cells or B cell-mediated antibodies induced by enteric vaccines and will examine the potential effect of host pre-existing immunity on vaccine-induced immune responses.

1.7 THESIS AIMS

Main Aim

To evaluate the immunogenicity of an oral live-attenuated rotavirus vaccine, Rotarix®, and a novel virus like-particle-based norovirus vaccine, *ex vivo* using tonsillar tissues (NALT) from children and adults and examine the relationship between pre-existing immunity and vaccine-induced T and B cells responses.

Specific Aims

1. To characterize the pre-existing immunity against rotavirus and NoV in children and adults. Virus-specific antibodies (IgG and IgA) will be analysed in serum samples by ELISA.
2. To evaluate the immunogenicity of Rotarix and NoV vaccine candidate *ex vivo* using tonsillar mononuclear cell cultures from children and adult.
3. To determine the relationship between the pre-existing natural immunity and enteric vaccine-induced mucosal immune response.

CHAPTER II

Material and Methods

CHAPTER II

Material and Methods

2.1 Study subjects

Ninety-four immunocompetent children (1.5-16 years) and adults (17-45 years) referred to adenotonsillectomy due to upper-airway obstructions or tonsillitis were included in this study. All subjects were recruited at Alder Hey Children's Hospital and Aintree University Hospital, Liverpool, UK. Patients who received immunosuppressant treatment, or with any known immunodeficiency were excluded from the study. The study was ethically approved by the National Research Ethics Committee (REC No: 14/SS/1058), and written informed consents were obtained from all subjects or their legal guardians.

2.2 Samples

2.2.1 Adenotonsillar tissues

Human tonsillar tissue samples were collected following the patient´s adenotonsillectomy. Fresh tonsillar tissues were stored in Hank's Balanced Salt Solution (HBSS) (Sigma Aldrich, UK) supplemented with 100 U/ml penicillin, 100 µg/ml streptomycin and 1% L-glutamine (all Sigma Aldrich, UK) and delivered to the Department of Clinical Infection, Microbiology, and Immunology at University of Liverpool for processing. Grossly inflamed tonsillar tissues were excluded from the study.

2.2.2 Peripheral Blood and Serum

Venous blood was collected from recruited patients undergoing adenotonsillectomy as mentioned above. Between 1-10 mL of blood were collected into a 25-ml universal tube containing 100 µl of heparin (LEO Pharma, UK). Whole blood was centrifuged at 400 x g for 10 min to collect serum samples which were then kept at -80°C until assay.

2.3 Vaccines and Viral Antigens

2.3.1 Live Attenuated Oral Rotavirus Vaccine

A live-attenuated oral vaccine against Rotavirus (Rotarix®), was purchased from GSK.

Rotarix®, referred to as RV1, is an oral rotavirus vaccine derived from the human rotavirus RIX4414 strain (live-attenuated, G1P[8] type). The oral RV1 suspension (1.5 mL) contains approximately 10^6 Cell Culture Infective Dose (CCID50) of live, attenuated rotavirus.

2.3.2 Inactivated rotavirus antigens

Rotavirus grade 3 antigens (Microbix Biosystems) consist of inactivated Group A rotavirus-derived antigens (SA-11-strain) partially purified from infected MA104 cell culture. Simian S11A rotavirus is a readily obtainable prototype group A rotavirus strain widely used for serological detection of rotavirus-specific human antibodies (97). This commercial antigen preparation derives from whole inactivated SA11 rotavirus particles, assuring a wide range of antigenic epitopes available and therefore used as coating antigen for measurement of rotavirus-specific human antibodies by ELISA (e.g., as surrogate for the evaluation of heterotypic response and/or pre-existing immunity to rotavirus).

2.3.3 Live Attenuated Influenza Vaccine

FluMist® (season 2011-2012, NR-36465, BEI resources, USA) is a trivalent live attenuated influenza vaccine (LAIV), derived from a reassortant of A/California/07/2009 (H1N1) pdm09, A/Perth/16/2009 (H3N2) and B/Brisbane/60/2008 influenza viruses. Each 0.2 mL formulation contains $10^{6.5}$-$10^{7.5}$ fluorescent focus units (FFU) of each of the three virus strains.

2.3.4 Norovirus-derived Virus Like Particles

Human norovirus virus-like particles (VLP) were produced on *Spodoptera frugiperda* (Sf9) insect cells by using a recombinant GII-4 norovirus-strain baculovirus[2] (BAC-GII4v2) previously described by Allen et al (98). Sf9 cells were grown and maintained at 27°C with shaking in SF900-II Insect Cell Media (Gibco™, Thermo-Fisher) supplemented with 2% FBS plus 1% of Antibiotic-Antimycotic (penicillin, streptomycin, and Amphotericin B) (Gibco™, Thermo-Fisher). Cell culture suspension of Sf9 insect cells were infected at multiplicity of infection (MOI) of between 2-3 PFU/cell with the rNoV baculovirus (BAC-GII4v2) and incubated at 28°C for 48-72 hours. Intracellular-phase VLPs were

[2] The recombinant baculovirus for NoV VLP production, i.e., BAC-GII4v2, was kindly provided by Dr Daniel Kelly (The London School of Hygiene & Tropical Medicine, London) and previously generated by Dr Allen´s method after cloning the major and minor structural proteins, VP1 and VP2, respectively, from a NoV positive clinical sample (GII-4 Sydney-2012 strain) into a bacmid expression system (98).

purified by sequential centrifugation and concentrated using 15%-60% sucrose gradient ultracentrifugation (Fig. 2.1). Purified fractions were analysed by sodium dodecyl sulphate (SDS)-12% polyacrylamide gel electrophoresis (PAGE) (NuPAGE kit, Invitrogen) according to manufacturer's instructions. Presence of the capsid protein was observed at 58KDa molecular weight (See **Appendix A**, Fig. A1). The protein concentration of the VLP preparation was measured using the Qubit Protein Assay Kit (Fisher Scientific, Leicestershire, UK). Purified human norovirus VLP, referred to as NoV1, were used and evaluated as a novel VLP-based vaccine candidate (Fig. 2.1).

2.4 Adjuvant: α-Galactosylceramide

α-Galactosylceramide (Adipogen, Caltag Medsystems Ltd, UK) was solubilized in DMSO following manufacturer's instructions. Briefly, α-GalCer was dissolved at 1mg/ml by heating at 80°C and sonicated for 2 h until completely dissolved. Stock solution was stored at -20°C until use and further diluted in 1X PBS at a desired concentration for mice and human tonsillar cell stimulation assays.

2.5 Antibodies

Antibody standards and enzyme-conjugated secondary antibodies used for enzyme-linked immunosorbent assays (ELISA) were obtained from SIGMA (Sigma Aldrich, UK), and will be detailed in each result chapter accordingly.

2.6 Tissue sample processing and cell isolation

Human palatine tonsils were washed with Hank's balanced salt solution (HBSS) upon arrival to remove any debris and contaminated blood and stored at 2-8°C until being processed. Tonsillar mononuclear cells (MNCs) were freshly isolated according to a previously described method (99). Briefly, tonsils were minced in HBSS with a sterile scalpel and filtered through a 70-μm cell strainer (Fisherbrand, Fisher Scientific UK) to collect cell suspension. MNCs were isolated by density gradient centrifugation at 400 x g for 30 mins using Ficoll-Paque Premium (Cytiva, UK). Tonsillar MNCs were collected and washed with Dulbecco's Phosphate-Buffered Saline (DPBS, 1X) (Gibco, Thermo Fisher Scientific UK) and finally resuspended in RPMI 1640 (Gibco, Thermo Fisher Scientific UK) supplemented with 10% heat-inactivated fetal bovine serum (FBS) (Sigma-Aldrich), 2 mmol/L L-Glutamine, 100 U/mL

penicillin and 100 U/mL streptomycin (Thermo Fisher Scientific, UK), and referred to as supplemented RPMI. Cells were counted using a haemocytometer and kept at a concentration of 4 x 10^6 cells/mL in supplemented RPMI until use.

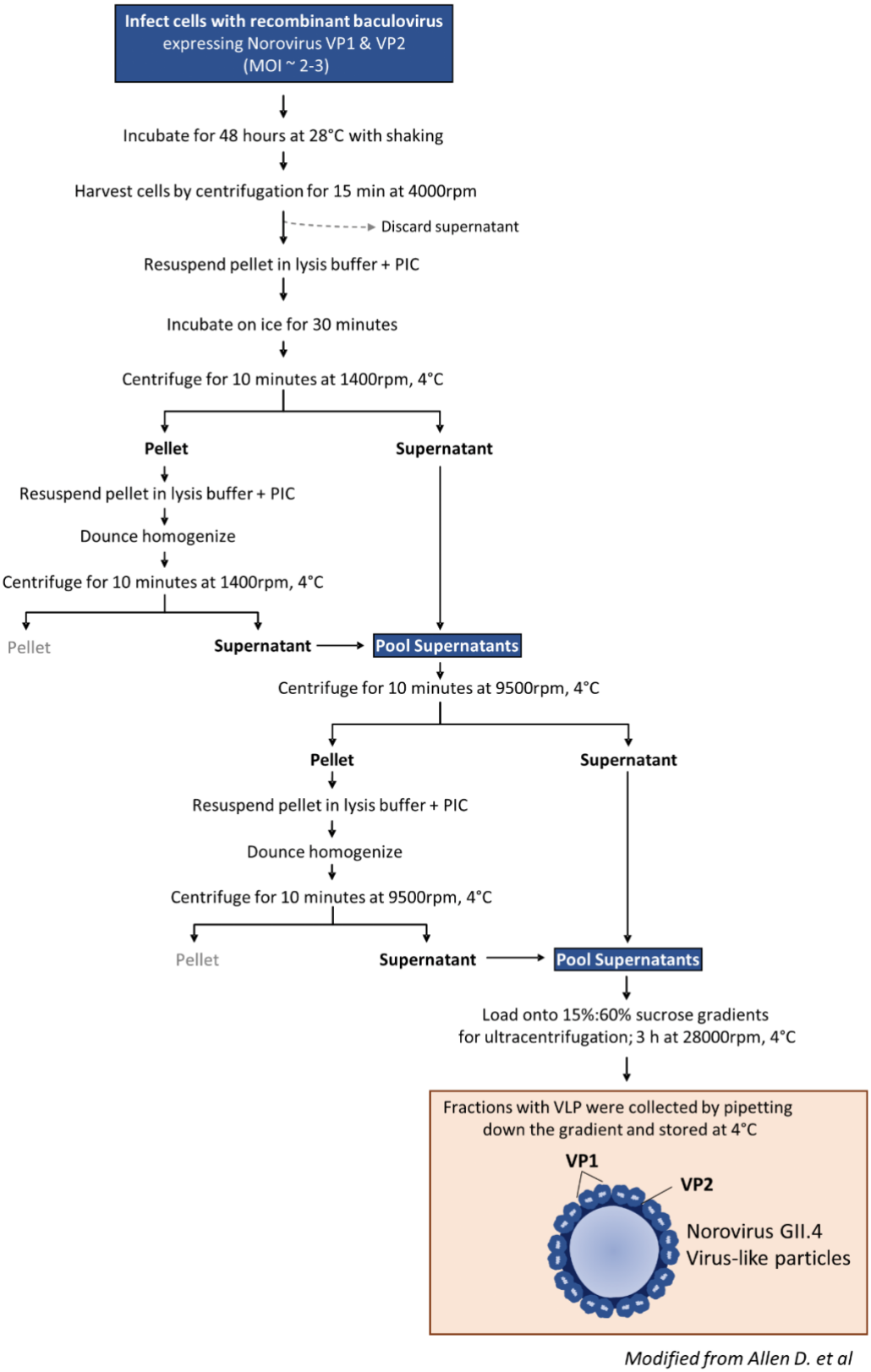

Figure 2.1. Norovirus virus like particles purification.

2.7 Magnetic cell separation

In some experiments, $CD45RO^+$ cells (memory and activated T cells) were depleted from tonsillar MNC in order to analyse naïve T cell response. Tonsillar MNCs were depleted of $CD45RO^+$ cells by using beads-based magnetic-activated cell separation (MACS) (Miltenyi Biotec, Germany) according to manufacturer´s instructions. Briefly, tonsillar MNCs ($5 \times 10^7 - 1 \times 10^8$ cells) were washed once with 1X DPBS (Gibco, Thermo Fisher Scientific UK) and resuspended in MACS buffer (0.5% BSA in 1X DPBS). Cells were incubated with CD45RO Microbeads (magnetic labelled anti-human CD45RO antibodies) for 15 min at 4°C. Cell suspension was washed with 5 mL of MACS buffer and centrifuged at 400 x g for 5 minutes. Cells were resuspended in 0.5 mL of MACS buffer and passed through an LS-column placed previously on a magnetic separator. Microbead-labelled cells ($CD45RO^+$ memory T cells) were magnetically retained in the LS-column, and $CD45RO^+$-depleted cells ($CD45RO^-$ MNCs) were eluted twice with 1 mL of MACS buffer and collected immediately into a new sterile universal tube. Finally, cells were centrifuged at 400 x g for 5 minutes and resuspended in supplemented RPMI until use as described before. Purity of $CD45RO^+$-depleted cells ($CD45RO^-$ MNC) (>99%) was confirmed by Flow cytometry (See **Appendix B**, Fig. B1).

2.8 Carboxyfluorescein succinimidyl ester (CFSE)

To monitor Human NALT T cell proliferation following vaccine stimulation, tonsillar MNCs (and $CD45RO^+$-depleted cells) were labelled with Carboxyfluorescein succinimidyl ester (CFSE) (CellTrace CFSE Cell Proliferation Kit, Thermo Scientific, UK). Briefly, tonsillar MNC ($5 \times 10^7 - 1 \times 10^8$ cells) were washed with 1X DPBS and centrifuged at 400 x g for 5 minutes. Cells were resuspended in 2 mL of 1X DPBS. A 1:4000 dilution from the 5mM CFSE stock was made by previously making a 2000-fold dilution in 1X DPBS and then adding 2 mL from this working stock to the resuspended cells (i.e., a final concentration of 1,25 μM of CFSE was used). Cells were mixed thoroughly and incubated at 37°C in 5% CO_2 for 8 minutes. CFSE staining was stopped by washing the cells with ice cold supplemented RPMI. Labelled cells were centrifuged at 400 x g for 5 minutes and resuspended in supplemented RPMI. Cells were counted using a haemocytometer and reconstituted at a concentration of 4×10^6 cells/mL in supplemented RPMI until use.

2.9 Flow cytometry

2.9.1 Cell surface and intracellular staining

Multicolour antibody panels were designed and used to evaluate tonsillar cell phenotypes and functionality by flow cytometry (FACS). Fluorochrome-conjugated monoclonal antibodies used for flow cytometry were purchased from Biolegend (UK). To stain human NALT cells for FACS analysis, tonsillar MNCs were harvested after individual vaccine stimulation. Briefly, cells were transferred to 1.5-mL microtubes, and washed with 1 mL of FACS staining buffer (0.2% BSA in 1X PBS) followed by centrifugation at 500 x g for 5 minutes. Cells were later resuspended with 50 µl of fluorochrome-conjugated antibody mix designed for cell surface markers (e.g., CD4, CD3, CD8) and incubated at 4°C for 30 minutes. For T cells analyses, tonsillar MNCs were stained with Pacific Blue or PE/Cy7 anti-human CD3 (clone HIT3a; Biolegend), PerCP/Cy5.5 anti-human CD8a (clone HIT8a; Biolegend) and APC/Cy7 or APC/Fire 750 anti-Human CD4 (clone RPAT4; Biolegend). Additionally, cells were stained with FITC anti-human CD49d (clone 9F1; Biolegend) and APC anti-human/mouse Integrin β7 (clone FIB504; Biolegend) for the analysis of gut homing $\alpha4^{+}\beta7^{+}$ tonsillar T cells. Stained cells were then washed by adding 1 mL of FACS buffer and centrifuged at 500 x g for 5 minutes. Cells were carefully resuspended in 300-500 µl of FACS buffer and analysed immediately by Flow cytometry. In case of intracellular staining (e.g., cytokines) was needed, surface-stained cells were resuspended in 200 µl of intracellular fixation buffer (eBioscience, UK) and incubated in the dark at room temperature for 30 min after mixing well by pipetting. Fixative solution was later washed out by adding 1 mL of 1X permeabilization buffer (eBioscience, UK) into the cells and centrifuging at 700 x g for 5 min. Last step was repeated by adding 1 mL of 1X permeabilization buffer. Permeabilized cells were resuspended with 30 µl of fluorochrome-conjugated antibodies mix for any intracellular cytokine (e.g., IFN-γ) and incubated in the dark for 30 minutes. Cells were washed by adding 1 mL of 1X permeabilization buffer and centrifuged at 1000 x g for 5 min. Supernatant was discarded and cells were finally resuspended in 200 µl of FACS buffer. All labelled cells were kept in the fridge at 2-8°C and protected from light until measured by flow cytometry.

2.9.1.1 Calculation of antibody cocktail volume

The total volume (µl) of each antibody needed for staining each sample/vial of cells was previously optimized for the assay. Single volumes were multiplied accordingly by the total number of vials to stain based on a final mix volume of 50 µl per vial. For example, if we wish to prepare 50 µl (i.e., one vial of cells) of surface antibody cocktail for T cells, using 2 µl of anti-human CD4, CD8 and CD3 antibodies per vial, respectively, we will need to consider a total antibody cocktail volume of 6 µl, plus 44 µl of FACS buffer to complete the final 50ul antibody mix volume (Table 1). Additionally, to prepare the same mix for 5 sample vials, you will need to multiply each antibody volume by 5 (see Table 1).

2.9.2 Zombie LIVE/DEAD labelling

Dead cells from tonsillar MNC were discriminated by flow cytometry using the Zombie Aqua™ Fixable Viability Kit (Biolegend, UK). Zombie dyes are amine-reactive fluorescent dyes able to penetrate cells with compromised membranes (Fig. 2.2). Thus, dead cells incorporate this dye into their cytoplasm while live cells exclude it (or will be slightly stained on surface). Dead cells are significatively represented by a brighter population due to an increased number of labelled proteins (Fig. 2.3). Cells were labelled with Zombie Aqua™ along with the surface antibodies staining mix following the same protocol for surface marker staining as described previously. Harvested cells were washed with 1 mL of FACS staining buffer (0.2% BSA in 1X PBS) and centrifuged at 500 x g for 5 minutes. Zombie dye was previously reconstituted in 100 ul of DMSO according to manufacturer's instructions and stored in 5 ul aliquots at -20°C until use. Zombie dye was added in the antibody cocktail mix and used at 1:1000 dilution (see Table 1).

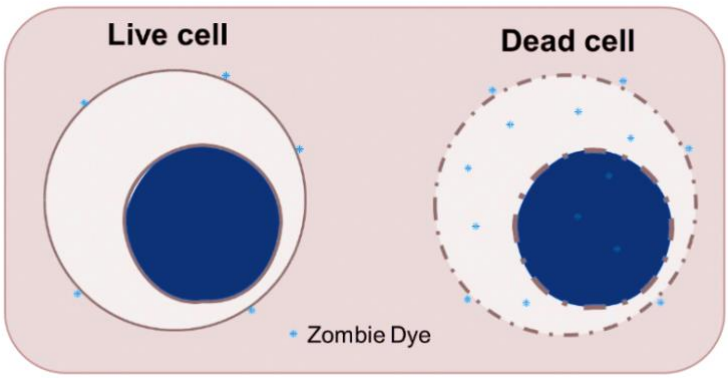

Figure 2.2. Zombie LIVE/DEAD labelling principle.

Table 1. Antibody cocktail volumes for flow cytometry staining.

Antibody Name	Volume per 1 vial	Volume per 5 vials
Anti-human CD3	2 µl	10 µl
Anti-human CD4	2 µl	10 µl
Anti-human CD8	2 µl	10 µl
FACS Buffer	44 µl	220 µl
TOTAL volume	50 µl	250 µl
Zombie Aqua™ dye	0.044 µl	0.22 µl

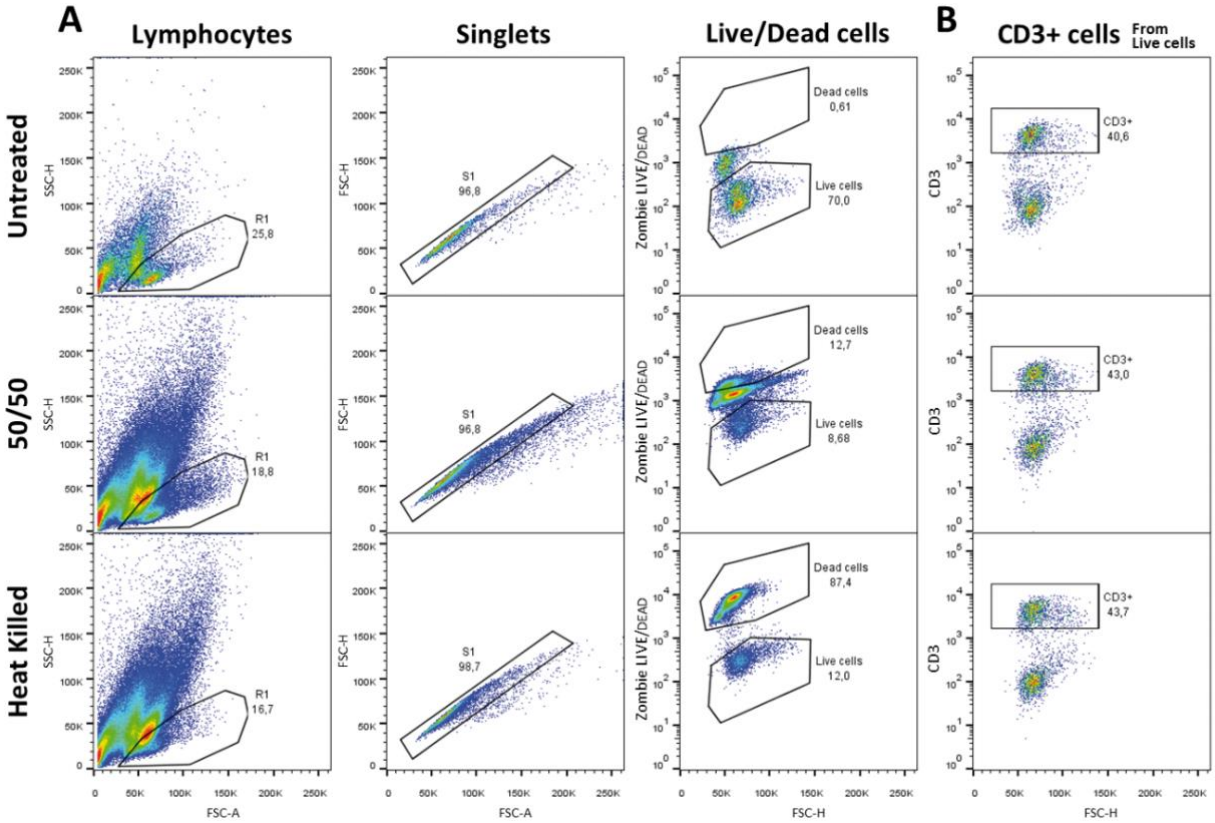

Figure 2.3. Cell viability analysis by Zombie LIVE/DEAD labelling. Human tonsillar MNCs were harvested 72 hours after processing and left untreated or heated at 56°C for 45 minutes for cell viability evaluation. A 1:1 mix of both controls (untreated and heat killed cells) were included as Live/dead control (50/50). Cells were stained with Zombie aqua LIVE/DEAD dye and PerCP-Cy7 anti-human CD3 antibody and analysed by flow cytometry. Representative dot plots show the percentage of both dead and live cells for (A) Total or (B) CD3+ tonsillar MNCs, respectively. Lymphocytes from whole tonsillar MNCs were gated based on cell size (FSC-H) and granularity (SSC-H), respectively. Doublets were excluded from the analysis by singlets selection.

2.9.3 Flow cytometry analysis

Fluorescence-labelled cells were measured immediately by flow cytometry. Briefly, cells were carefully transferred to a FACS tube (Corning, UK) and acquired using a BD FACS Canto II flow cytometer (BD Biosciences, USA). The number of recorded events was dependent upon each study. FACS data was analysed using FlowJo X v10.0.7 software. Cell population and gating strategies were specified in each result chapter Appendix.

2.10 Enzyme-linked Immunosorbent Assay (ELISA)

2.10.1 Measurement of IFN-γ concentration

Human tonsillar cell culture supernatants were collected at day 3 following vaccine stimulation (i.e., Rotarix or Norovirus VLPs) for the measurement of IFN-γ production by enzyme-linked immunosorbent assay (ELISA). Interferon-γ concentrations were determined using the Human IFN-γ Duo set ELISA kit (R&D Systems, USA) according to manufacturer´s instructions. Briefly, 96-well flat bottom plates (High binding, Corning™ Costar™, USA) were coated with 100 µl per well of 3 µg/ml Mouse Anti-Human IFN-γ capture antibody previously reconstituted in 1X PBS. Plates were sealed and incubated overnight at 4°C. Plates were then washed 3 times with 300 µl of washing buffer (0.05% Tween-20 in 1X PBS) and blocked with 200 µl/well of Reagent Diluent (2% BSA in 1X PBS) at room temperature for 60-90 min. For IFN-γ standard, a 10-fold dilution from the reconstituted recombinant Human IFN-γ Standard (190 ng/mL stock) was added in duplicates to the first wells followed by a 2-fold serial dilution. A 5-fold dilution was used for cell culture supernatants. Both standard and samples were diluted in Reagent diluent and used at 100 µl and 50 µl per well, respectively. Plate was incubated for 2 hours at room temperature and washed 3 times afterwards. A 100 µl of 1:60 diluted Biotinylated Mouse Anti-Human IFN-γ Detection Antibody was added to each well and incubated for another 2 hours at room temperature. Then, 100 µl of the working dilution of Streptavidin-HRP B was added to each well and incubated for 30 minutes at room temperature. Finally, 100 µl/well of TMB (SIGMA) were added and incubated for 10-20 min until colour development. The absorbance was read at 450nm after addition of 2N H_2SO_4 by using an ELISA plate reader (Thermo Scientific, UK).

2.10.2 Detection of virus-specific antibody production by tonsillar MNC

Supernatants from tonsillar MNC cultures were collected at day 7 and 14 post stimulation with Rotavirus or Norovirus vaccines and analysed for virus-specific antibody production by ELISA, respectively. Standardized protocols for each antibody response were specified in chapter IV. Antibody reference standards and enzyme-conjugated antibodies used for ELISA were obtained from SIGMA (Sigma Aldrich, UK), and will be detailed in each result chapter accordingly.

2.10.3 Detection of Norovirus-specific antibody production in mice

Norovirus-specific IgA and IgG levels from NoV1-immunized mice were quantified by ELISA. Procedure standardization for each antibody response with mouse experimental details were specified in chapter III. Immunoglobulin standards and enzyme-conjugated antibodies used for ELISA were obtained from SIGMA (Sigma Aldrich, UK), and will be detailed in each chapter accordingly.

2.11 Statistical analysis

All statistical analyses were performed using GraphPad Prism 9.0. Two groups difference were analysed using paired t-test. Fold change analyses against unstimulated control were included considering tonsillar MNCs inherent baseline response and/or activation due to continuous exposure to external antigens; Fold-changes analyses were made by two-way ANOVA multiple comparisons. Correlations between variables were analysed using Pearson´s correlation coefficient. Linear regressions (2nd order polynomial) were performed accordingly as a representative fit to express the relationship between data. $P<0.05$ was considered statistically significant.

CHAPTER III

Evaluation of norovirus-specific systemic and mucosal antibody response in mice following oral immunisation with norovirus VLP-based vaccine candidate

CHAPTER III

Evaluation of norovirus-specific systemic and mucosal antibody response in mice following oral immunisation with norovirus VLP-based vaccine candidate

Difficulties to culture noroviruses have been a major obstacle to study in dept the virus immunobiology and develop effective antiviral strategies. Although there is no licensed NoV vaccine available, pre-clinical and advanced clinical studies with parenteral non-live subunit vaccines candidates, mainly based on NoV virus-like particles (VLPs) have been developed (70, 71). The expression of NoV capsid protein VP1 leads to self-assembly of non-infectious, yet immunogenic, VLPs (100). These NoV capsid-based particles are morphologically and antigenically similar to native virions, and can be synthetized in large quantities, being a promising vaccine candidate for norovirus disease. Adjuvants have been also included in most VLP-based vaccine formulations, including several vaccine candidates for NoV infection (73, 77, 78). The use of adjuvants as immunomodulatory molecules improves vaccine safety and immunogenicity in subunit vaccines promoting a stronger response, especially among unexposed and/or low-responders individuals, such as infants (76). Based on these properties, we evaluated the immunogenicity of human norovirus VLPs by examining the systemic and mucosal antibody response in mice after repeated oral immunisation with norovirus GII-4 Sydney-2012 strain-derived VLPs (comprised of NoV viral capsid structural proteins VP1 and VP2; coined NoV1) as a potential vaccine candidate. Moreover, we evaluated the potential role of a-Galactosylceramide (α-GalCer) as mucosal adjuvant to promote a stronger VLP-induced immune response. These findings will work as a proof of concept for the evaluation of α-GalCer with viral antigens and their translation in human NALT model.

3.1 Immunization with NoV virus-like particles using adjuvant α-Galactosylceramide

An *in vivo* experiment, summarized in Figure 3.1, was performed to evaluate the immunogenicity of norovirus VLP and the role of α-Galactosylceramide (α-GalCer) as mucosal adjuvant in mice. This

experiment was performed by former laboratory members[3] as part of a collaboration from Professor Miren Iturriza-Gomara at Institute of Infection, Veterinary and Ecological Sciences (former institute of Infection and Global health, IGH), University of Liverpool. This chapter presents the results from analysis of the samples collected from the experiment described in Figure 3.1 which were processed and analysed as part of this thesis.

3.1.1 NoV1: Norovirus VLP-based vaccine candidate

Norovirus GII-4 strain virus like particles, comprised of norovirus viral capsid structural proteins VP1 and VP2, were produced on Sf9 insect cells infected with a recombinant baculovirus, BAC-GII4v2, as previously described by Allen et al. (98). Norovirus VLPs were purified by ultracentrifugation through a sucrose cushion as previously detailed in Materials and methods section in **Chapter II** (98). Purified norovirus VLPs were further evaluated as a novel VLP-based vaccine candidate, referred to as NoV1.

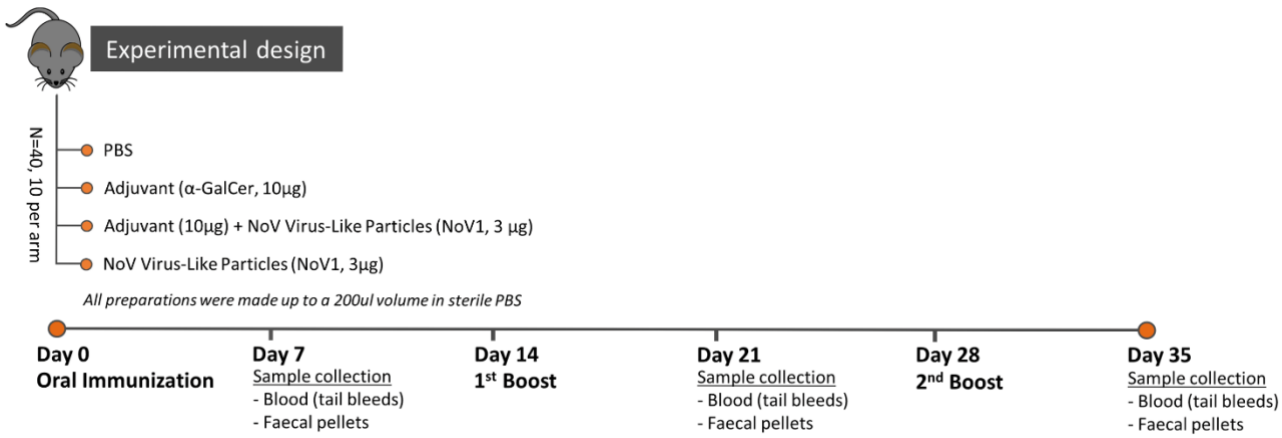

Figure 3.1. Mice oral immunization schedule for Norovirus VLP and α-GalCer evaluation. C57BL/6 mice (N=40, 10 per arm) were orally immunised with 3 ug of NoV VLP (NoV1) or in combination with 10µg of α-GalCer adjuvant. Control mice were given PBS or α-GalCer, respectively. Mice were distributed in two groups of 5 animals each per arm. A boost was applied at day 14 and 28 post immunization. Blood from tails was collected at days 7, 21 and 35 post immunization. Faecal pellets were pooled per cage at same intervals.

[3] Performed by Dr Stavros Panagiotou and Dr Daniel Kelly at The University of Liverpool

3.1.2 Oral immunization and sample collection.

Eight-weeks old, females, C57BL/6 mice (N=40, 10 per arm) were immunised by orally administering 3 μg of NoV1, in the presence or absence of 10 μg α-Galactosylceramide (α-GalCer) (Adipogen Life Sciences) as adjuvant. Additionally, same-dose boosts were applied at day 14 and 28 post-immunization, comprising a total 3-dose immunization regimen. All preparations were made up to 200μl volume in sterile 1X PBS (Thermo Fisher Scientific, UK). Control mice were given 1X PBS and 10 μg of α-GalCer, separately. Mice were distributed in 2 cages with 5 animal each, per treatment, respectively. Mice were closely monitored for the visual development of clinical signs of side-effects according to specific COSHH assessment standards by the Department of Clinical Infection Microbiology Immunology, University of Liverpool. Blood samples were collected by tail bleed at days 7, 21 and 35 post immunization. Stool pellets were collected and pooled per cage, i.e., five animals per treatment in duplicate, following the same time intervals (Fig. 3.1). Faecal samples were weighted and processed by making a 10% wt/vol suspension, depending on the weight of each sample, in sterile 1X PBS. Samples were centrifuged at 400g for 5 min and supernatants were collected for ELISA measurements. All samples were stored at 80°C until use for virus-specific antibody analyses.

3.2 Development and optimization of an in-house Enzyme-Linked Immunosorbent Assay for detection of norovirus-specific antibodies

An in-house indirect ELISA (Enzyme-Linked Immunosorbent Assay) for immunological quantification of norovirus-specific antibodies in mouse serum and stool samples was developed to evaluate the immunogenic performance of NoV1 and the adjuvant role of α-GalCer in mice. A standardised protocol was optimized for both IgG and IgA antibodies measurements using the above-mentioned purified norovirus virus-like particles, NoV1, as a coating antigen (Fig. 3.2).

3.2.1 Preparation of Norovirus VLP-coated microtiter plates

Ninety-six microtiter plates (High binding, Corning™ Costar™) were coated directly with 100 μl of 5 μg/mL NoV-VLP (0.5 μg per well). Assay coating conditions were previously chosen according to optimal signal/background ratio values from three different VLP coating concentrations (0.5, 1.0 and 2.0 μg/well) (Fig. 3.2. B). Virus-like particles were diluted in carbonate-bicarbonate buffer, pH 9.6

(Sigma-Aldrich). Plates were covered with adhesive seal and kept 48 hours at 4°C. Non-specific protein binding was blocked by adding 250 µl/well of 5% Skimmed milk in 1X PBS for 60 minutes at 37°C. Microtiter plates were kept in a humidity chamber through all assay incubations to minimize the liquid evaporation and cross contamination.

3.2.2 Preparation of IgG and IgA Standard

Purified mouse immunoglobulins were used as theorical norovirus-specific antibodies standard due to lack of specific mouse NoV-specific polyclonal antibodies available. A 100-fold or 20-fold dilution of purified mouse IgG (PMP01, BioRad) or mouse IgA (553476, BD Biosciences) were added directly to 96-microtiter plates, respectively, to prepare a standard curve in each experiment. Briefly, 2-fold serial dilutions were performed seven times in duplicate for IgG (starting concentration 10 µg/mL) or IgA (starting concentration 25 µg/mL) using carbonate-bicarbonate buffer, pH 9.6. Plates were incubated for 48 h at 4°C for immunoglobulins adsorption along with NoV-VLPs.

3.2.3 Norovirus-specific IgG and IgA detection in serum

Assay performance using NoV VLP-coated plates was evaluated by testing serum samples from mice immunized with NoV1 and α-GalCer adjuvant. The presence of NoV-specific antibodies was assessed from mouse sera collected at day 21 post immunization (i.e., 7 days after the first boost). Sera from PBS control group were also included to determine the assay specificity.

NoV VLP-precoated plates were washed 3 times with 300 µl of 1X PBS containing 0.05% Tween-20 (washing buffer). Plates were loaded with 50 µl of mice serum dilutions (50-fold for control sera, and 50- or 100-fold for the immunized groups), prepared in 1% Skimmed Milk/1X PBS (dilution Buffer), and incubated for 90 min at 37°C on a humidity chamber. Dilution buffer was used as a negative control. Plates were washed 3 times after sample incubation and 100 µl of horseradish peroxidase conjugated secondary antibody for IgG (goat anti-mouse IgG, sc-2005, Santa Cruz Biotechnology) or IgA (goat anti-mouse IgA, 1040-05, Southern Biotech) were added. Enzyme-conjugated secondary antibodies were used at 1:4000 or 1:1000 dilution for mouse IgG or IgA detection, respectively. Plates were incubated for 60 min at 37°C and washed again as mentioned above. Lastly, a 100 µl per well of supersensitive 3´3´5´5´-TMB peroxidase substrate (Sigma Aldrich, UK) was added, and plates were

incubated in darkness for 10-20 min. Absorbances readings were recorded 10 to 20 min after the stop solution (H_2SO_4, [2N]) addition at 450 nm by using a Multiskan Spectrum spectrophotometer (Thermo Fisher Scientific, UK). Quantitative analyses were performed using 4-Parameter Logistic (4PL) curve fitting by MyAssays software (MyAssays Limited, UK). Assay steps were summarized in **Figure 3.2**.

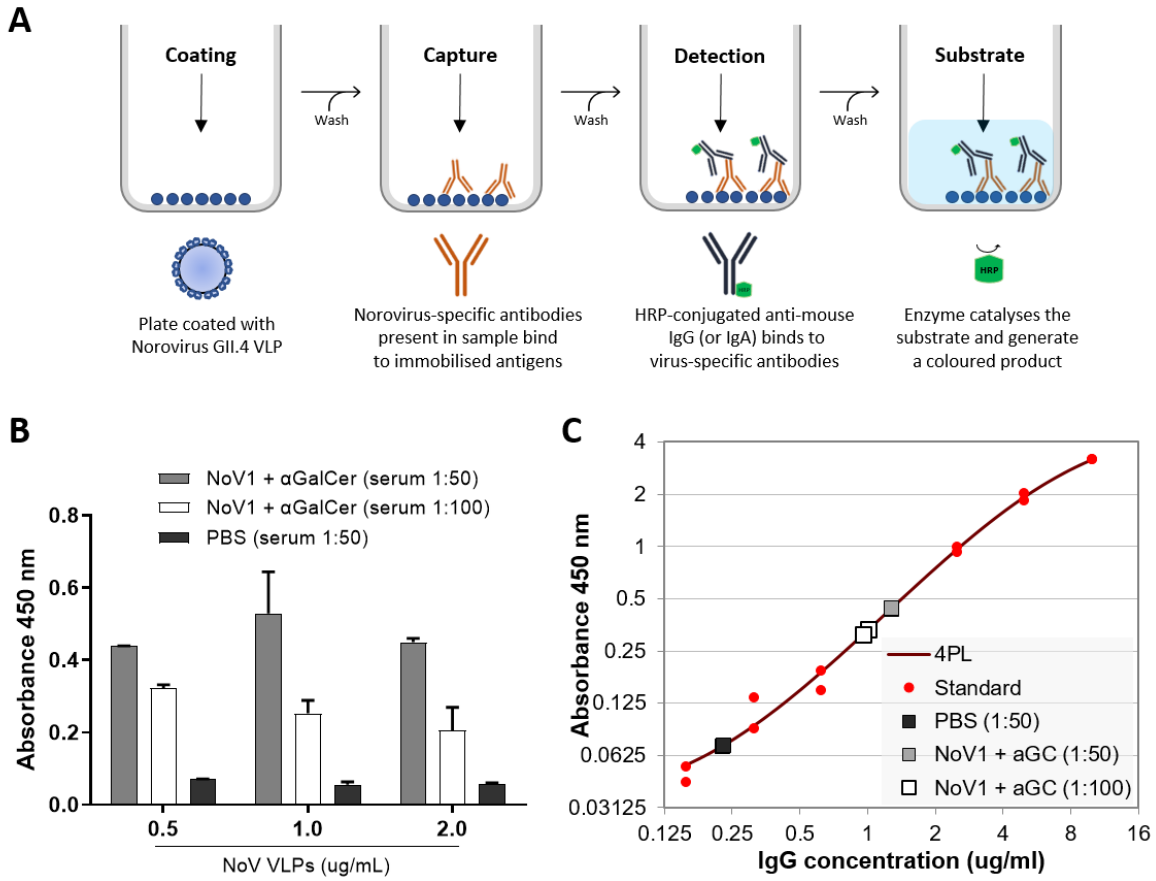

Figure 3.2. In-house ELISA for norovirus-specific antibodies detection. An indirect ELISA for detection of IgG or IgA antibodies against norovirus was developed using 96-well microtiter plates coated with GII.4 norovirus virus-like particles (NoV-VLPs) (A). Representative data from virus-specific serum IgG levels evaluated in C57BL/6 mice 21 days after immunization with NoV-VLP (NoV1) and α-GalCer adjuvant, or with PBS as negative control (B, C). Absorbances from sera dilutions (1:50 or 1:100) were recorded at 450 nm using different assay coating concentration (0.5, 1.0 and 2.0 µg/well) (B). A standard curve using purified mouse IgG (BioRad) was included. Data was quantified using a 4-parameter logistic (4PL, red line) curve regression by MyAssays software (C).

3.2.4 Norovirus IgG assay optimisation results

As shown in figure 3.2, a significative presence of norovirus-specific IgG antibodies was successfully detected from mice immune sera using ELISA test described above. Absorbance values were not altered by different VLP coating concentrations, suggesting an appropriate adsorption of NoV-VLP to the well surface (Fig. 3.2. B). No significant improvement in particles adsorption were observed using purified porcine gastric mucin type III (Sigma)[4] pre-treated microtiter plates (data not shown). Additionally, an optimal assay specificity was evidenced by low background absorbance values observed in PBS control groups (Fig. 3.2. B). No unspecific signal was detected using dilution buffer as negative control. Therefore, considering the assay performance and to minimize the consumption of a critical reagent, the lower VLP-coating concentration (0.5 μg/well) was chosen. Assay quantification using 0.5 μg/well of NoV-antigen coating for both VLP-stimulated and PBS control groups are described in **Figure 3.2**. As shown in figure 3.2 C, a symmetrical sigmoidal curve using four-parameter logistic regression (MyAssays) were observed after 20 min of HPR-substrate addition. A starting IgG concentration of 10 μg/mL was assigned using purified mouse IgG as a reference standard. Theoretical norovirus-specific IgG concentrations were interpolated from the standard curve based on standard curve absorbance values (Fig. 3.2. C).

3.3 Norovirus-specific systemic and mucosal antibody response after repeated oral immunization with α-GalCer and norovirus VLPs.

The immunogenicity of human norovirus-VLP based vaccine candidate, NoV1, and the adjuvanticity of α-GalCer, was evaluated in mice by examining both systemic and mucosal antibody response following a 3-dose immunization regimen, as previously described in **Figure 3.1**. Norovirus-specific IgA and IgG levels from mice immunization experiments were quantified using the in-house ELISA methodology as described above. Briefly, 96-well microtiter plates were coated with 0.5 μg/well of NoV VLPs in carbonate-bicarbonate buffer at 4°C. For IgG systemic response evaluation, plates were incubated with individual mouse serum dilutions (100-fold dilution for control sera and 100, 200 or

[4] Human NoV VLPs can bind to glycoproteins from animal gastric mucosa (e.g., purified porcine gastric mucin type III) through the carbohydrate moieties (101).

400-fold sera dilution for immunized groups). A 40-fold dilution of mouse sera was used in parallel for IgA detection in all experimental groups. Additionally, detection of NoV-specific IgA in stool pellets was performed following the same assay conditions. Stool pellets were previously weighted by group and homogenized in 1X PBS to a final 10% w/v solution. Stool samples were finally added in duplicate following a 2-fold dilution series pattern from 1:5 to 1:40 per well. Norovirus-specific antibody detection was done using HRP conjugated anti-mouse IgA or anti mouse IgG antibodies and supersensitive TMB as a chromogen. Assay quantification was performed against 2-fold serial dilutions of commercial immunoglobulin standard for mouse IgG (starting at 10 μg/ml) or IgA (starting at 25 μg/ml), respectively. Data analysis was performed using four parameter logistic regression curves by MyAssays software. Assay cut-off threshold for positive readings was defined as the average absorbance from PBS-treated control group (negative control) plus 3 times the standard deviation (SD) of same control group absorbances: All ELISA measurements were performed in duplicate.

$$Assay\ Cutoff = Average\ (OD\ Values\ of\ PBS\ control) + 3 \times SD(OD\ Values\ of\ PBS\ control)$$

The presence of norovirus-specific antibody levels in serum and stool samples were calculated using the average of two positive readings, i.e., values over the assay cut-off threshold and within the standard curve linear range.

3.3.1 NoV1 vaccination induces Norovirus-specific IgG and IgA levels

The immunogenicity of the norovirus VLP-based candidate vaccine, NoV1, was recorded from 2 cages of 5 animals each, per arm (N=40, 10 per arm) after orally delivered in the presence and absence of the adjuvant α-GalCer (detailed in **Figure 3.1).**

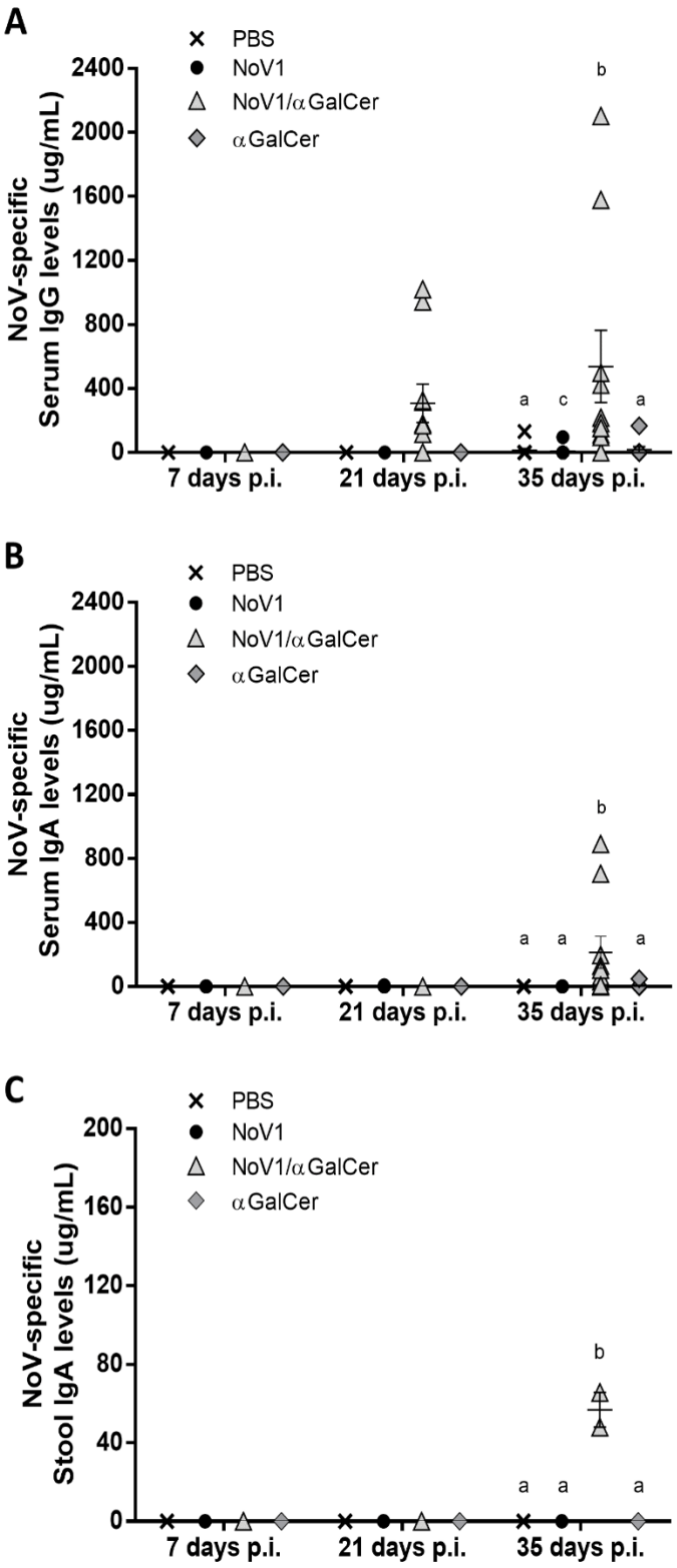

Figure. 3.3. Repeated oral immunization with Norovirus VLPs and α-GalCer adjuvant induces a robust norovirus-specific antibody response in mice. C57BL/6 mice (N=40, 10 per arm) were orally immunised with 3 μg of VLP-based norovirus vaccine candidate (NoV1) alone or in combination with 10 μg of α-GalCer adjuvant. Negative control groups were administered PBS or α-GalCer, respectively. Boost doses were applied 14 and 28 days after immunization. Serum norovirus-specific IgG (A) and IgA (B) antibodies were measured by ELISA at days 7, 21 and 35 post immunization (p.i.). The presence of virus-specific IgA antibodies in stool samples was evaluated at same time intervals (C). Data analysis was performed by four parameter logistic curve regression using MyAssays. Assay cut-off threshold for positive readings was defined as the mean OD value of PBS control group (X) + 3SD. Data were represented as mean + SEM. Stool pellets were pooled per cage (2 cages with 5 animals each per treatment arm). Statistical analysis was performed in GraphPad Prism by 2way ANOVA: n=10 per group, a, b: $p<0.0001$, b, c: $p = 0.0003$.

As shown in **Figure 3.3**. a robust NoV-specific antibody response was induced after the oral delivery of NoV1 vaccine in combination with α-GalCer adjuvant (NoV1/α-GalCer). A systemic IgG response was observed after the first and second vaccine boost, as evidenced in mice sera from day 21 and 35 post-oral immunization, respectively (Fig. 3.3. A). A cut-off threshold of 1 μg/mL was considered for positive readings, which was estimated as the mean plus 3 times the SD absorbance values from the PBS negative control group. Interestingly, the highest serum IgG production was reached 7 days after completed the 3-dose immunization regimen (35 days p.i.) exclusively using NoV1 in combination with α-GalCer (Fig. 3.3. A). No substantial serum NoV-IgG levels were observed after NoV1 administration alone. In addition, a significant production of NoV-specific IgA antibodies was detected in mice sera 35 days after VLP immunization in presence of α-GalCer adjuvant (Fig. 3.3. B). A cut-off threshold over 0.2 μg/mL was considered for positive serum NoV-IgA readings, as previously calculated from PBS control group absorbance values. Similarly, no significant serum NoV-IgA response was observed using NoV1 vaccine in absence of α-GalCer adjuvant.

Furthermore, a strong mucosal immune response was evidenced by the presence of NoV-specific IgA antibodies in stool samples from NoV1/α-GalCer immunized mice (Fig. 3.3. C). Concentration values over 3.125 μg/mL (cut-off threshold) were considered as positive for NoV-IgA readings in stool samples. Notably, mucosal NoV-specific IgA levels were only detected in mice stool after receiving the 3-dose immunization regimen with NoV1/α-GalCer (Fig. 3.3. C). No NoV-specific IgA was detected in stool using either NoV1 or α-GalCer adjuvant alone.

3.4 Conclusion

In this chapter, we successfully presented an in-house ELISA-based method for the detection and quantification of norovirus specific antibodies in serum and stool samples from mice. This method consisted of an indirect ELISA, with GII.4 NoV VLPs directly adsorbed on 96-well plates. Although polyclonal antibodies (102) or porcine gastric mucin (101) can be used to capture NoV VLPs to ELISA plates, other authors have suggested that when NoV VLPs are directly adsorbed to microtiter plates, conformational changes may occur exposing masked VLP epitopes for recognition (102). Nevertheless, no changes in OD signal were observed when plates were pre-treated with PGM type III before NoV

VLP coating following our experimental conditions. In fact, experimental settings such as coating temperature and blocking agents are crucial for a correct VLP adsorption (103).

We also evaluated both systemic and mucosal immune responses in mice after a repeated oral immunization with GII.4-SYD NoV-derived VLPs (NoV1). Notably from NoV1-immunized groups, only the ones adjuvanted with the sponge-derived sphingolipid and iNKT cell activator; α-GalCer, were able to develop a systemic and mucosal immune response after a 3-dose sequential oral immunization regimen, as shown by increased levels of NoV-specific serum IgG and IgA and stool NoV-specific IgA, respectively. Although other studies have described the mucosal adjuvanticity of α-GalCer when orally administered with whole-killed bacteria vaccines (34) (35), here we provided the first evidence on the role of α-GalCer as a mucosal adjuvant for virus-derived antigens and VLP delivery. Interestingly, a lack of immune response was observed following the first and second dose of NoV1 alone. This result contrast with other studies where high serum levels of NoV-specific antibodies has been obtained after one dose of GII.4 NoV VLPs (10 μg; via intramuscular, intradermal or intranasal delivery) (104-106), highlighting the immunogenicity of NoV VLP per se. Although VLP parental administration was unable to induce mucosal responses (106), these studies might suggest a dose-response re-evaluation including both higher and lower NoV1 dose for future experiments. Importantly, as presented in this chapter, the high immunogenic response for NoV1 in combination with α-GalCer support a dose sparing effect and evidenced both the role of α-GalCer as a mucosal adjuvant and the use of human norovirus-derived VLP as orally delivered immunogens. Although similar results have been reported for IM delivery of GII.4 NoV VLPs co-administered with Al(OH)3 or MPLA adjuvants, no mucosal IgA antibodies were detected, indicating that mucosal delivery of NoV VLPs is needed for induction of strong mucosal responses (106). Thus, our findings support the potential for a mucosal delivery of a non-replicating NoV VLP, for a human Norovirus vaccination. Moreover, this chapter provides an important proof of concept for the use of α-GalCer with particulate viral antigens (e.g., NoV-VLPs) and for subsequent NoV1 translation into our human NALT model, using human tonsillar tissues as a key mucosal compartment mediating mucosal immunity. These results will be presented accordingly in Chapter V and VI and will contribute to our understanding of the mucosal immune response against human NoV.

CHAPTER IV

Serological Evaluation of Pre-Existing Immunity to Rotavirus and Norovirus in Humans by Enzyme-linked Immunosorbent Assay (ELISA)

CHAPTER IV

Serological Evaluation of Pre-Existing Immunity to Rotavirus and Norovirus in Humans by Enzyme-linked Immunosorbent Assay (ELISA)

4.1 PART I: Optimisation of Enzyme-linked Immunosorbent Assays (ELISA) for Rotavirus-and Norovirus-specific antibody detection in Human samples

ELISA is a widely used method for laboratory diagnosis of enteric viruses, such as rotavirus and norovirus. This technique provides a quantitative tool to identify the status of infection and to evaluate the immune response of a subject. The presence of virus antigens and virus-specific antibodies can be found in mucosal secretions like saliva or stool, or systemically in serum samples. Additionally, ELISA can be extrapolated for vaccine studies in *ex vivo* cell culture systems by analysing correlates of protection for a particular infection or disease in cell culture supernatants. In order to characterise the pre-existing levels and production of rotavirus and norovirus-specific antibodies in human samples and evaluate the antibody response to enteric vaccines, described in Chapter VI, we first developed and optimized different ELISA protocols, which will be presented accordingly on this Chapter.

4.1.1 ELISA optimization for detection of rotavirus-specific human antibodies

4.1.1.1 Detection of rotavirus-specific human IgG by ELISA

Serum levels of rotavirus-specific immunoglobulin G (IgG) were evaluated by ELISA. An indirect ELISA protocol was performed and optimized by evaluating different concentrations of coating antigen. Ninety-six well microtiter plates (High binding, Corning™ Costar™) were coated overnight at 4°C with either 10, 50 or 100-fold dilution of rotavirus antigens[5] (Microbix Biosystems). Plates were washed five times with 300 µl of washing buffer (0.05% Tween-20 in 1X PBS) using a microplate washing machine and blocked for 60 minutes with 10% FBS in 1X PBS (Blocking buffer).

Rotavirus IgG antibodies in huma serum were estimated by reference to a standard curve (107). A 50 mg IgG/mL solution of human intravenous immunoglobulin (IVIg) (Intratect, Biotest Pharma, UK) was

[5] Group A rotavirus-antigens purified from Simian rotavirus SA11-infected MA104 cell culture supernatants.

used as an IgG reference standard. IVIg is a human normal immunoglobin solution prepared from pooled plasma of ≥ 1000 human donors and contains a broad spectrum of natural IgG subclasses against several infectious agents. The presence of anti-rotavirus antibodies in commercially available immunoglobulin preparations has been described previously by others (107, 108). Therefore, given the high prevalence of rotavirus during childhood and recurrent exposures throughout life, and due to unavailability of specific standard reagent, IVIg was considered a suitable assay reference standard. Briefly, 100 µl per well of IVIg at a standard dilution of 1:200 was incorporated in duplicate and diluted serially by 2-fold using blocking buffer. Blocking buffer was also used as a negative control. Plates were incubated at room temperature with 200 rpm agitation for 90 min and then washed five times with 300 µl of washing buffer. Rotavirus-specific IgG levels were detected using 50 µl of 1:2000 mouse monoclonal anti-human IgG-Alkaline Phosphatase conjugated antibody (Sigma Aldrich, UK) and incubated for 90 minutes. Absorbances were recorded at 405nm from 30 minutes after p-Nitrophenyl Phosphate (pNPP) (Sigma-Aldrich) substrate addition (see appendix C) by using the Multiskan Spectrum spectrophotometer (Thermo Fisher Scientific, UK). Quantitative analyses were performed using 4-Parameter Logistic (4PL) curve fitting by MyAssays online software (MyAssays Limited, UK).

Steps for indirect ELISA protocol were summarized in **Figure 4.1**. As shown in figure 4.1 B, symmetrical sigmoidal curves were observed after 30 min of pNPP substrate addition indicating the presence of rotavirus-specific IgG antibodies in the commercial human immunoglobulin preparation. Absorbance readings showed similar magnitudes for all three rotavirus-antigen dilutions used for plate coating (Fig. 4.1. B). The highest signal/background ratio was observed at 100-fold of rotavirus antigen dilution and considered for all assays.

Although a 200-fold dilution of IVIg stock was preliminary defined as 250 Units of rotavirus-specific IgG antibodies per mL of serum, an indirect ELISA for total IgG was performed in parallel to estimate the absolute amount of rotavirus-specific IgG antibodies present in the IVIg reference standard. Serial dilutions of the IVIg stock solution (50 mg/mL) were prepared in duplicate on a 96-well microtiter plate (High binding, Corning™ Costar™) with or without rotavirus antigen coating (Fig. 4.1. C). Doubling

dilutions of IVIg starting from 1:2000 (i.e., 25µg IgG per ml) were used for total IgG detection; and 1:400 (i.e., 125 rotavirus-specific IgG U/ml) for rotavirus IgG detection, respectively.

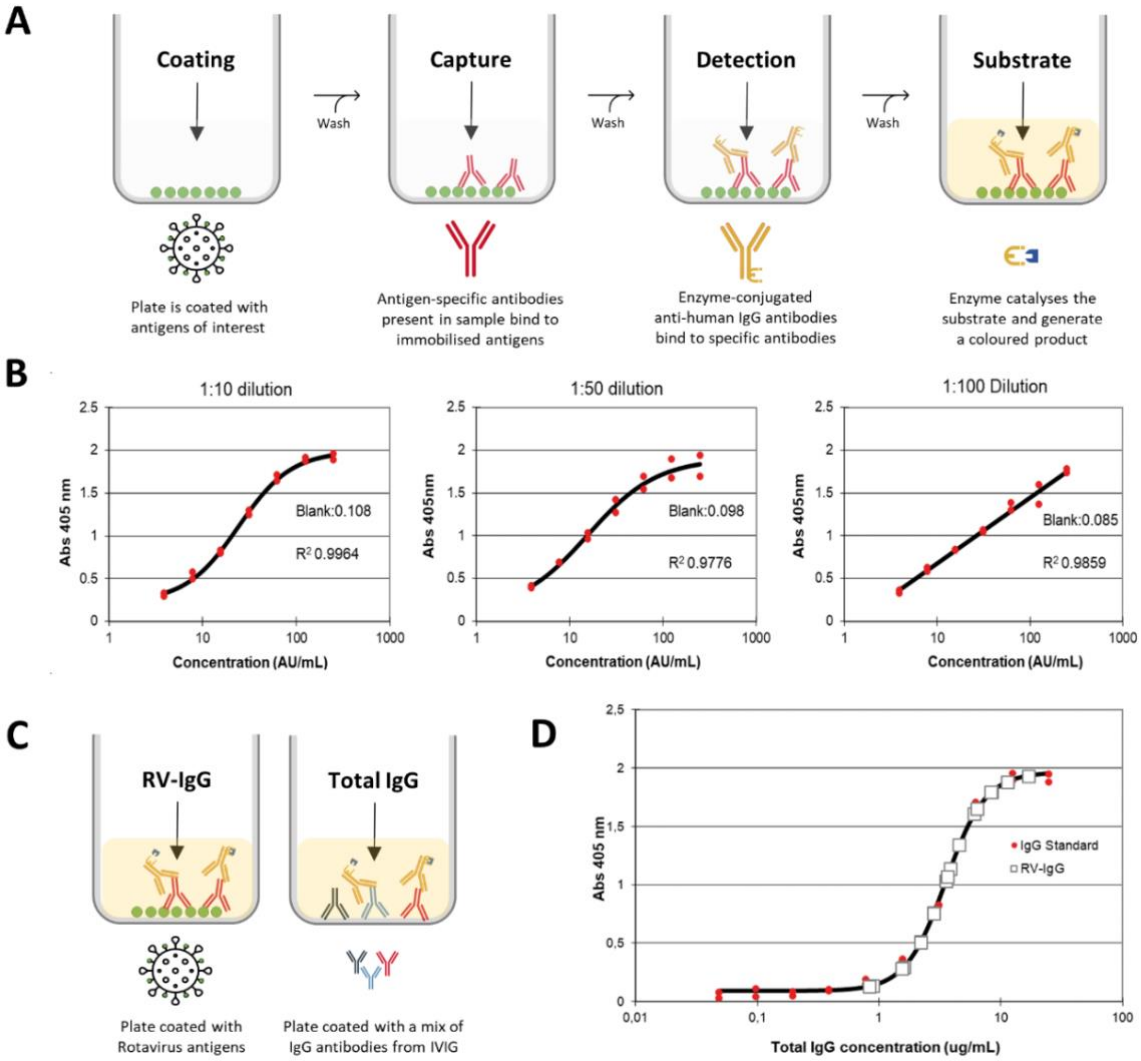

Figure 4.1. Detection of rotavirus-specific IgG in human plasma solution by ELISA. An indirect ELISA for rotavirus-specific IgG detection in human intravenous immunoglobulin (IVIg) solution was assessed (A). Absorbances were measured at 405nm after 60 min from substrate addition. (B) Representative curves for rotavirus-specific antibodies in human IVIg solution for 10, 50 and 100-fold dilutions of rotavirus-antigen coating. (C) Total IgG levels in IVIg were also measured by ELISA. (D) Two-fold serial dilutions of IVIg for total (red circles) and virus-specific (white squares) IgG detection were used, respectively. Quantitative analyses of rotavirus-specific antibodies using four-parameter-logistic (4PL) curve fit were performed by MyAssays software.

ELISA was performed following the same steps as described above. Absorbance readings were collected 60 minutes after pNPP substrate addition to obtain a well-defined saturation curve (Fig. 4.1). For rotavirus-specific IgG measurements, IVIg serial dilutions were analysed as unknown samples and

OD values were converted into the equivalent antibody IgG concentration by reference to the IVIg standard curve, i.e., by extrapolating the antibodies amount from the linear range of the total IgG standard curve (Fig. 4.1. D). An approximated concentration of 6.6 mg/mL of RV-specific IgG antibodies was observed in the 50 mg/mL IVIg standard solution and used as a reference amount for calculation of virus-specific IgG concentrations in the following experiments, with a starting dilution of 1:400 for standard curve preparation. Additionally, a 400-fold dilution for human serum samples, and a 1:10 dilution for cell culture supernatants from tonsillar MNCs, were the most suitable for rotavirus-IgG ELISA detection (data not shown) and used for all the assays (**Table 2**).

4.1.1.2 Detection of rotavirus-specific human IgA by ELISA

Primary and secondary infections caused by rotavirus can promote the production of immunoglobulin A (IgA) in serum, saliva and primarily in the small intestine mucosa (109). Following similar conditions as previously described for human IgG evaluation, we designed an indirect ELISA protocol to detect the presence of rotavirus-specific IgA in human samples by using a solution of purified human IgA from human colostrum as a reference standard. Purified human IgA was purchased from Sigma-Aldrich as a commercial isolate from pooled normal human colostrum. A total protein concentration of 2.1 mg/mL from IgA stock was obtained after absorbance measurements at 280 nm according to manufacturer's instructions. Ninety-six well flat bottom plates (High binding, Corning™ Costar™) were coated overnight at 4°C with 100-fold dilution of rotavirus antigens (Group A rotavirus, Microbix Biosystems). In parallel, twelve two-fold serial dilutions of purified human IgA from human colostrum (Sigma-Aldrich) were included and adsorbed as a coating protein to directly quantify the total IgA levels (Fig. 4.2. A). Serial dilutions were made from 25-fold diluted purified human colostrum IgA stock (84 µg/mL total protein). Plates were washed three times with 300 µl of washing buffer (0.05% Tween-20 in 1X PBS) and blocked for 120 minutes with 10% FBS in 1X PBS (Blocking buffer). To evaluate the presence of rotavirus-specific IgA antibodies, a 1:3 dilution of purified human IgA from human colostrum (700 µg/mL total protein) was added in duplicate as an unknown sample and diluted serially by 2-fold (Fig. 4.2. A). Fifty-microliters from a pool of human serum samples were also included as a positive control. Same volumes of blocking buffer were added to all the remaining wells coated earlier

with human colostrum IgA. ELISA plates were incubated overnight at 4°C with 200 rpm agitation. Immunoglobulin A levels were detected by using 50 µl of 1:1000 mouse monoclonal anti-human IgA-Alkaline Phosphatase conjugated antibody (Sigma Aldrich, UK). Plates were incubated for 2 hrs at room temperature. Absorbance was frequently monitored after pNPP substrate addition and recorded at 405nm by using Multiskan Spectrum spectrophotometer (Thermo Fisher Scientific, UK). Quantitative analyses were performed by MyAssays software using a 4PL curve fitting. Rotavirus-specific IgA levels were calculated following the same methodology described above, by using the total IgA standard curve from human colostrum IgA as reference. As shown in figure 4.2. B, sigmoidal regression curves were observed for both total IgA and rotavirus-specific IgA assays after 120 minutes from substrate addition. Absorbance values from human colostrum IgA dilutions, i.e., unknown sample, evidenced the presence of rotavirus-specific IgA in commercially purified human colostrum (Fig. 4.2. B). OD values fitted within the linear range of the total IgA standard curve and were equivalent to a final concentration of 60 µg/mL of rotavirus-specific IgA from purified colostrum IgA solution (**Table 2).**

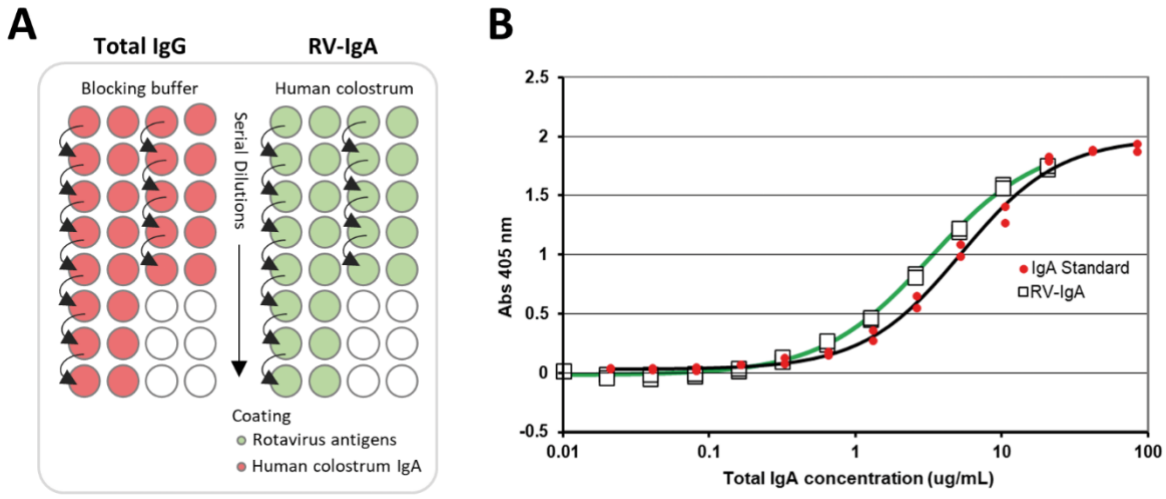

Figure. 4.2. Detection of total and rotavirus-specific IgA antibodies in human colostrum. The presence of rotavirus-specific IgA antibodies in a commercial purified human colostrum was assessed by ELISA using a Total IgA standard curve as reference. (A) Plates were coated overnight with purified human colostrum IgA (red) or with rotavirus-specific antigens (green), respectively. Two-fold serial dilution of purified IgA from human colostrum were added as unknown samples. (B) Representative four-parameter-logistic (4PL) curve fit for total IgA (black line) and rotavirus-specific IgA (green line) in purified human colostrum. Absorbances were measured at 405nm after 120 minutes from substrate addition. Quantitative analyses using 4PL curves were performed by MyAssays software.

4.1.2 ELISA optimization for detection of norovirus-specific human antibodies

As described previously in Chapter III, norovirus-specific antibodies in serum and stool samples from mice were successfully detected by ELISA using purified norovirus virus-like particles as a coating antigen. Norovirus VLP were generated from a positive clinical sample, GII-4 Sydney-2012 strain (GII.4-SYD), which mainly consist of major capsid protein VP1. Mapping studies have described B and T cell epitopes within VP1 domains, being relevant for potential vaccines evaluation (44, 110). Therefore, and based on the methodology used in mice, we assessed the capacity to detect and quantify norovirus-specific antibodies in human samples by ELISA, particularly from serum and tonsillar cell culture supernatants from recruited patients, by using passively adsorbed human norovirus-VLPs as coating proteins.

4.1.2.1 Detection of norovirus-specific human IgG by ELISA

The presence of norovirus-specific human IgG antibodies was evaluated by ELISA using IVIg (Intratect, Biotest Pharma) as a reference sample. An indirect ELISA protocol was performed and optimized for this approach, following a similar methodology described for the detection of rotavirus-specific antibodies in human samples. Ninety-six microtiter plates (High binding, Corning™ Costar™) were coated with 100 µl of 5 µg/mL norovirus-VLP (0.5 ug per well). Norovirus VLP were diluted in carbonate-bicarbonate buffer (Sigma-Aldrich). Coating concentration was determined from previous assays using mice samples (See Chapter III). As shown in **Figure 4.3**, plates were divided for both total and norovirus-specific IgG detection, respectively. Two-fold serial dilutions from IVIg solution, starting at 1:500 (100 µg/mL), were used as coating for total IgG detection (Fig. 4.3. B). Plates were adhesive sealed and incubated 48 hrs at 4°C. To prevent liquids evaporation, microtiter plates were kept in a humidity chamber during all incubations along this protocol. Plates were washed three times with 300 µl of washing buffer (0.05% TWEEN-20 in 1X PBS) and then blocked with 200 µl of 2% BSA (Sigma-Aldrich) in 1X PBS (VLP-blocking buffer) for 60 min at 37°C. Plates content were discarded before samples addition and gently blotted on an absorbent towel. For NoV-specific IgG measurement, 100 µl of 1:100 human IVIg solution were added at the top wells from the VLP-coated section and two-fold serial dilutions were prepared in duplicate. Additionally, 50 µl of 200-fold diluted human serum

samples from previous recruited patients, were included as unknown samples. Plates were incubated for 2 h at 37°C in a humidity chamber.

Due to low signal/background ratio observed in human tonsillar cell culture supernatants (data not shown), a biotin-streptavidin system was included in this methodology to increase the sensitivity of this assay and improve ELISA detection. (See summary in Fig. 4.3. A).

Plate contents were discarded, and wells were washed three times. Washing buffer remnants were gently blotted on an absorbent towel. Norovirus-specific IgG detection was performed using 1:4000 goat anti-Human IgG (γ-chain specific)-Biotinylated antibody (Sigma Aldrich, UK). Plates were incubated for 90 min at 37°C. Streptavidin-conjugated HRP (DY998, R&D systems, UK) was added later according to manufacturer's instructions after washing steps. A 1:40 dilution was made using VLP-blocking buffer. Plates were incubated for 60 min at 37°C. Finally, supersensitive TMB peroxidase substrate (Sigma Aldrich, UK) was added (100 µl/well) and incubated in darkness for 10-20 min. Absorbances were monitored over time at 650nm and recorded at 450nm after stop solution addition (H_2SO_4, [2N]).

As shown in Figure 4.3, a HRP saturation curve was obtained for total IgG measurements at 45 min after substrate addition. Absorbance values from norovirus-specific IgG levels in human IVIg dilutions fitted within the total IgG standard curve and evidenced the presence of virus-specific IgG in commercial purified human normal serum sample (IVIg) (Fig. 4.3. C). Extrapolated measurements by 4PL-curve analysis revealed a total concentration of 1.3 mg/mL NoV-specific IgG antibodies in purified IVIg solution. Two-fold serial dilutions of 1:1600 human IVIg solution were further used as a reference human NoV-IgG standard curve (see **Table 2**). Additionally, NoV-specific IgG antibodies were also detected in human serum samples from recruited children and adults' subjects (Fig. 4.3. C). The presence of pre-existing virus-specific antibodies in human serum samples will be detailed in Part II of this chapter.

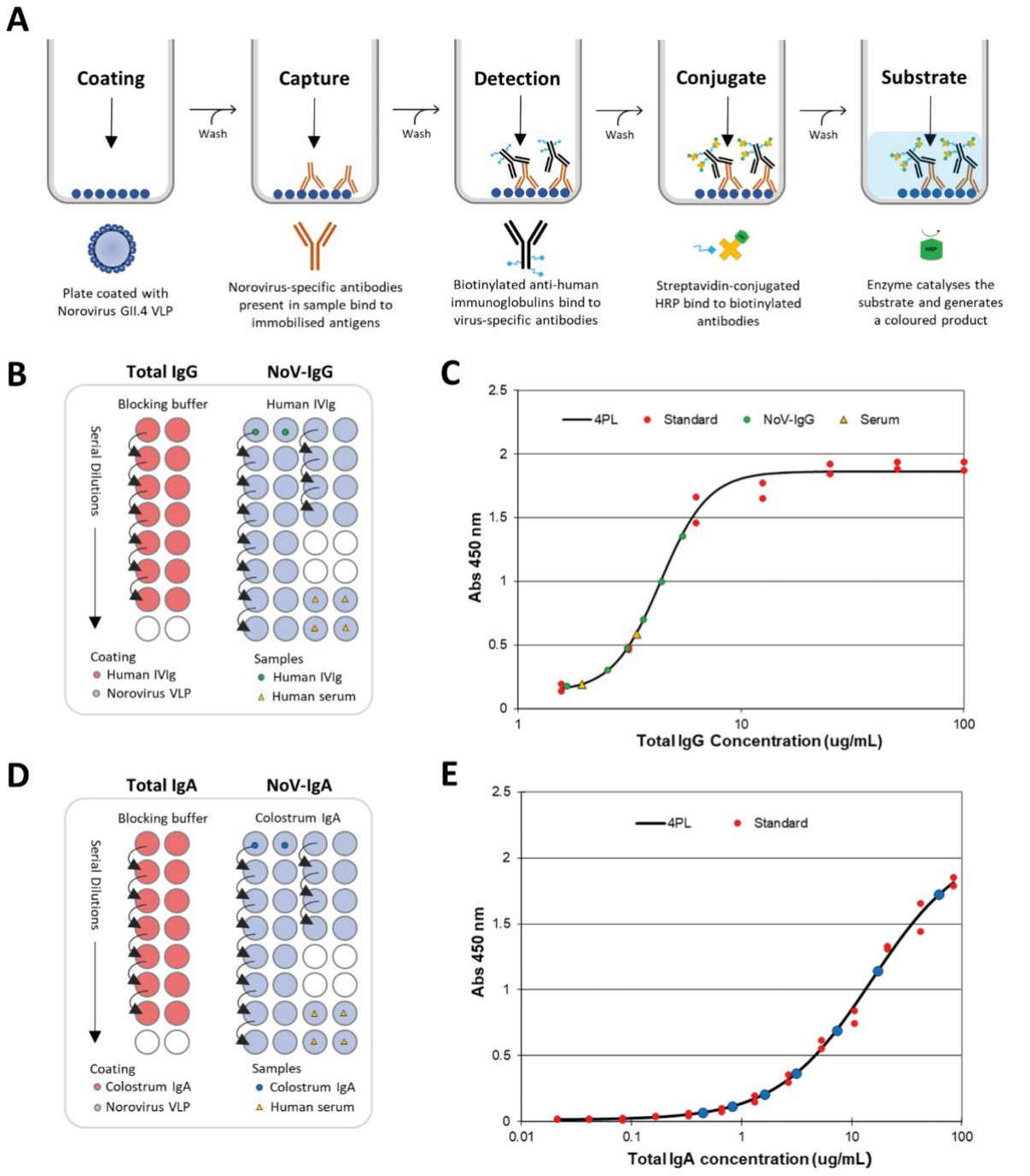

Figure. 4.3. Detection of Norovirus-specific antibodies in human samples by ELISA. Norovirus-specific antibodies were measured by ELISA using GII.4 norovirus virus-like particles adsorbed plates (A). Levels of IgG (B, C) and IgA (D, E) antibodies were detected from human purified intravenous immunoglobulin (IVIg) and colostrum IgA solution, respectively. Total immunoglobin analyses were performed in parallel to quantify the amount of virus-specific antibodies in samples (B, D). Two-fold serial dilutions from purified solutions were used as protein coating and reference samples, respectively (B, D). Representative curve fit analyses for both total and virus-specific IgG (C) or IgA (E) assays. Absorbances were monitored at 650nm after substrate addition. Quantitative analyses using 4-paremeter logistic curves were performed by MyAssays software.

4.1.2.2 Detection of norovirus-specific human IgA by ELISA

Following the same ELISA methodology as described above, we evaluated the presence of norovirus-specific human immunoglobulin A in a purified solution of IgA antibodies from human colostrum (Sigma-Aldrich). Assay steps and plate design were summarized in **Figure 4.3** accordingly. For total IgA detection, two-fold serial dilutions from human colostrum IgA solution, starting at 1:50 (42 µg/mL), were carefully adsorbed in ninety-six microtiter plates (High binding, Corning™ Costar™) for 48 hrs at 4°C (Fig. 4.3. B). In parallel, 50 µl per well from 3-fold diluted human colostrum IgA solution were serially diluted by 2-fold to evaluate the presence of NoV-specific IgA antibodies. Additionally, 50 µl of 20-fold diluted human serum samples were included as unknown samples. Plates were incubated for 2 h at 37°C in a humidity chamber. Norovirus-specific IgA detection was done using 1:1000 rabbit anti-Human IgA (α -chain specific)-Biotinylated antibody (Sigma Aldrich, UK). Plates were incubated for 90 min at 37°C. Additionally, Streptavidin-conjugated HRP (DY998, R&D systems, UK) was added following manufacturer's instructions. Absorbances were monitored at 650nm and recorded at 450nm after TMB substrate addition (Sigma Aldrich, UK). Figure 4.3 E shows HRP saturation curve for total IgA measurements after 60 min of substate addition. Absorbance from norovirus-specific IgA measurements were clearly distributed within the total IgA standard curve, showing the presence of virus-specific IgA antibodies in purified IgA from commercial human colostrum (Fig. 4.3. E).

Table 2. Assays details for Virus-specific antibody detection by ELISA

Virus-specific IgG detection		For Rotavirus assays	For Norovirus assays
Standard	Human IVIg	6.6 mg/mL of RV-specific IgG	1.3 mg/mL NoV-specific IgG
Samples	Human serum	Use 1:400 or 1:800 dilution	Use 1:400 or 1:800 dilution
	TS cell supernatants	Use 1:10 dilution	Use 1:5 dilution
Virus-specific IgA detection		For Rotavirus assays	For Norovirus assays
Standard	Human colostrum IgA	60 µg/mL of RV-specific IgA	800 µg/mL NoV-specific IgA
Samples	Human serum	Use 1:20 dilution	Use 1:50 dilution
	TS cell supernatants	Use 1:10 or 1:5 dilution	Use 1:5 dilution

An estimated concentration of 800 µg/ml NoV-specific IgA antibodies were detected in human colostrum sample by 4PL-curve analysis using Myassays software. Additionally, absorbances values from human serum samples were over the detection range (data not shown), considering a higher sample dilution for the next assays (**Table 2**).

4.1.2.3 Detection of human serum antibodies against enteric viruses by ELISA

Once the protocols for both rotavirus and norovirus specific antibody detection were standardized, we evaluated the assay performance using random serum samples from immunocompetent children and adults referred to adenotonsillectomy included in this study (Table 3). Sample dilutions were performed as described in **Table 2**. Representative curves for virus-specific IgG antibodies are summarized in **Figure 4.4**. Sigmoidal saturation curves from IVIg standard were observed for both rotavirus and norovirus antibody detection (Fig. 4.4). As observed in figure 4.4, a higher level of rotavirus-specific IgG antibodies was detected in adult samples as compared to children. Although the antibody titres in the measured serum samples fitted within assay detection range, respectively, an extra dilution (1:800) was included in future analyses, especially for those samples with high levels of virus-specific antibodies. A detailed analysis of the presence of pre-existing virus-specific antibodies in human serum samples will be presented in Part II of this chapter.

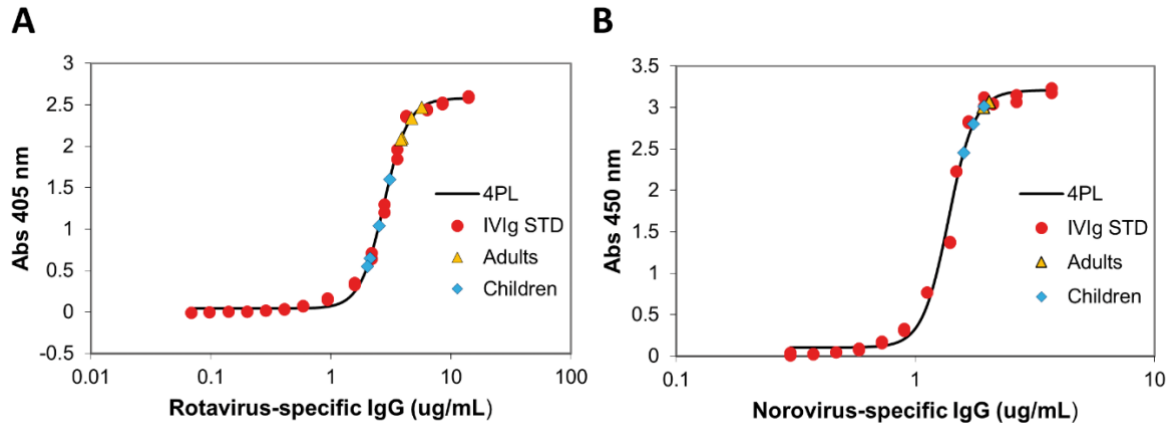

Figure 4.4. Detection of virus-specific IgG antibodies in human serum samples by ELISA. Presence of virus-specific antibodies were evaluated in children and adult serum samples by an in-house ELISA method using Group A rotavirus antigens (A) or GII.4 norovirus virus-like particles (B) adsorbed plates. Human purified intravenous immunoglobulin (IVIg) was used as a reference standard (red dots). Representative four parameter logistic (4PL) curve fit analyses indicate the presence of (A) rotavirus or (B) NoV specific IgG antibodies in children (blue diamond) and adults (yellow triangle). Quantitative analyses using 4PL were performed by MyAssays software.

4.2 PART II: Pre-existing immunity to Rotavirus and Norovirus in human sera

A wide range of specific host factors, e.g., genetic, gut microbiota or pre-existing immunity, can shape our immunological status and influence the quality of the immune response to vaccination (86, 111). These factors have also been associated with host intrinsic elements/demographics, such as age, gender, and socioeconomical factors (1-3). The efficacies of live orally-delivered vaccines, such as OPV and ORV, have been shown considerable variation among countries with different socioeconomic settings, where poor vaccine effectiveness has been evidenced in low-and-middle-income countries (LMIC) (51-53). It has been suggested that pre-existing immunity, i.e., the baseline presence of antigen-specific antibodies due to maternal–foetal transmission, natural infection, or vaccination, as one important baseline factor that may impact vaccine-induced immune responses and effectiveness (112). Previous exposure to prevalent virus strains, which share similar antigenic regions with LAV, Viral-vectored or VLP-based vaccines may impair the normal processing of and potentially decrease their efficacies (92, 95, 112, 113). In this section, we aimed to examine the level of pre-existing immunity to rotavirus and norovirus in children and adults by measuring the presence of virus-specific antibodies in serum samples using ELISA.

4.2.1 Pre-existing serum levels of human rotavirus-specific antibodies

Serum samples were collected from ninety-four immunocompetent children (1.5-16 years) and adults (17-45 years) referred to adenotonsillectomy due to upper-airway obstructions or tonsillitis (Table 3). Patients who received immunosuppressant treatment, or with any known immunodeficiency were excluded from this study. Baseline presence of rotavirus-specific IgG and IgA levels in sera were determined by ELISA as previously described above (*section 4.1*). Briefly, whole blood from recruited patients was centrifuged at 400 x g for 10 min to collect serum samples and kept at -80°C until assay. Ninety-six well microtiter plates (High binding, Corning™ Costar™) were coated overnight with a 100-fold diluted SA11 rotavirus antigens (Group A rotavirus, Microbix Biosystems).

Human serum samples (1:400 dilution) were added to the well and incubated at room temperature, with 200 rpm agitation for 90 min. Virus-specific antibodies detection was performed using alkaline phosphatase conjugated mouse anti-human IgG or anti-human IgA, respectively

Table 3. Characteristic of recruited patients for rotavirus immunity analyses.

	Total subjects (N=94)	**Children (N=73)**	**Adults (N=21)**
Age range (median)	**1.5-45 (5)**	1.5-16 (4)	17-45 (23)
Sex, N of females (%)	**51 (54)**	34 (45)	17 (81)
Serum RV-IgG Titers (μg/ml), mean ± SD, (Geometric mean titer)	**986.7 ± 581.3 (810.7)**	853.1 ± 472.6 (710.4)	1430.0 ± 693.5 (1528.7)
Serum RV-IgA Titers, (μg/ml), mean ± SD, (Geometric mean titer)	**45.3 ± 37.2 (28.79)**	41.1 ± 35.4 (25.01)	60.6 ± 40.3 (47.65)

Absorbance values were collected at 405nm after PNPP substrate addition with an ELISA plate reader (Multiskan Spectrum spectrophotometer, Thermo Fisher Scientific, UK). Quantitative analyses were performed using 4-Parameter Logistic (4PL) curve fitting by MyAssays online software (MyAssays Limited, UK).

An heterogenous distribution of rotavirus-specific serum antibody levels were detected among patients (Fig. 4.5). Pre-existing rotavirus-specific IgG titres in sera were significantly higher than rotavirus-specific IgA levels with a geometric mean titre (GMT) of 810.7 ug/mL and 28.8 ug/mL, respectively (Fig. 4.5. B). A positive correlation (Pearson r: 0.50, $P<0.001$) between rotavirus-specific IgG levels and patients´ age was observed (Fig. 4.5. C). Higher rotavirus-specific IgG levels were evidenced among adults (mean of 1430.0 ± 693.5 ug/mL) as compared to children (mean of 853.1 ± 472.6 ug/mL) and significantly increased by age groups (Fig. 4.5. C, E). A similar increase was also observed for serum rotavirus-specific IgA antibodies (Pearson r: 0.25, $P<0.04$) with significantly higher IgA presence among adults (mean of 60.7 ± 40.3 ug/mL) as compared to children (mean of 41.05 ± 35.4 ug/mL) (Fig. 4.5. E, F). These results evidenced a baseline presence of rotavirus-specific antibodies in human sera and were used as an indicator of "pre-existing immunity" among recruited patients for further RV1 vaccine immunogenicity analysis for T cell and B cells presented in Chapters V and VI, respectively.

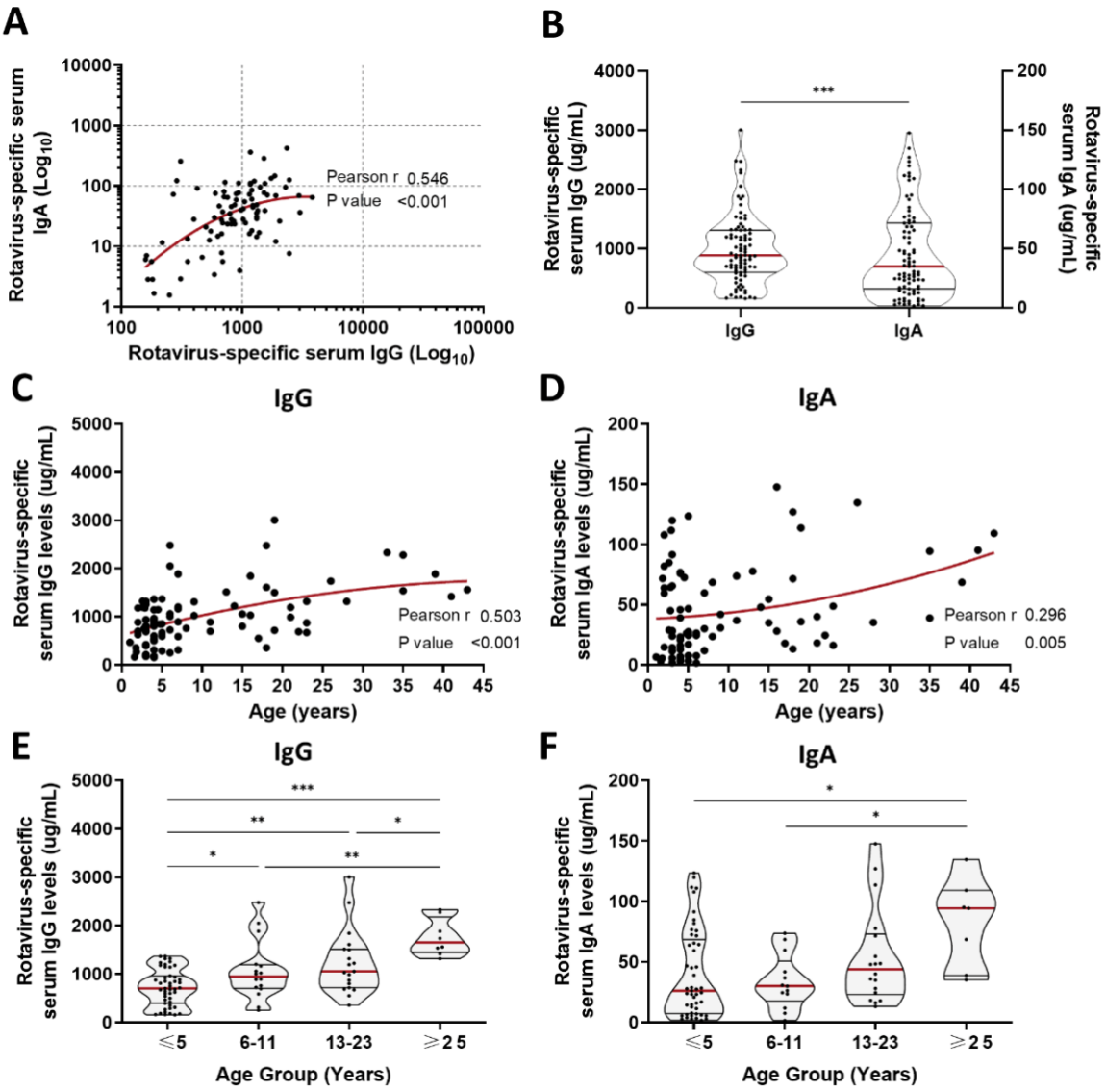

Figure 4.5. Serum Rotavirus-specific antibodies titres increases with age. Ninety-four serum samples from children (1.5-16 years) and adults (17-45 years) were analysed by ELISA for rotavirus-specific IgG and IgA detection. (A, B). Correlation between rotavirus-specific antibody levels and patient age (C, D), and antibody levels by age-group (E, F) were analysed by GraphPad prism 9 software, *P <0.05, ** P <0.01, *** P <0.001.

4.2.2 Pre-existing serum antibody levels to human Norovirus

Fifty immunocompetent children (1.5-16 years, median: 4 years) and adults (17-45 years, median: 23 years) referred to adenotonsillectomy due to upper-airway obstructions or tonsillitis were included in this analysis. Serum samples from patients were collected to evaluate their baseline IgG antibody levels to norovirus (i.e., Pre-existing immunity) (Table 4). The presence of norovirus-specific IgG in sera was determined by ELISA as described above (*section 4.1.2*).

Table 4. Characteristic of recruited patients for rotavirus immunity analyses.

	Total subjects (N=50)	**Children (N=37)**	**Adults (N=13)**
Age range (median)	**1.5-45 (5)**	1.5-16 (4)	17-45 (23)
Sex, N of females (%)	**26 (52)**	16 (43)	10 (77)
Serum NoV-IgG Titers (µg/ml), mean ± SD, (Geometric mean titer)	**331.6 ± 244.1 (236.3)**	284.3 ± 230.7 (196.3)	455.2 ± 243.3 (383.7)

Briefly, 96-well microtiter plates (Corning™ Costar™) were coated overnight with 5 µg/mL norovirus-VLP and incubated with patients´ serum samples for 2 h at 37°C. Levels of norovirus-specific IgG antibodies were detected by using a combination of Biotinylated-anti-Human IgG antibody and Streptavidin-conjugated HRP. Absorbances were recorded after TMB substrate addition at 450 nm by an ELISA plate reader and quantified using 4-Parameter Logistic (4PL) curve fitting by MyAssays software (MyAssays Ltd., UK). Pre-existing serum anti-NoV-specific IgG antibodies were shown to positively correlate with patients age (Pearson r: 0.50, P<0.001) (Fig. 4.6. A), and appeared significantly increased after the first few years in life (Fig. 4.6. B), with NoV-specific IgG geometric mean titres of 383.7 ug/mL and 196.3 ug/mL for adults and children, respectively (Table 4).

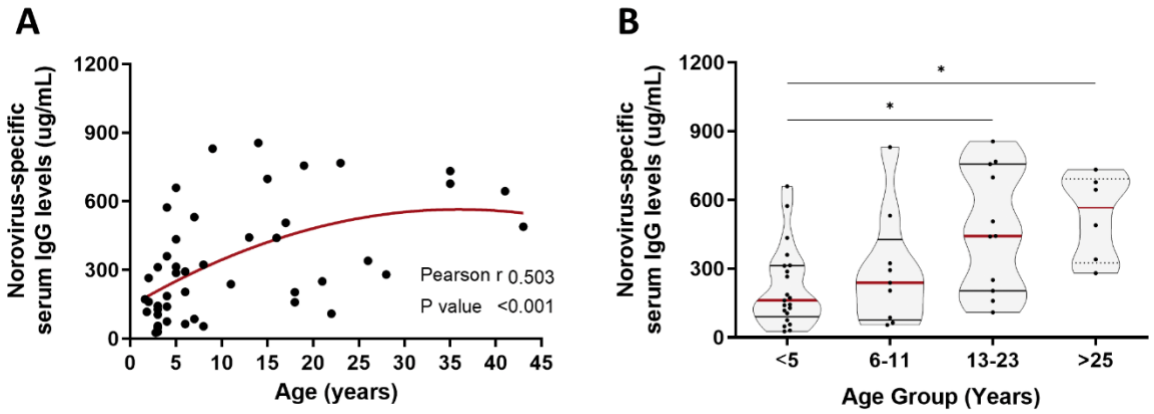

Figure 4.6. Serum Norovirus-specific antibodies titres distribution with age. Fifty serum samples from children (1.5-16 years, median: 4 years) and adults (17-45 years, median: 23 years) were analysed by ELISA for NoV-specific IgG detection. Correlation between NoV-specific antibody levels and patients age (A) and NoV-specific antibody levels by age-group (B) were performed by GraphPad prism 9 software, *P <0.05, *** P <0.001.

4.3 Conclusion

In this chapter, we provided the methodology and design of an in-house indirect ELISA for both rotavirus and norovirus specific antibodies detection in human serum samples. Serum rotavirus-specific levels were determined by a modified indirect ELISA previously described by Grimwood et al (114). This method involved coating microwell ELISA plates with G3, SA11 antigen, followed by addition of serum samples in test. Currently, simian-derived rotavirus antigens (SA11 strain) are easily obtainable and a commercially available source of group A rotavirus, providing a wide range of antigenic epitopes used widely for serological detection of rotavirus-specific human antibodies (97, 114, 115). Thus, by directly adsorbing a commercial rotavirus antigen preparation derived from whole inactivated SA11 rotavirus particles into 96-well EIA plates, we successfully detected a baseline presence of serum rotavirus-specific IgG and rotavirus-specific IgA titres among recruited patients.

Interestingly, we showed that pre-existing rotavirus-specific serum antibody levels follow an heterogenous distribution and increased with patients' age. This cohort was recruited from Liverpool`s hospitals within the UK and included children (1.5-16 years) and adults (17-45 years) referred to adenotonsillectomy from 2017 to 2021. Despite we were not able to access to the vaccination history of these patients, by considering both patients' age and recruitment date we can infer that all subjects who born since 2013 (Rotarix® vaccine was incorporated in UK's national immunization program in 2013) has been vaccinated. However, no significant differences were observed between "vaccinated" and unvaccinated groups (data not shown) suggesting that the variable rotavirus-specific antibody levels detected in this study were not due to patients' vaccination history. Moreover, our results are in line with a birth-cohort study where pre-existing serum anti-rotavirus IgG and IgA titres increased children age and with previous rotavirus infections, supporting their protective role against rotavirus infection and illness (116). Thus, although natural rotavirus infection (117) and rotavirus vaccination have proven to elicit a heterotypic immune response (58, 118), the use of a non-vaccine strain (SA11-derived antigens) for antibody detection may help to reduce possible inaccuracies associated to Rotarix® (G1P[8]) vaccination history and reflect instead the natural rotavirus history from this cohort. These may explain the higher titres of both IgG and IgA rotavirus-specific antibodies found in adults as

compared to children serum samples, suggesting that a cumulative pre-existing immunity may be associated with multiple rotavirus infections throughout life as described elsewhere for rotavirus (119) (116) and influenza virus (120).

Additionally, by using GII.4-SYD-derived NoV VLPs as coating antigens, we showed that pre-existing serum levels of GII.4 NoV-specific IgG antibodies followed a similar pattern and significantly increased with age. These findings are consistent with the high global prevalence of GII.4 NoV strains suggesting that patient's natural exposure history to NoV begins after the first few years in life and accumulates throughout the years (121-123). A similar increasing trend has been observed in children`s serum IgG antibody levels against NoV GI.3 and GII.4 VLPs and rotavirus VP 6 protein, all of which remained at high levels at the age of four (124).

Therefore, by analysing a wider group-age cohort, our findings showed a representative picture of the pre-existing immunity to both rotavirus and norovirus in children and adults and provided a valuable immune parameter to evaluate the potential impact of immunological imprinting on the mucosal immune response to enteric vaccines.

CHAPTER V

Evaluation of T Cell Responses elicited by Enteric Vaccines in Ex Vivo Human NALT

CHAPTER V

Evaluation of T Cell Responses elicited by Enteric Vaccines in *Ex Vivo* Human NALT

As major components of mucosal-associated lymphoid tissues (MALT), Human Nasopharynx associated lymphoid tissues (NALT) sits at the entrance of the Oro-respiratory tract, where are frequently exposed to foreign antigens and thereby containing a substantial proportion of antigen-experienced cells. Human adenotonsillar tissues (i.e., NALT) contain a diverse repertoire of T cells, including both central memory and effector memory T cells, and are recognized as important induction sites for adaptive immune responses. T lymphocytes play essential protective roles against many infections. T cells can recognise and target virus-infected cells as well as promote the production of antibodies. Thus, the activation of a robust and long-term T cell response may considered crucial for vaccine effectiveness (125). Although there still sparse data on the underlying T-cell immune responses to both norovirus and rotavirus infection (and vaccination), the current understanding achieved through animal models have shown a crucial role for T-cells in suppression and clearance of infection of rotavirus (126) and Murine NoV (127) and generation of antibody responses associated with protection (128). Thus, to study the mucosal immunity activated by enteric vaccines, we have examined the magnitude of human tonsillar T cell immune responses to a live attenuated oral Rotavirus vaccine (RV1), and a VLP-based Norovirus vaccine candidate (NoV1). The cellular immune responses in human NALT following vaccine stimulation were focused on three parameters; 1) the frequency of IFN-γ-producing T cells, 2) the level of tonsillar T cell proliferative response, and 3) the capacity of T cells to express gut-homing receptors in response to above mentioned vaccines.

5.1 Human NALT samples

Tonsils from 33 immunocompetent patients; 21 children (2-16 years, median: 4 years) and 12 adults (19-41 years, median: 23 years); were collected following adenotonsillectomy procedures due to upper-airway obstructions or tonsillitis. All subjects analysed in this chapter were recruited at Alder Hey Children's Hospital and Aintree University Hospital, Liverpool, UK. Patients who received

immunosuppressant treatment, or with any known immunodeficiency were excluded from the study. Processing and isolation of mononuclear cells (MNCs) from patient`s tonsillar tissues were performed as described in Materials and Methods (Chapter II). Variation in data sample size (n) per T cell outcomes were due to 1) intrinsic conditions of some samples after fresh tonsil collection: tissue inflammation, or damage; and/or low tonsillar MNC viability and/or 2) sample use for dose-response standardization experiments. Grossly inflamed tonsillar tissues were excluded from the study.

5.2 PART I: T cell response to Rotavirus vaccine in human NALT

5.2.1 Methodology

Human tonsils tissues were collected from 15 patients undergoing adenotonsillectomy to evaluate the immunogenicity of Rotarix (RV1), a live attenuated oral vaccine against human rotavirus. Processing and isolation of mononuclear cells (MNCs) from human tonsillar tissues were performed as described in Materials and Methods (Chapter II). Briefly, tonsillar MNC were cultured at a density of 2 x 10^6 cells/well (volume 0.5 ml) on 48-well plates (CytoOne®, STARLAB International GmbH, UK) and stimulated with 1 x 10^3 cell culture infectious dose 50% (CCID50) per mL of RV1 (Rotarix®, GSK) or media alone as unstimulated control (supplemented RPMI). Optimal RV1 dose was selected based on tonsillar T cell and B cell antibody response (see **Appendix C**, Fig.C1). Tonsillar MNC were incubated at 37°C with 5% CO_2 and T cell responses following vaccine stimulation were measured at day 3 for IFN-γ production, and day 5 for T cell proliferative response and expression of gut homing markers, respectively.

5.2.2 IFN-γ response to Rotavirus Vaccine

Interferon-γ has been widely recognized as a key cytokine in the clearance of many viral infections and thus, their expression/production by mucosal T cells can be a good indicator for activation of the antigen-specific T cell response elicited by enteric vaccines. We evaluated the frequency of IFN-γ producing T cells in Human NALTs following RV1 stimulation. Fresh tonsillar MNC from 12 individuals undergoing adenotonsillectomy were stimulated with 1 x 10^3 CCID50 mL^{-1} of RV1 and analysed 72 h later by IFN-γ intracellular staining and by FACS. All cells were treated with 1x Brefeldin (Biolegend) for 12-18 hours prior to cell harvesting. PMA/ionomycin (cell activation cocktail,

Biolegend) was used as a positive control according to manufacturer's instructions. Gating strategies used for tonsillar T cells and IFN-γ expression are shown in **Appendix D** (Fig. D1). As shown in **Figure 5.1**, rotavirus vaccine stimulation induced a marked IFN-γ production in human tonsillar MNC (Fig. 5.1). Increased frequencies of both $CD4^+$ and $CD8^+$ IFN-γ producing T cells were observed 3 days after vaccine stimulation as compared to unstimulated controls (Fig. 5.1. A-C, G, H). Additionally, increased IFN-γ secretion was also detected by ELISA in RV1-stimulated human tonsillar cell culture supernatants (Fig. 5.1. I, n=12).

5.2.3 Human Tonsillar T cell proliferation

A main characteristic of T cell activation is a proliferative response follow an infection or antigen exposure. Tonsillar MNC from 13 individuals undergoing adenotonsillectomy were stimulated with RV1 (1×10^3 CCID50 mL^{-1}) and evaluated 5 days later for cell proliferation using CFSE staining. Anti-human CD3 antibody (Ultra-LEAF™ purified HIT3a, Biolegend) was used as a T cell activation positive control. Both $CD4^+$ and $CD8^+$ T cell proliferation levels were analysed by FACS following rotavirus vaccine stimulation (RV1). Gating strategies used for CFSE dilution/cell proliferation analyses are shown in **Appendix D** (Fig. D2).

As summarized in **Figure 5.1**, rotavirus vaccine elicited marked $CD4^+$ and $CD8^+$ T cell proliferative responses in NALT of children and adults (n=13, 4 adults) (Fig. 5.1. D-F). Unlike PBMCs, tonsillar MNCs are frequently exposed to external antigens and may contain activated cells as evidenced by the base level of proliferation in the unstimulated medium controls in some subjects (Fig. 5.1. D). Notably, an increased T cell proliferative response was observed in RV1-stimulated tonsillar MNCs as compared to unstimulated control after analysis using fold increases (Fig. 5.1. G, H).

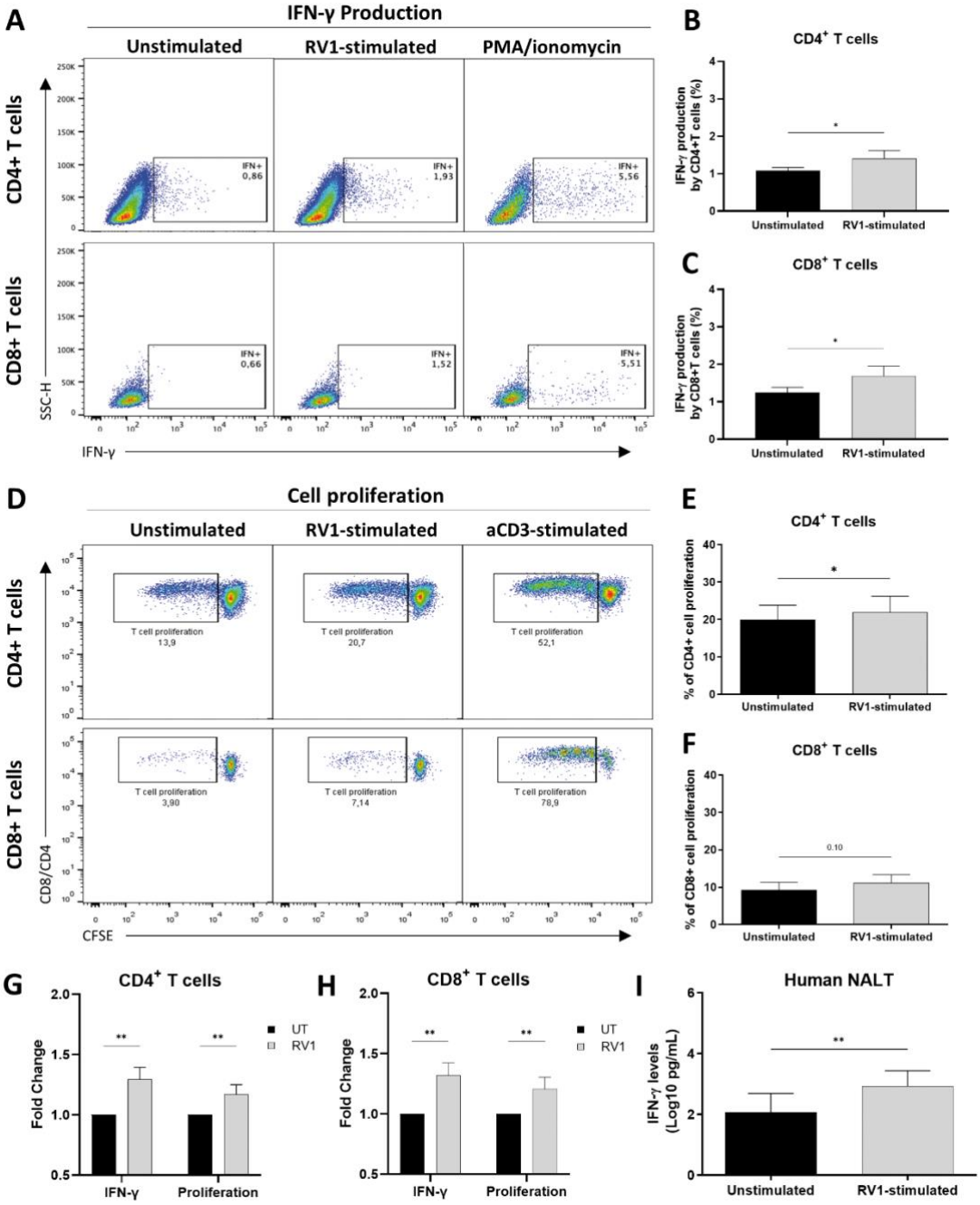

Figure. 5.1. Rotavirus Vaccine activates T cell immune response on human NALTs. Human tonsillar MNC were stimulated with $1x10^3$ CCID50 mL^{-1} of Rotarix vaccine (RV1) or left with media alone as an unstimulated control (UT). IFN-γ expression (A-C) and cell proliferative response (D-F) from tonsillar $CD4^+$ and $CD8^+$ T cells were analysed after 3 or 5 days by flow cytometry, respectively (n=13). Fold changes were obtained dividing RV1-stimulated values by unstimulated counterpart (G, H). IFN-γ secretion in cell culture supernatants was measured by ELISA at day 3 post-stimulation (I). Bars and error bars represent means + SEM. Statistical analysis was performed by GraphPad paired t-test or 2way ANOVA (Fold change). * P <0.05, ** P<0.01.

5.2.4 Gut-Homing receptor expression in human tonsillar T cells following RV1 stimulation

Oral delivered vaccines, such as rotavirus and poliovirus vaccines, have been widely used in many parts of the world and are associated with protective immunity in the gastrointestinal tract (42, 43). The migration and homing of lymphocytes from/to mucosal induction sites, such as gut-associated lymphoid tissues (GALT), have important implications in vaccine development and induction of specific immune responses (129, 130). The expression of α4β7 integrins, one of the main gut-homing receptors expressed by lymphocytes in the gastrointestinal (GI) tract, can predispose the homing of activated T cells to effector sites in the gut mucosa (131). Although the existence of a common mucosal immune system has been well described (129, 132), data is lacking on the expression of gut-homing receptors at related mucosal induction sites other than intestinal tract following enteric vaccines stimulation. Here, we examined the expression of α4β7 integrins in human NALTs in response to stimulation by RV1, a live attenuated oral Rotavirus vaccine. Freshly isolated tonsillar MNCs from 15 healthy donors were stimulated with RV1 (1×10^3 CCID50 mL^{-1}) as described above and analysed 5 days later for gut-homing receptor expression by flow cytometry. A combination of FITC-labelled anti-human CD49d, i.e., Integrin α4, (clone 9F1; Biolegend) and APC-labelled anti-human/mouse Integrin β7 (clone FIB504; Biolegend) antibodies were used for the analysis of gut-homing receptor in human tonsillar MNCs. Double positive ($\alpha4^+\beta7^+$) populations were selected as gut-homing receptor expressing cells by flow cytometry (**Appendix D**, Fig. D3). Representative figures demonstrating expression of α4β7 gut-homing receptor in $CD4^+$ and $CD8^+$ T cell populations were shown in **Figure 5.2** (Fig. 5.2. A, B). Increased levels of $\alpha4^+\beta7^+$ cells were observed in RV1-stimulated tonsillar MNCs as compared to unstimulated controls (Fig. 5.2. C-E).

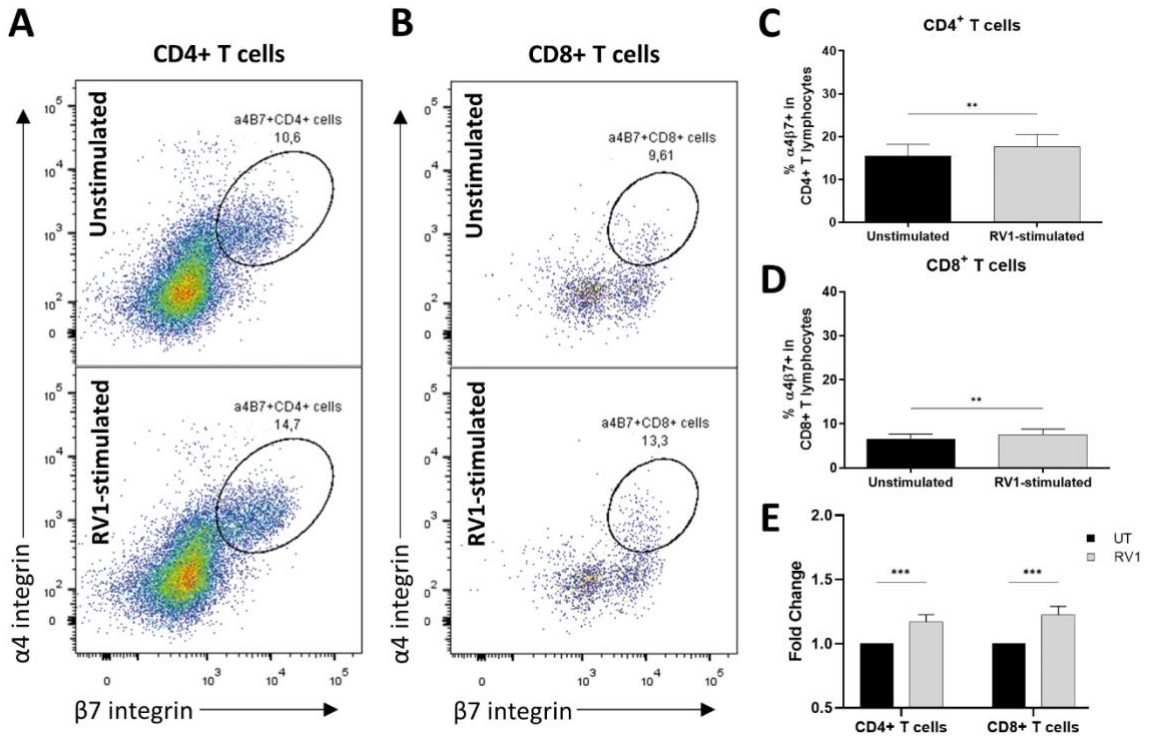

Figure 5.2. Expression of gut homing receptor on T cells from RV1-stimulated tonsillar MNC. Human tonsillar MNC were stimulated with rotavirus vaccine (RV1, 1 x 10^3 CCID50 mL^{-1}) and analysed after 5 days for the expression of α4β7 homing receptor by flow cytometry. Representative dot plots show the expression of α4β7 in $CD4^+$ (A) or $CD8^+$ (B) tonsillar T cells. Top right values represent the percentage of gut-homing receptor expressing cells as defined by double positive populations ($\alpha4^+\beta7^+$ cells) among $CD4^+$ or $CD8^+$ T cells (circles), respectively. Population percentages were summarized for $CD4^+$ (C) and $CD8^+$ (D) tonsillar T cells (n=15). Fold increase analysis as compared to unstimulated control was also included (E). Data were presented as means + SEM. Statistical analyses were performed by GraphPad paired t-test or 2way ANOVA (fold change), *P <0.05, **P<0.01, *** P <0.001.

5.2.5 Rotavirus Vaccine response in human naïve tonsillar T cells

As NALT has previously been shown to be important for polio vaccine-induced immunity, it raised the possibility that orally delivered enteric vaccines may also utilise NALT as additional induction sites for immunity (38). We therefore examined the induction of primary T cell response by rotavirus vaccine by using naïve T cells from tonsillar MNC.

As CD45RO is expressed on the cell surface of memory and activated, but not naïve T cells, the activation of naïve T cell response was studied using $CD45RO^+$ T cell depleted tonsillar MNC by

magnetic cell sorting. Briefly, memory T cells ($CD45RO^+$ cells) were removed using MACS columns (Miltenyi Biotec, Germany) according to manufacturer´s instructions. $CD45RO^+$ cell depleted tonsillar MNC from the same subjects described above were used. As shown in **Appendix B**, the efficiency of $CD45RO^+$ T cell depletion procedure was over 99% (i.e., >99% of $CD45RO^+$ $CD4^+$ and $CD8^+$ T cells were removed following the magnetic cell sorting procedure) (Appendix B, Fig. B1). $CD45RO^+$ cell-depleted tonsillar MNCs (n=14, 5 adult) were stimulated with RV1 (1 x 10^3 CCID50 mL^{-1}) and analysed 3 or 5 days later for IFN-γ production or cell proliferation respectively, as previously described.

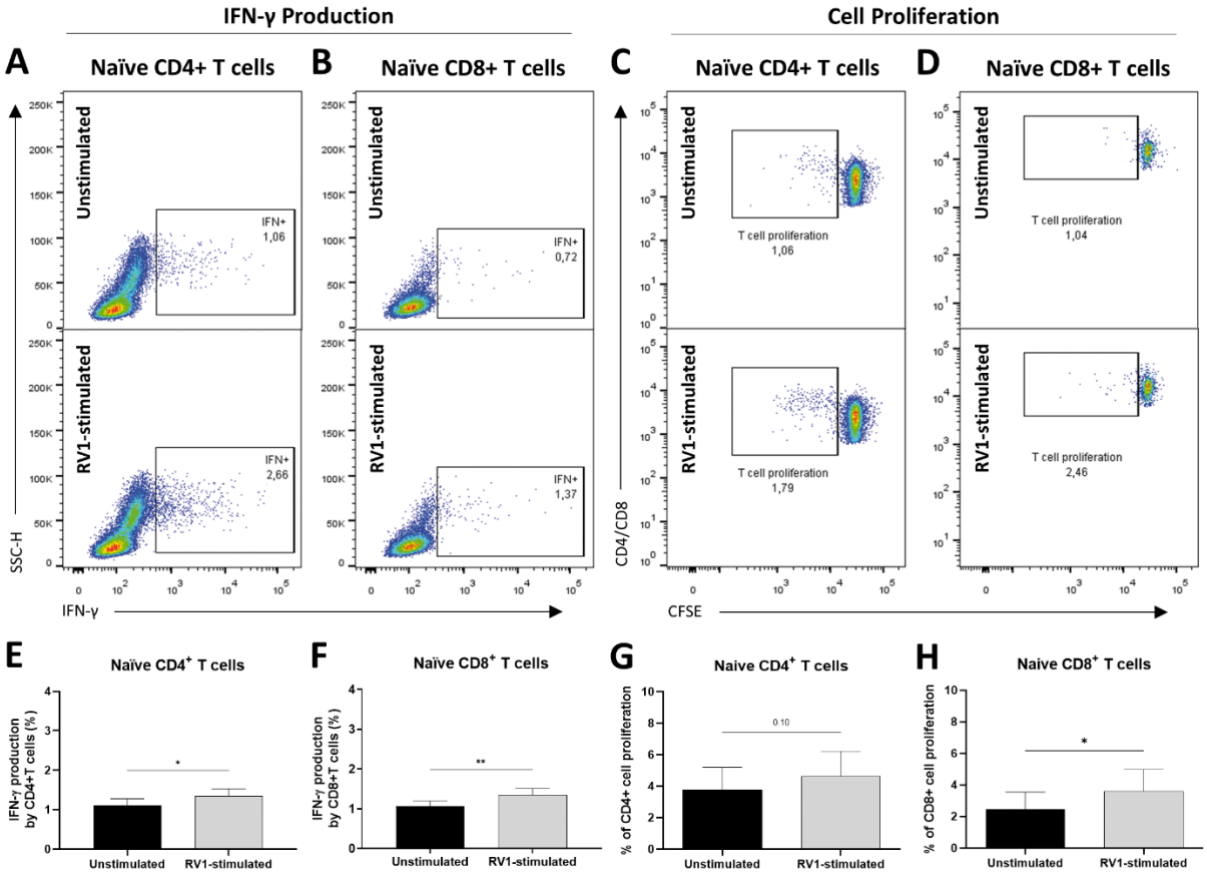

Figure 5.3. Rotavirus Vaccine induces a marked T cell immune response in naïve tonsillar T cells. $CD45RO^+$ cell-depleted tonsillar MNCs were stimulated with rotavirus vaccine (RV1, 1 x 10^3 CCID50 mL^{-1}) and compared to unstimulated control by flow cytometry analysis. Representatives dot plots shows the percentages of IFN-γ expression (A, B) and cell proliferative response (C, D) from $CD45RO^+$ cell-depleted (naïve) tonsillar T cells (n=15) at 3- or 5-days following vaccine stimulation, respectively. Percentages were summarized for $CD4^+$ (E, G) and $CD8^+$ (F, H) naïve tonsillar T cells. Bars and error bars represent means + SEM. Statistical analysis was performed using GraphPad Prism 9, paired t-test * P <0.05, ** P <0.01.

As shown in **Figure 5.3**, an increased cellular response was observed for naïve tonsillar T cells following rotavirus vaccine stimulation. These were evidenced by a high frequency of both $CD4^+$ and $CD8^+$ IFN-γ producing T cells from RV1-stimulated naïve T cells (Fig. 5.3. A, B, E, F). Additionally, as shown in Figure 5.3, an increase was also observed in $CD4^+$ and $CD8^+$ T cell proliferation from naïve tonsillar T cells following stimulation with rotavirus vaccine as compared to unstimulated controls (Fig. 5.3. G, H).

5.3 PART II: T cell response to VLP-based NoV vaccine candidate in human NALT

While several monovalent and multivalent VLP-based vaccine candidates against human NoV have been developed, different doses, adjuvants formulations and delivery routes are still being evaluated (70, 71). Based on our promising findings previously shown in mice by following repeated oral immunizations with NoV1, a VLP-based GII.4-Norovirus vaccine candidate, in combination with α-GalCer as a mucosal adjuvant (see **Chapter III**), we have further evaluated the mucosal immune response to NoV1, using tonsillar tissues as an ex vivo human NALT culture model. As presented above for the rotavirus vaccine, an analysis approach comprised by T cell proliferative and IFN-γ response and T cell gut-homing receptors expression levels, was followed to evaluate the cellular immune response of human NALT following NoV1 vaccine stimulation.

5.3.1 Methodology

Human tonsils were collected from 10 immunocompetent patients undergoing adenotonsillectomy to evaluate the immunogenicity of NoV1 vaccine. Tissue processing and mononuclear cell isolation of mononuclear cells (MNCs) were performed as previously described in Materials and Methods (Chapter II, Section 2.6). Briefly, 500 µl of freshly isolated tonsillar MNC (4×10^6 cells/mL) were seeded on 48-well plates (CytoOne®, STARLAB International GmbH, UK). Cells were immediately stimulated with 50 ng of purified VLP-based NoV vaccine candidate, NoV1, in presence or absence of pre-warmed 50 ng α-GalCer. All solutions were made in supplemented RPMI. A volume of 10 ul was added per well obtaining a final working dose of 0.1 µg/ml of either vaccine or adjuvant, respectively. Supplemented RPMI media alone was used as unstimulated control. Vaccine dose selection was based on tonsillar T cell proliferative and B cell antibody responses (see **Appendix C**, Fig.C1). Adjuvant formulation was

chosen from cell viability analyses when used in combination with optimal NoV1 vaccine dose (data not shown). Tonsillar MNC were incubated with 5% CO_2 at 37°C and evaluated at day 3 and day 5 following vaccine stimulation for T cell responses: intracellular IFN-γ production, T cell proliferative response and expression of gut homing receptors, respectively.

5.3.2 IFN-γ response to norovirus VLP

Vaccine studies in mice have widely evidenced the importance of T cell stimulation and activation through increased IFN- γ levels. Both $CD4^+$ and $CD8^+$ T cells can recognize norovirus VP1 peptides (110, 133) and upregulate IFN-γ production contributing to the control of norovirus infection *in vivo* (127). In order to characterize the immune response to norovirus VLP *ex vivo*, we evaluated the frequency of IFN-γ producing T cells in Human NALTs following NoV1 stimulation. Tonsillar MNC from ten immunocompetent subjects were stimulated with 0.1 μg/ml of NoV1 and analysed after 72 h for intracellular IFN-γ production by flow cytometry. Cells were also stimulated with 0.1 μg/ml of α-GalCer alone or in combination with NoV1. Cells were pre-treated 12-18 hours prior to cell harvesting with 1x Brefeldin (Biolegend) and PMA/ionomycin (cell activation cocktail, Biolegend) according to manufacturer's instructions. Interferon-γ producing tonsillar T cells were analysed by flow cytometry according to gating strategies used for rotavirus vaccine experiments (**Appendix D**, Fig. D1). As shown in **Figure 5.4**, frequencies of both $CD4^+$ and $CD8^+$ IFN-γ producing T cells were observed 3 days after NoV1 vaccine stimulation (Fig. 5.4. A-C). Increased IFN-γ levels were observed in VLP-stimulated human tonsillar MNC using fold increase analyses against unstimulated control (Fig. 5.4. G, H). IFN-γ secretion was also detected by ELISA in cell culture supernatants from NoV1-stimulated tonsillar MNC (Fig. 5.4. I, n=7). No significant differences were observed using α-GalCer as adjuvant (Fig. 5.4).

5.3.3 Human Tonsillar T cell proliferation to norovirus VLPs

Tonsillar MNC from 10 healthy subjects were labelled with CFSE and stimulated with 0.1 μg/ml of VLP-based vaccine candidate (NoV1) in presence or absence of α-GalCer as adjuvant. One μl per well of anti-human CD3 antibody (Ultra-LEAF™ purified HIT3a, Biolegend) was used as a positive cell activation control. Cell proliferative response from both $CD4^+$ and $CD8^+$ tonsillar T cells was evaluated by flow cytometry after 5 days of stimulation.

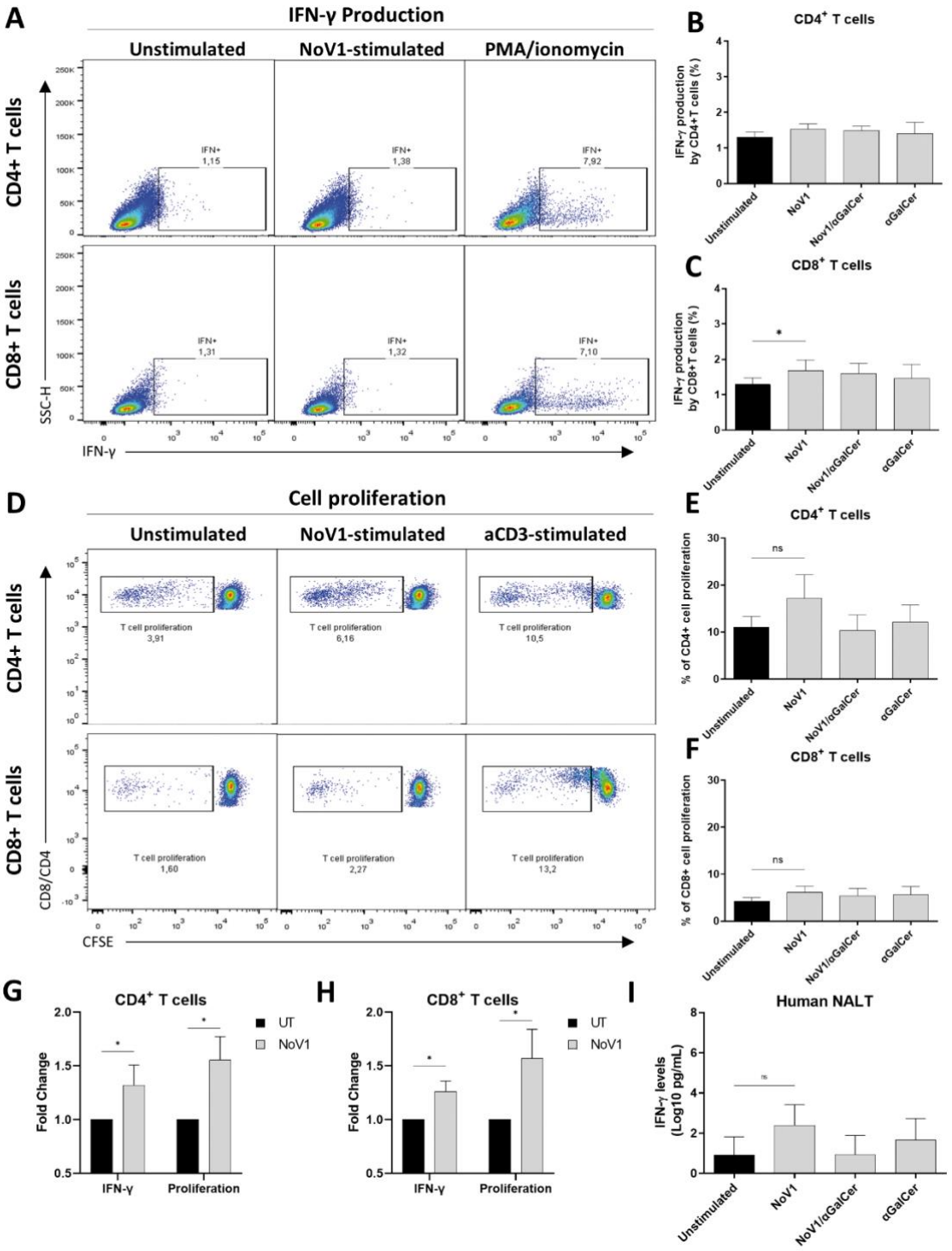

Figure 5.4. Norovirus VLP activates T cell immune response in human NALT. Human tonsillar MNC were stimulated with 0.1 μg/ml of VLP-based norovirus vaccine candidate (NoV1) in presence (NoV1/αGalCer) or absence (αGalCer) of α-GalCer adjuvant. Media was used for unstimulated control (UT). CD4+ and CD8+ T cells were analysed after 3 or 5 days by flow cytometry for IFN-γ expression (A-C) (n=7) and cell proliferation levels (D-F) (n=10). Fold increases were compared between NoV1-stimulated and UT values (G, H). Presence of IFN-γ in cell culture supernatants was measured at day 3 post-stimulation by ELISA (I). Data were presented as mean + SEM. Statistical analysis was performed by GraphPad paired t-test or 2way ANOVA (fold change) * P <0.05.

Gating strategies for T cell populations and CFSE dilution analyses are described in **Appendix D** (Fig. D2). As shown in **Figure 5.4**, VLP-based vaccine stimulation elicited a mild T cell proliferative response in human NALT (Fig. 5.4. D-F). Although preactivated cells from unstimulated tonsillar tissues were observed, fold increase analyses revealed a higher $CD4^+$ and $CD8^+$ T cell proliferative response in NoV1-stimulated tonsillar cells (Fig. 5.4. G, H).

5.3.4 Gut-Homing receptor expression in human tonsillar T cells following VLP stimulation

The expression of α4β7 gut-homing receptor has been used as a biomarker for mucosal immunity in oral vaccine studies, such as OPV and other norovirus vaccine candidates (134, 135). However, little is known about α4β7 expression levels in mucosal T cells using VLP vaccines. Here, we evaluated the expression of α4β7 receptor in human NALTs in response to NoV1 vaccine stimulation as a VLP-based norovirus immunogen. Freshly isolated human tonsillar MNCs from 8 healthy volunteers were stimulated with 0.1 μg/ml of NoV1 in presence or absence of 0.1 μg/ml α-GalCer as a mucosal adjuvant. Tonsillar T cells were analysed after 5 days post-stimulation for α4β7 gut-homing receptor expression by flow cytometry as previously described for live-attenuated rotavirus vaccine experiments (**Appendix D**, Fig. D3). Background fluorescence was subtracted from double positive ($\alpha4^+\beta7^+$) frequency analyses by using either fluorescence minus two (FM2) (Fig. D3) or isotype controls (data not shown). Representatives dot plots for α4β7 gut-homing receptor expression in human $CD4^+$ and $CD8^+$ T cell populations were shown in **Figure 5.5.** (Fig. 5.5. A, B). Interestingly, a higher frequency and fold increase of α4β7-expressing tonsillar T cells were observed following VLP vaccine stimulation (NoV1) when compared to unstimulated controls (Fig. 5.5. C-E). The same trend was observed for the NoV1/α-GalCer combination, however, VLP effect was not substantially potentiated by α-GalCer adjuvant.

5.3.5 Human tonsillar naïve T cell response to norovirus VLP vaccine

We evaluated the capacity of the NoV1 candidate, as a particulate immunogen, to induce a primary mucosal response in human NALT. For this purpose and following a similar approach as described for the live-attenuated rotavirus vaccine, naïve T cells from human tonsillar MNC ($CD45RO^+$ depleted cells, n=8) were stimulated with either 0.1 μg/ml of NoV VLPs (NoV1) or media alone as unstimulated control (UT). Additionally, we evaluated the adjuvanticity of α-GalCer during cell culture stimulation

by using 0.1 μg/ml α-GalCer alone or in combination with the NoV1 vaccine candidate. Human tonsillar T cells were harvested after 3- or 5-days post-stimulation and analysed for IFN-γ production or cell proliferation, respectively. Memory T cells were successfully removed from Tonsillar MNCs preparation using MACS column-based cell separation (Miltenyi Biotec, Germany) (Appendix B)

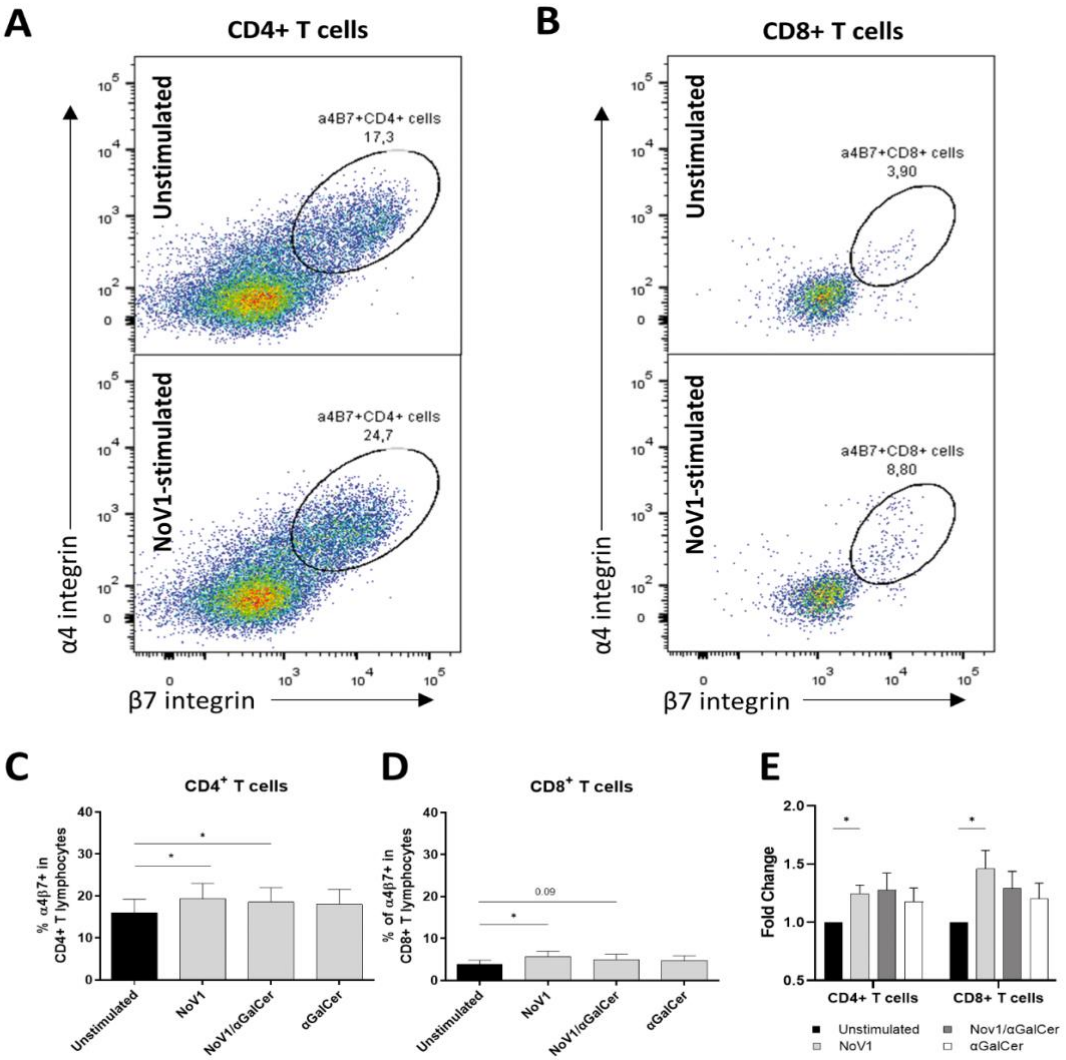

Figure 5.5. Norovirus VLP vaccine promotes α4β7 gut-homing receptor expression in human tonsillar T cells. Human tonsillar MNC were stimulated with norovirus VLP vaccine (NoV1, 0.1 μg/ml) or left with media as unstimulated control (UT) and analysed 5 days later for α4β7 gut-homing receptor the expression by flow cytometry. Adjuvant alone (α-GalCer) or in combination with the NoV1 (NoV1/αGalCer) was also assessed. Representative dot plots show the gut-homing receptor expression in human tonsillar $CD4^+$ (A) or $CD8^+$ (B) T cells. Frequency of double positive populations ($\alpha4^+\beta7^+$) were summarized for $CD4^+$ (C) and $CD8^+$ (D) T cells. Fold increase analyses against paired UT control were also included (E). Data were presented as means + SEM. Statistical analyses were performed by GraphPad, paired t-test or 2way ANOVA (fold change), *P <0.05.

As shown in **Figure 5.6**, T cell response was induced modestly by the NoV1 vaccine candidate in human NALT (Fig. 5.6). Interestingly, a significant increase of both IFN-γ and cell proliferative response was observed in tonsillar $CD8^+$ T cells following NoV1 vaccine stimulation (Fig. 5.6. F, H).

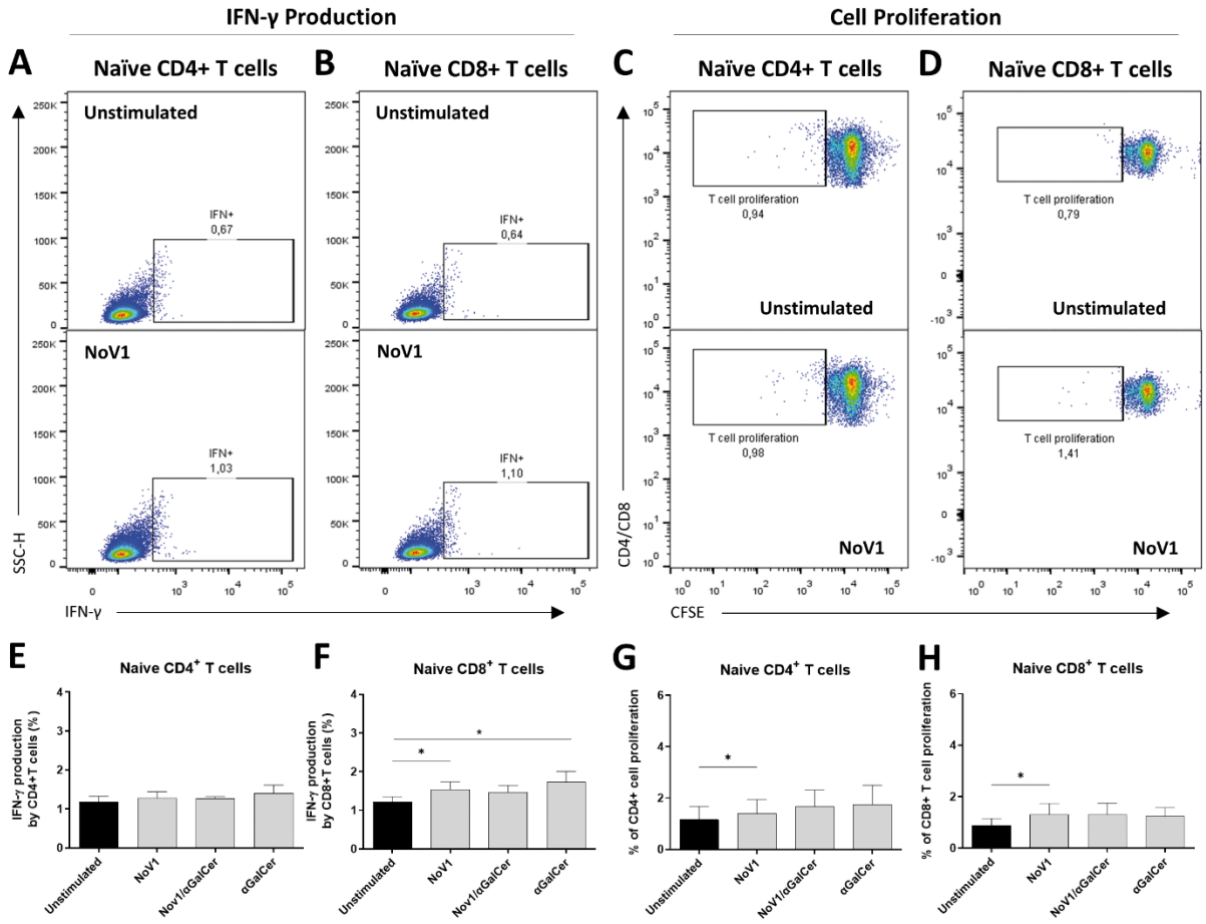

Figure 5.6. Norovirus VLP vaccine-induced response in naïve tonsillar T cells. $CD45RO^+$ cell-depleted tonsillar MNCs (naïve T cells) were stimulated with 0.1 μg/ml of VLP-based Norovirus vaccine candidate (NoV1), in presence or absence of α-GalCer adjuvant (NoV1/αGalCer or αGalCer, respectively), and compared to unstimulated control (UT) by flow cytometry analyses. Representatives dot plots shows the percentages of IFN-γ (A, B) and cell proliferation (C, D) from naïve tonsillar T cells at 3- or 5-days post-stimulation, respectively. Data were summarized for naïve $CD4^+$ (E, G) and $CD8^+$ (F, H) tonsillar T cells. Bars and error bars represent means + SEM. Statistical analysis was performed by GraphPad Prism 9, paired t-test * $P < 0.05$.

5.4 PART III: Evaluation of the Effect of Pre-Existing Immunity on Rotavirus and Norovirus Vaccine-Induced T cell immune responses.

As detailed on previous sections of this Chapter, tonsillar T cell responses to rotavirus vaccine (RV1) and VLP-based NoV vaccine candidate (NoV1) stimulation were analysed with three main outcomes: 1) the frequency of IFN-γ-producing T cells, 2) the tonsillar T cell proliferative response, and 3) the T cell expression of the gut-homing receptor α4β7. These findings provided relevant information to elucidate the role of T cell-mediated immunity to both rotavirus and norovirus. Given the current evidence on reduced efficacies of rotavirus vaccines in LMICs (92), we further analysed the relationship between vaccine-induced mucosal T cell responses and pre-existing immunity to rotavirus and norovirus; defined in Chapter IV as the baseline presence of virus-specific antibodies in sera, as a potential factor that may impact on vaccines immunogenicity and effectiveness. These findings will contribute to better understand the relationship between T cell immunity and seroconversion rates and the role of vaccine-induced T cell response as a potential immune correlate of protection to rotavirus and norovirus.

5.4.1 Relationship between Pre-existing Immunity and rotavirus vaccine-induced Mucosal T cell response

We first analysed the relationship between RV1-induced mucosal T cell responses and pre-existing serum anti-rotavirus antibody levels. Data on rotavirus pre-existing immunity were collected from 33 children (2-16 years, median: 4 years) and adults (19-41 years, median: 23 years) undergoing adenotonsillectomy and paired with tonsillar T cell immune responses detected *ex vivo* following RV1-stimulation. Fold change of T cell responses, i.e., the ratio of RV1-stimulated with respect to unstimulated control (baseline), and Log10-transformed serum antibody levels (Elisa Units; EU) were used for respective correlation analyses. For T cell outcomes, vaccine responder subjects were defined as all values over baseline (Fold Change >1); whereas values $\leq$1 as non-responders. Finally, correlations between patients´ pre-existing serum antibody levels to rotavirus and RV1-induced mucosal T cell responses were performed using GraphPad Prism 9 software. Pearson correlation coefficient (r) and linear regression were included for all analyses.

The distribution of RV1 vaccine responders and non-responders for every T cell outcome evaluated previously in tonsillar MNCs is shown in **Figure 5.7.** We found that pre-existing anti-rotavirus IgG levels in sera positively correlated with vaccine-induced gut homing receptor α4β7 expression in tonsillar $CD4^+$ T cells (N=19, Pearson r=0.5 p<0.047) (Fig. 5.7. C). On contrary, we observed no significant correlation between the mucosal T cell response indicators (i.e., IFN-γ and T cell proliferative response) and the pre-existing serum antibody titres (Fig. 5.7). However, when analysed individually, a group of non-responder children with low frequency of IFN-γ-producing $CD4^+$ and $CD8^+$ cells (i.e., fold Change ≤1) shown a significant inverse correlation with their pre-existing immunity (Pearson r:0.76 and 0.75 for $CD4^+$ and $CD8^+$, respectively) (Fig. 5.8). No associations were observed between RV1-induced T cell proliferative response and serum pre-existing anti-rotavirus IgG levels.

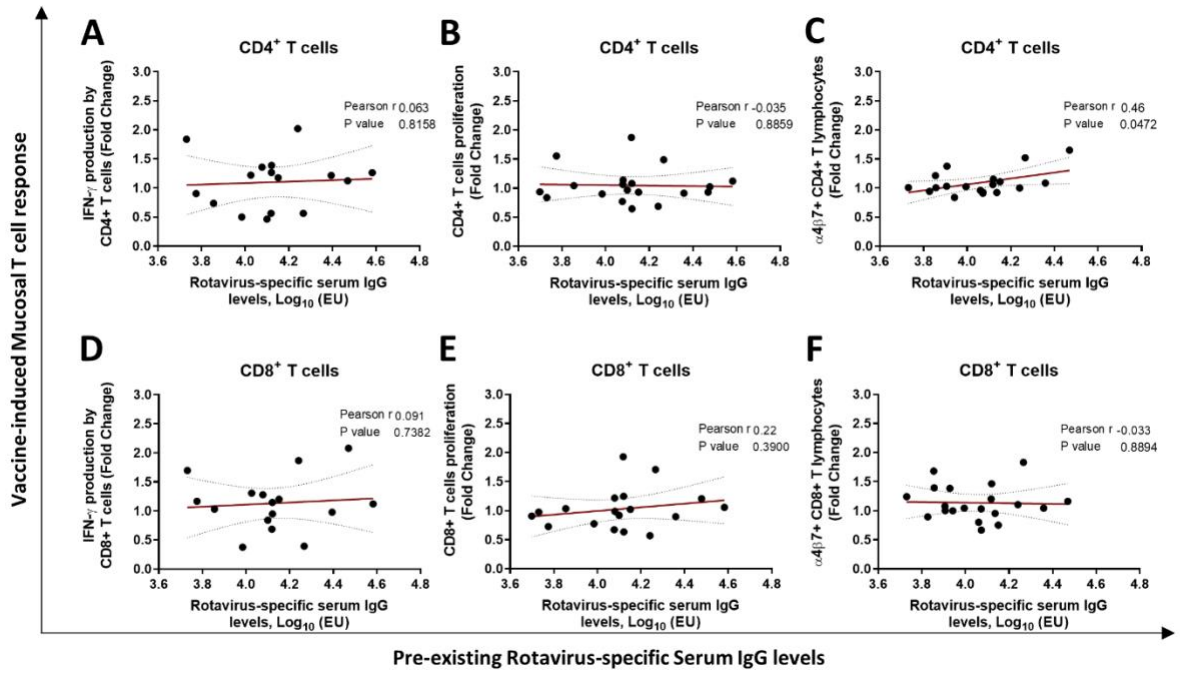

Figure 5.7. Relationship between pre-existing anti-rotavirus IgG levels and Mucosal T cell response to rotavirus vaccine. Fold Change mucosal $CD4^+$ (A, B, C) and $CD8^+$ (D, E, F) T cell responses from Rotarix (RV1)-stimulated human tonsillar MNC were correlated with patients' rotavirus-specific serum IgG titres (Log10-transformed ELISA units; EU). Fold increase data for IFN-γ expression (A, D), T cell proliferative response (B, E) and α4β7 homing receptor expression (C, F) were included in the analyses. Statistical analyses including Pearson correlation coefficient (r) and linear regression (red line) were performed by GraphPad prism 9.

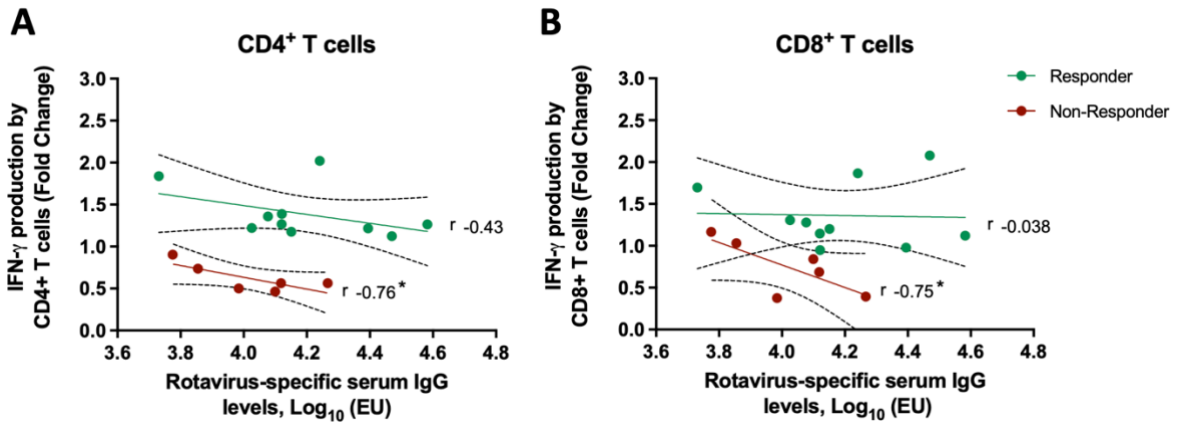

Figure 5.8. Relationship between pre-existing anti-rotavirus IgG levels and RV1-induced mucosal IFN-γ-producing T cell response. Fold Change of IFN-γ-producing $CD4^+$ (A) and $CD8^+$ (B) mucosal T cell responses from RV1-stimulated human tonsillar MNC were correlated with patients' rotavirus-specific serum IgG titres (Log_{10}-transformed ELISA units; EU). RV1 responders (values > 1; green) and non-responders (values ≤1; red) were defined based on tonsillar T cell outcomes as the ratio between RV1-stimulated and unstimulated control. Pearson correlation coefficient (r) and linear regression analyses were performed by GraphPad prism 9; * P <0.05.

5.4.2 Pre-existing norovirus immunity effect on NoV1 vaccine-induced Mucosal T cell response

We further examined whether there is any effect of pre-existing immunity to human norovirus on tonsillar T cell immune responses induced by a VLP-based norovirus vaccine candidate (NoV1). Data on pre-existing NoV-specific antibodies were collected from 11 children (4-16 years, mean: 6 years) and adults (28-41 years, mean: 32 years) and paired with *ex vivo* tonsillar T cell immune responses induced by NoV1 (i.e., IFN-γ-production, proliferative response and gut-homing α4β7 receptor expression by human tonsillar T Cells). Fold change data between NoV1-stimulated and unstimulated control from T cell outcomes were considered for correlation analyses against patients´ pre-existing immunity. Pearson correlation coefficient (r) and linear regression analyses were included using GraphPad prism 9.

As shown in **Figure 5.9,** a positive trend was observed for correlation between pre-existing serum IgG levels to norovirus and vaccine-induced IFN-γ expression in tonsillar $CD4^+$ T cells (N=10, r=0.68, p<0.04) and $CD8^+$ T cells (N=10, r=0.58, p<0.07) (Fig. 5.9. A, D). Interestingly, this trend was significantly correlated when NoV1 was adjuvanted with α-Galcer (Appendix E, n=10; $CD4^+$ T cells, r=0.75 p<0.01; $CD8^+$ T cells, r=0.77, p<0.01). No significant associations were found between NoV pre-existing immunity and the proliferative response or gut-homing receptor expression by NoV1-stimulated tonsillar T cells, respectively (Fig. 5.9).

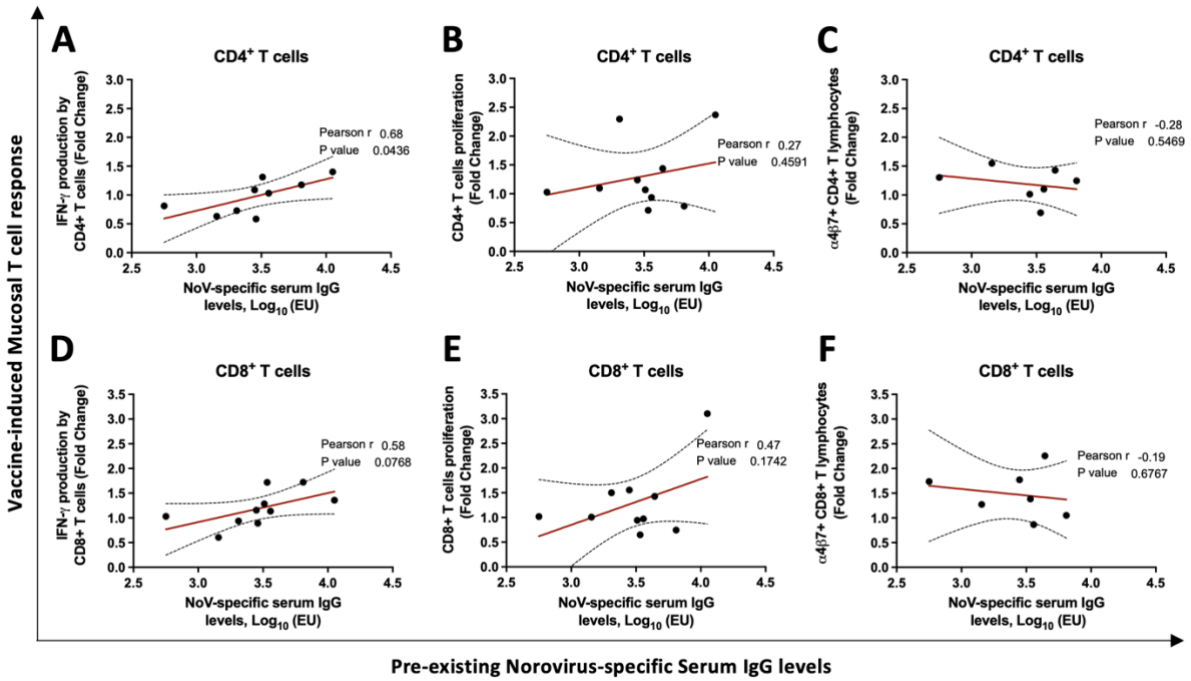

Figure 5.9. Effect of pre-existing norovirus immunity on NoV1 vaccine-induced Mucosal T cell response. CD4+ (A-C) and CD8+ (D-F) mucosal T cell responses recorded after stimulation of human tonsillar MNC with a VLP-based norovirus vaccine candidate (NoV1) were paired and correlated with patients' norovirus-specific serum IgG titres (Log_{10}-transformed ELISA units; EU). Fold increase data from and IFN-γ production (A, D) T cell proliferation (B, E) and α4β7 homing receptor expression (C, F) by T cells were considered in the analyses. Pearson correlation (r) and linear regression (red line) were performed by GraphPad prism 9 software.

5.5 Conclusion

On this chapter, we performed a comprehensive evaluation of the mucosal T cell immune response to rotavirus and norovirus antigens using children and adults NALTs. We showed that Rotarix®, a live-attenuated oral rotavirus vaccine (RV1), elicited a marked T cell response in tonsillar MNC; with increased frequencies of both $CD4^+$ and $CD8^+$ IFN-γ producing T cells and T cell proliferative responses. Moreover, using $CD45RO^+$cell depleted tonsillar MNC, we found that RV1 induced a significant native T cell response in both children and adults NALTs. In parallel, we found a modest yet significant increase of both IFN-γ and cell proliferative response in tonsillar T cells following stimulation with non-replicating NoV VLPs (NoV1) as a potential vaccine candidate.

Evidence from animal models and human studies (particularly using human PMBCs) have described cell-mediated responses following stimulation with rotavirus (126)(62, 136, 137) or NoV antigens (127) (138) (124), respectively. However, there still sparse data on the underlying T cell immune responses to rotavirus vaccination (139) and norovirus candidate vaccines trials. Clinical trials studies for rotavirus vaccines have observed a reduction in viral shedding implying the generation of local protective immune response mediated by mucosal effectors (140). In this regard, murine models have described mucosal immune responses, characterized by Th1 cellular responses and higher production of IFN-γ after parenteral rotavirus vaccination (141). Similarly, increased IFN-γ production in human PBMCs have been observed after NoV-VLP immunizations (138)**.** Notably, we showed that NoV1-induced IFN-γ response in tonsillar T cells positively correlated with patients` pre-existing immunity to GII.4 NoV. On contrary, a trend of inverse correlation was observed particularly in those individuals who demonstrated low/no mucosal T cell response following RV1-stimulation.

Therefore, using human NALT as a mucosal model, our findings confirm that either a live attenuated rotavirus vaccines or particulate norovirus antigens were able to induce at different degrees, a cell-mediated immune response**.** Importantly, to the best of our knowledge, this is the first *ex vivo* study to describe the magnitude of local mucosal T cell responses elicited by rotavirus vaccines and VLP-based NoV antigens in children and adults.

In term of gut-homing response, we described an increased expression of the gut-homing receptor α4β7 in both RV1 and NoV1-stimulated human tonsillar T cells. Studies using human PBMCs have described increased proportions of rotavirus-experienced T cells expressing the gut homing receptor α4β7 in children following acute rotavirus infection and vaccination (63, 142, 143). In this line, we found high frequencies of α4β7-expressing $CD4^+$ and $CD8^+$ T cells in NALT of children and adults following RV1-stimulation, however, only a mild increase was observed using non-replicating NoV VLPs alone or in combination with αGalCer. This may suggest the need for a strong stimulus or dose adjustment to activate a NoV-specific T cell memory repertoire among patients when using particulate antigens. Although there is no evidence to date about T cell gut-homing properties following NoV antigens stimulation, previous studies have found VLP-specific B cells expressing β7 homing marker after human PBMCs stimulation with human NoV-like particle vaccines (144, 145), highlighting the importance of considering B-cell mediated response for future NoV studies (data currently in progress).

Collectively, our results support the role of human NALT (e.g., tonsils) as important induction sites for adaptive immune responses induced by rotavirus and norovirus vaccines. Our findings suggest human NALT may be an important reservoir of activated memory and effector T cells with potential intestinal homing-properties. Further studies are needed to evaluate whether immune protection to rotavirus and norovirus is mediated by homing of immune cells to the gut mucosa.

Finally, this chapter provided insights into the use of tonsils as an important source of human immune tissue to study key cell-mediated responses induced by non-parenteral vaccines and underlying immune mechanisms of protection for mucosal vaccines and adjuvants. Given the high cell density obtained from freshly collected tonsillar MNCs, the use of new molecular tools such as antigen loaded-tetramers may be considered in future human NALT studies to elucidate with higher sensitivity the presence antigen-specific T cells responses induced by vaccine and could help to overcome the high inherent baseline activation human tonsillar MNCs.

CHAPTER VI

Evaluation of B Cell Antibody Response to Enteric vaccines in *ex vivo* Human NALT

CHAPTER VI

Evaluation of B Cell Antibody Response to Enteric vaccines in *ex vivo* Human NALT

B cells are responsible for the production of antigen-specific antibody responses and the development of long-term protective humoral immunity against infectious diseases. B cells also remains a crucial parameter of protection induced by vaccines. Many studies have described the formation of germinal centre (GC) structures and a predominant B cell distribution within human tonsillar tissues (37, 39, 146). Here we assessed the mucosal B cell antibody response to a live-attenuated rotavirus vaccine and a VLP-based norovirus vaccine candidate in human NALT, using tonsillar tissues as an *ex vivo* system to examine the antigen-specific mucosal immune response to enteric vaccines.

6.1 PART I: Mucosal B cell antibody response to Rotavirus vaccine in human NALT

Human tonsillar tissues were collected from 41 immunocompetent subjects (aged 2-43) undergoing adenotonsillectomy to evaluate the mucosal B cell antibody response following stimulation of tonsillar MNC with a live-attenuated rotavirus vaccine (Rotarix®, GSK) (RV1). Tissue processing and isolation of mononuclear cells (MNCs) from human tonsils were performed as described in Materials and methods (Chapter II, section 2.6 - *Tissue Processing and cell isolation*).

6.1.1 Methodology

The magnitude of mucosal B cell antibody response to rotavirus vaccine stimulation was evaluated by co-culturing the vaccine with tonsillar MNC. Briefly, human tonsillar MNC were stimulated with 1 x 10^3 CCID50 mL^{-1} of RV1, or with media alone as unstimulated control (UT), and incubated for up to 14 days at 37°C with 5% CO_2. Cell culture supernatants (100-200 µl per stimulation) were collected at 7- and 14-days post-stimulation. Equal volumes of fresh media (supplemented RPMI) were replaced per well at day 7 following supernatants collection. The Rotavirus vaccine dose for stimulation was previously selected based on T cell and B cell responses in Human NALTs (see **Appendix C**, Fig.C1). The presence of rotavirus-specific IgG and IgA antibodies in tonsillar cell culture supernatants were quantified by ELISA as previously described in **Chapter IV** (see section 4.1).

Briefly, ninety-six well microtiter plates (High binding, Corning™ Costar™) were coated overnight at 4°C with 100-fold dilution of purified rotavirus antigens (Microbix Biosystems). 100 ul of tonsillar cell culture supernatants (1:10 dilution) was subsequently added per well for antibody detection. Quantification of rotavirus-specific IgG and IgA antibodies was done against reference standard curves of human intravenous immunoglobulin (IVIg) (Intratect, Biotest Pharma, UK) or purified IgA from human colostrum, respectively. Two-fold serial dilutions of reference standard were made, starting at 16.5 µg/ml or 20 µg/ml of RV-specific IgG or IgA respectively (summarized in Chapter IV, Table 4). Assay cut-off threshold for positive readings was defined as the average absorbance from unstimulated controls + 3SD. Quantitative analysis was done using 4-Parameter logistic curve fitting (MyAssays Limited, UK).

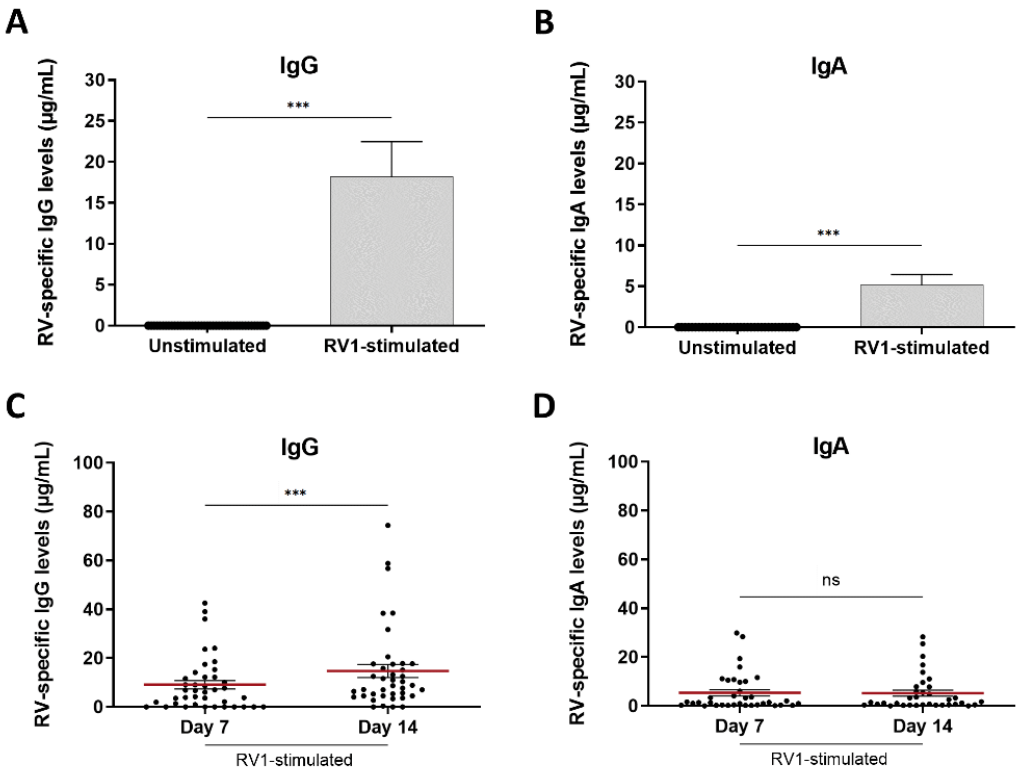

Figure. 6.1. Rotavirus vaccine induces the production of rotavirus-specific antibodies in human tonsillar MNC. Culture supernatants from human tonsillar MNCs were collected at 7- and 14-days post stimulation with RV1 vaccine (10^3 CCID50/mL). Rotavirus-specific IgG (A, C) and IgA (B, D) antibody levels were quantified by ELISA; A and B shows data collected at day 14 post RV1-stimulation. Data were presented as mean plus SEM. Statistical analysis was performed by GraphPad 9, using paired t-test. *** P <0.001; ns, not significant.

6.1.2 Rotavirus-specific antibody production in human NALT

As shown in Figure 6.1, significant rotavirus-specific antibody responses were detected in human tonsillar cell culture supernatants following RV1 vaccine stimulation. We observed that a Rotarix dose of 10^3 CCID50/mL induced production of both rotavirus-specific IgG (N=41) and IgA (N=33) antibodies in human tonsillar MNC after 14 days of stimulation as compared to unstimulated controls (Fig. 6.1 A, B). Rotavirus-specific IgG levels were also observed at day 7 after RV1 vaccine stimulation, followed by a further increase at day 14 (Fig. 6.1. C). Additionally, human mucosal rotavirus-specific IgA antibody production was also observed at day 7 post RV1-stimulation (Fig. 6.1. D).

Interestingly, the mucosal IgG and IgA antibody responses following rotavirus vaccine stimulation were shown to be positively correlated with sample donors age (Fig. 6.2). As shown in Figure 6.2, stronger responses in rotavirus-specific IgG (Fig. 6.2. B) and IgA (Fig. 6.2. D) antibodies were observed in tonsillar MNC from adults as compared to children following RV1 vaccine stimulation.

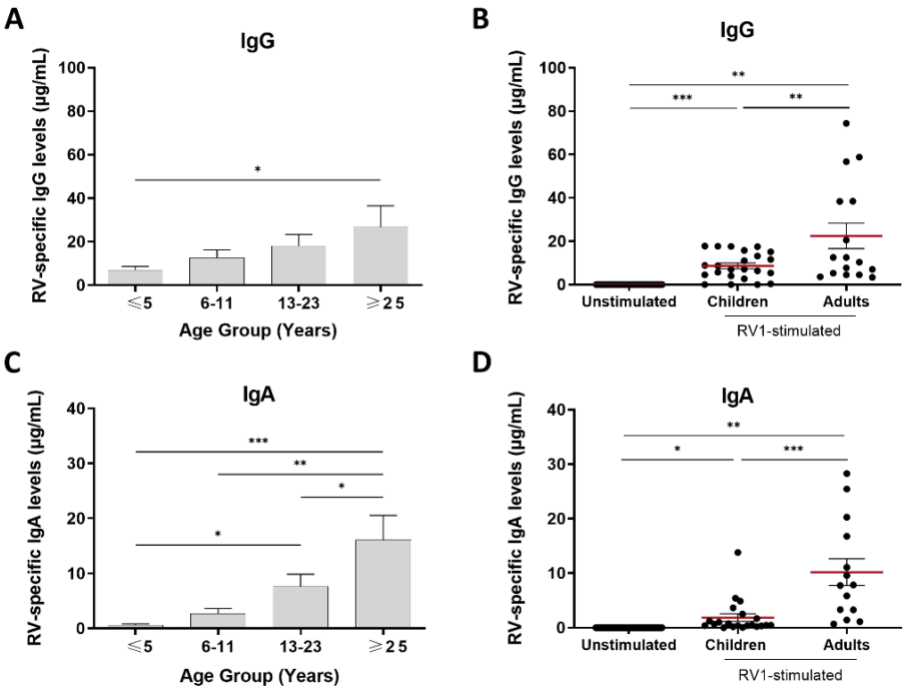

Figure 6.2. Rotavirus vaccine-induced antibody responses in human NALT by Age. Rotavirus-specific IgG (A, B) and IgA (C, D) antibody responses to rotavirus vaccine stimulation in human NALT (day 14) were analysed in association with donors' age. Data were obtained from 40 patients, including 23 children (2-16 years; age median: 4.8 years) and 17 adults (17-45 years; age median 24.5 years), and presented as mean + SEM. Statistical analysis was performed by GraphPad 9, using paired t-test. *P <0.05; ** P <0.01; ***P <0.001.

6.2 PART II: Antibody response to VLP-based Norovirus vaccine in human NALT

It was previously shown that our VLP-based norovirus vaccine candidate (referred as NoV1) induced both systemic and mucosal norovirus-specific antibody responses in mice after 3-dose oral immunizations in combination with α-GalCer adjuvant (NoV1/α-GalCer) (detailed in Chapter III). Here, we further characterized the immunogenicity of this particulate norovirus vaccine by studying the mucosal B cell antibody response in human NALT following NoV1 stimulation. Additionally, we also evaluated the adjuvant effect of α-GalCer on the *ex vivo* NoV1-induced mucosal antibody response.

6.2.1 Methodology

Human tonsillar tissues were collected from 20 immunocompetent patients (aged 2.9-43) undergoing elective adenotonsillectomy and processed for tonsillar mononuclear cells (MNCs) isolation as described in Chapter II, section 2.6. Human tonsillar B cell antibody response to NoV1 was evaluated under the same *ex vivo* conditions as described for T cells assays (Chapter V, section 5.2.1). Briefly, tonsillar MNC were stimulated with 0.1 μg/ml of NoV1, or with media alone as unstimulated control, and incubated at 5% CO_2, 37°C for 14 days. The adjuvanticity of α-GalCer was evaluated in parallel by using 0.1 μg/ml of α-GalCer alone or combined with NoV1 for human tonsillar MNC stimulation. Both vaccine and adjuvant concentrations were previously chosen according to cell viability analyses (data not shown) and optimal immune responses in human NALT (see Appendix C, Fig.C1). Aliquots of 100-150 μl from cell culture supernatants were collected at days 7 and 14 post-stimulation and production of norovirus-specific IgG antibodies were quantified by ELISA, as described in Chapter IV - section 4.1. Ninety-six well microtiter plates (High binding, Corning™ Costar™) were coated with norovirus VP1-based VLP as coating antigen and incubated for 48 h at 4°C. 100 ul of each supernatant sample (1:4 dilution) was applied to each well for antibody analysis. Quantification of NoV-specific IgG was done against a reference IVIg (Intratect, Biotest Pharma, UK) standard curve starting at 1:800 dilution from stock (1340 μg/ml NoV-specific IgG). Antibody levels were presented as stimulated minus unstimulated control. Quantitative analysis was done using 4-Parameter logistic curve fitting (MyAssays Limited, UK).

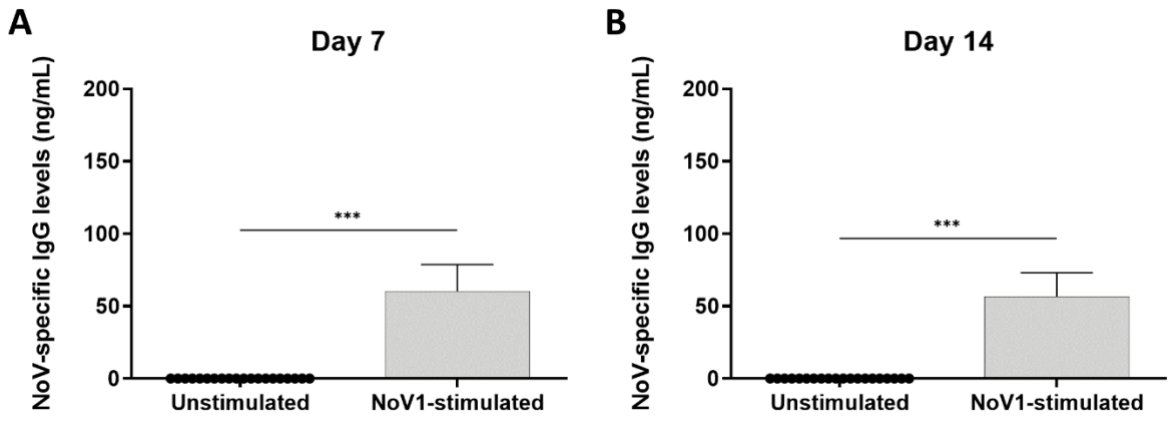

Figure 6.3. Norovirus VLP vaccine induces the production of NoV-specific IgG in human tonsillar MNC. Culture supernatants from tonsillar MNCs were collected 7-and 14-days post stimulation with 0.1μg/ml of VLP-based vaccine candidate (NoV1). Norovirus-specific IgG antibodies were detected by ELISA using norovirus VLP as coating antigen and quantified against a IVIg reference standard curve. Data were represented as mean + SEM. Statistical analyses were performed by GraphPad 9 using paired t test; ***P <0.001.

6.2.2 Mucosal B cell antibody response to Norovirus VLP Vaccine in Human NALT

B cell-mediated mucosal IgG response to norovirus was determined by ELISA following human NALT *ex vivo* stimulation with NoV1. As shown in Figure 6.3, significant levels of norovirus-specific IgG antibody were observed in human tonsillar cell culture supernatants after stimulation with NoV1 vaccine (n=20; 10 adults). Marked production of norovirus-specific IgG antibodies was detected at both 7-and-14 days after vaccine stimulation as compared to unstimulated controls (Fig. 6.3. A, B).

Furthermore, we evaluated the adjuvant capacity of α-GalCer during NoV1 vaccine stimulation in human NALT. Notably, an increased norovirus-specific IgG response was observed using the NoV1/α-GalCer combination as compared to either vaccine or adjuvant alone controls (Fig. 6.4). Norovirus-specific IgG responses were observed in human tonsillar cell culture supernatants at both day 7 and day 14 following NoV1/α-GalCer stimulation (Fig. 6.4)

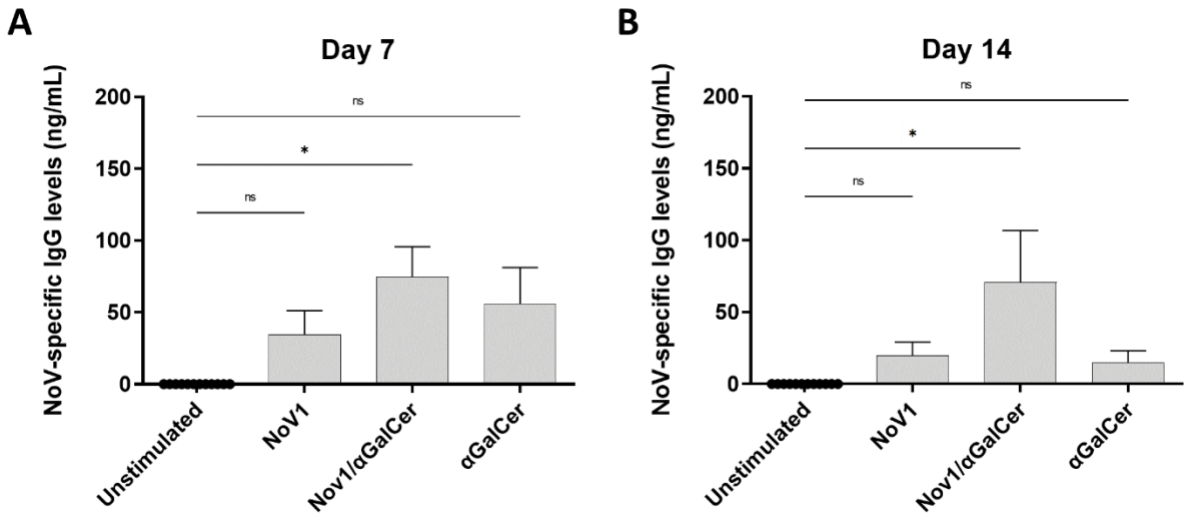

Figure 6.4. α-GalCer enhances NoV1 vaccine-induced IgG production to norovirus in human tonsillar MNC. Human tonsillar MNC were stimulated for 14 days with either 0.1μg/ml norovirus VLP vaccine (NoV1) alone or in combination with 0.1μg/ml α-GalCer (NoV1/α-GalCer). Presence of norovirus-specific IgG antibodies in cell culture supernatants were evaluated by ELISA at day 7 (A) and day 14 (B) post-stimulation. Data was represented as mean + SEM. Statistical analyses were performed by GraphPad 9 using ANOVA multiple comparison *p <0.05, ns: not significant.

6.3 PART III: Evaluation of the Effect of Pre-Existing Immunity on Rotavirus and Norovirus Vaccine-Induced Antibody Immune Responses.

On this section, we aimed to examine the relationship between pre-existing immunity, i.e., serum virus-specific antibody levels as described in Chapter IV, and the mucosal antibody response induced by a live-attenuated monovalent rotavirus vaccine (RV1). In addition, we also studied the relationship between pre-existing immunity to human NoV and the mucosal antibody response induced by VLP-based NoV vaccine candidate (NoV1).

For correlation analyses, samples with undetectable antibody titre for each assay (virus-specific IgG and IgA) were assigned a value of half of the lower detection limit as previously described elsewhere (147). The lower limit of detection was calculated from the respective 4-Parameter Logistic (4PL) standard curves derived from purified human IgG or IgA by MyAssays software using parameter “a”; which represent the minimum value that can be obtained (i.e., at dose zero or unstimulated control). Final concentration values for all samples were multiplied by 10 (referred as ELISA units, EU) and then Log_{10}-transformed for correlation analyses.

6.3.1 Relationship between Pre-existing Immunity and Rotavirus Vaccine-Induced Mucosal B Cell Antibody Response

Mucosal antibody responses in tonsillar MNC following rotavirus vaccine stimulation were studied using tonsillar tissue samples from fifty-one children (2-16 years, median: 5 years) and adults (17-43 years, median: 23 years) as described above. The relationship between the mucosal antibody response and pre-existing immunity, i.e., rotavirus-specific antibody levels in sera, was further analysed.

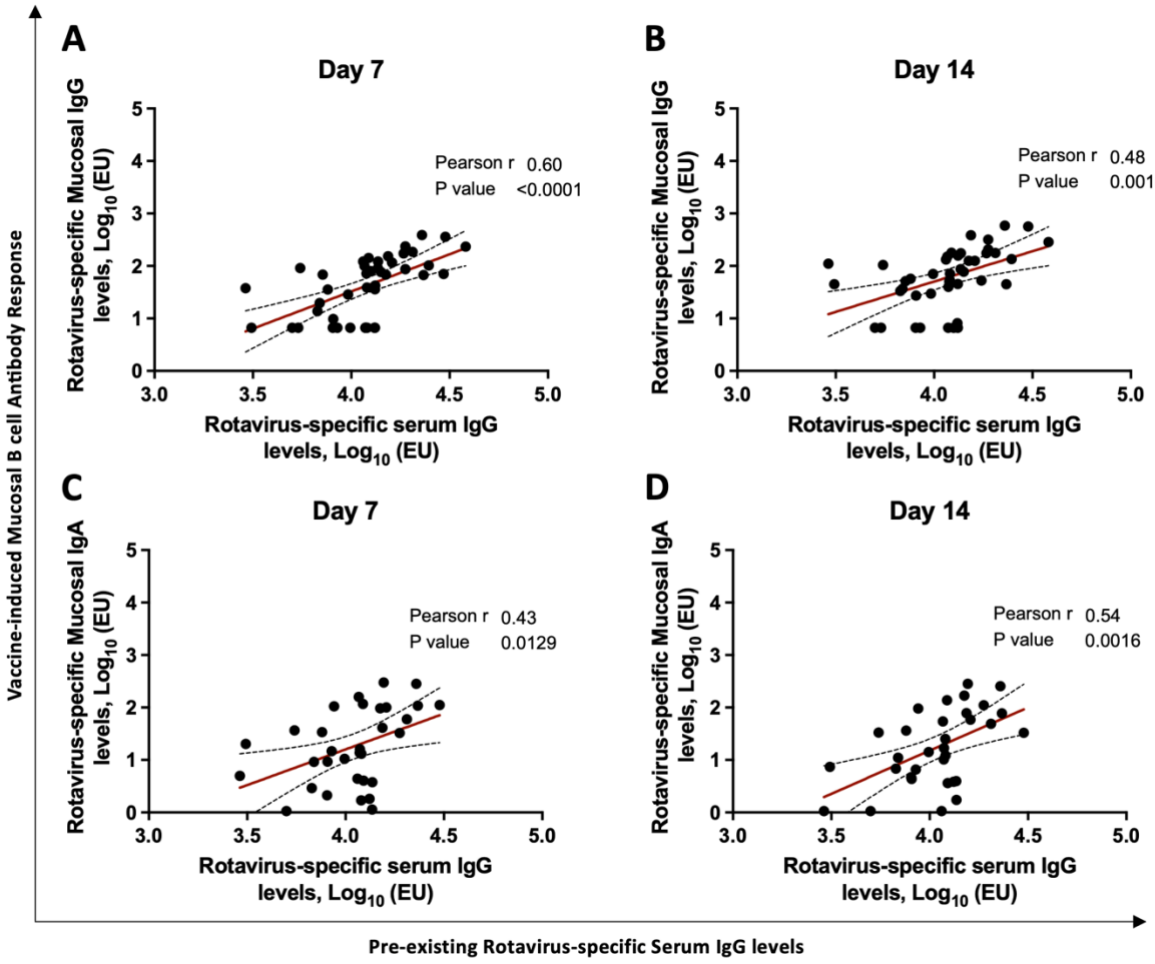

Figure 6.5. Rotavirus vaccine-induced Mucosal B cell antibody response correlates with pre-existing virus-specific serum antibody titres. Culture supernatants from human tonsillar MNCs were collected at 7-and 14-days after RV1 vaccine stimulation and rotavirus-specific antibody levels were determined by ELISA. Log_{10}-transformed data from vaccine-induced mucosal B cell IgG (A, B) and IgA (C, D) responses to rotavirus and patients' pre-existing rotavirus-specific serum IgG titres were correlated respectively. Statistical analysis using Pearson correlation (r) was performed by GraphPad prism 9; Red line: linear regression.

As shown in **Figure 6.5**, the tonsillar B cell antibody response following rotavirus vaccine stimulation was positively correlated with rotavirus-specific IgG titres found in patients´ sera. Statistical analyses using Pearson correlation and linear regression were performed using GraphPad prism 9. A strong correlation was observed between pre-existing serum anti-rotavirus IgG antibodies and RV1-induced IgG responses in tonsillar MNC at day 7 (N= 44, Pearson r: 0.60, P<0.001) and day 14 (N= 44, Pearson r: 0.48, P<0.001) post vaccine stimulation (Fig. 6.5. A, B). Additionally, a positive correlation was also observed for rotavirus-specific IgA responses in tonsillar MNC and pre-existing serum IgG levels (Fig. 6.5. C, D) (N= 33; Pearson r: 0.43, P<0.01, and r: 0.54, P<0.002 were observed at D7 and D14 respectively).

6.3.2 Pre-existing Immunity and vaccine-induced antibody response to human Norovirus

Fifty immunocompetent children (1.5-16 years, median: 4 years) and adults (17-45 years, median: 23 years) referred to adenotonsillectomy due to upper-airway obstructions or tonsillitis were included in this study. From the total recruited participants, 20 were analysed for NoV1-induced mucosal B cell antibody response in human NALTs and further used for correlations analyses based on their pre-existing immunity data (i.e., serum NoV-specific serum IgG levels). As shown in **Figure 6.6**, NoV1-induced IgG response in the tonsillar MNC was positively correlated with the serum pre-existing immunity to norovirus. A positive correlation was observed between serum NoV-specific IgG levels and NoV1-induced IgG response from day 7 (Pearson r: 0.45, P<0.068) and day 14 (Pearson r: 0.64, P<0.005) post stimulation (Fig. 6.6. C, D). A positive trend was also observed between patients pre-existing norovirus immunity and the virus-specific mucosal IgG response induced by NoV1 vaccine in combination with α-GalCer adjuvant (data not shown).

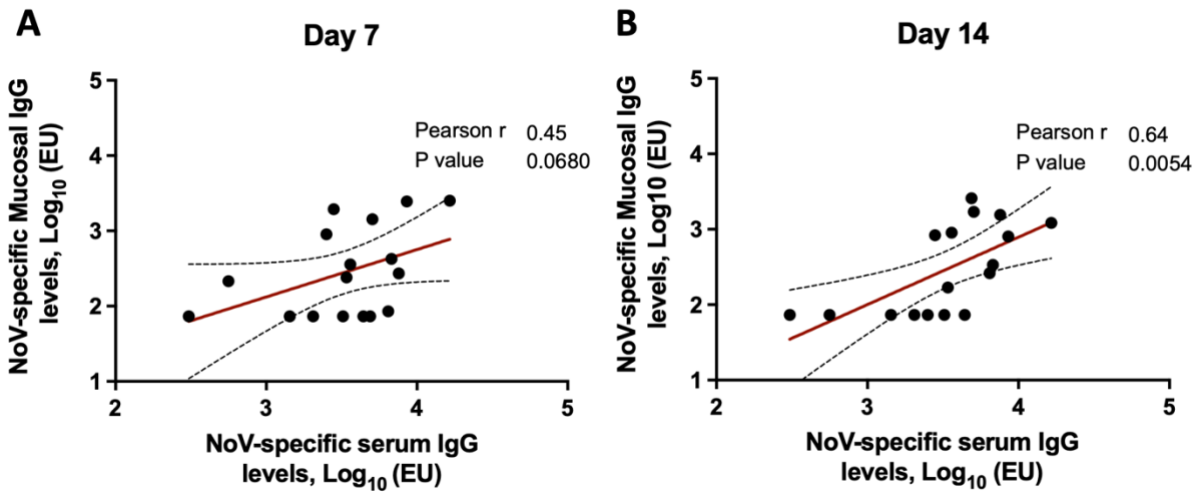

Figure 6.6. Relationships between pre-existing serum anti-NoV IgG antibody levels and NoV1 vaccine-induced Mucosal IgG antibody response. Log_{10}-transformed data from serum anti-NoV IgG titres were analysed in association with NoV1 vaccine-induced mucosal B cell IgG responses from day 7 (C) or day 14 (D). Statistical analysis using Pearson correlation (r) were performed by GraphPad prism 9; Red line: linear regression.

6.4 Conclusion

In this chapter, we described the mucosal B cell antibody response to rotavirus vaccine and VLP-based norovirus antigens using human tonsillar tissues from children and adults as a key compartment for mucosal immunity.

We show that a live attenuated rotavirus vaccine (RV1, Rotarix®) induced a robust virus-specific mucosal B cell antibody response in NALT of children and adults. Particularly, we show that both IgG and IgA rotavirus-specific antibodies significantly increased following tonsillar MNC stimulation with RV1 and positively correlated with patients' pre-existing immunity to rotavirus. These results confirm the high efficacy and immunogenicity of Rotarix in the UK, where high shedding and seroconversion rates has been described in RV1-vaccinated infants, born even from mothers with high RV-IgA levels in breast milk and serum (148). In this line, our results suggest that patient`s pre-existing immunity (shown as baseline IgG levels to rotavirus) may reflect the immunogenic nature of cumulative rotavirus exposures (i.e., early exposures and mild or asymptomatic re-infection), which translates to high vaccine-induced mucosal responses in subjects from high-income countries. However, pre-existing antibodies has been negatively correlated with oral-rotavirus vaccine response in LMIC (148) and

merits further study, considering for example a broad human NALT cohort, particularly from developing countries.

On the other hand, we also showed that non-replicating NoV VLP-based antigens (NoV1) significantly induced GII.4 norovirus-specific IgG responses in NALT of children and adults. Interestingly, the NoV1-induced mucosal antibody response positively correlated with patients pre-existing serum anti-NoV IgG levels and may indicate a potential a correlate of immune protection against norovirus. HBGA-blocking antibodies have been widely correlated with protection against norovirus illness and disease severity and must be considered in future vaccines studies using human NALT (64). Interestingly, NoV1 when co-administered with α-Galactosylceramide (α-GalCer) showed a higher NoV1-specific mucosal antibody response in NALT of children and adults. Non-parenteral coadministration of α-GalCer with immunizing antigen results in enhanced production of antigen-specific antibodies in mice (149). Thus, our result provides new evidence about the mucosal adjuvanticity of α-GalCer, as previously described for experimental oral-delivered vaccines against enterotoxigenic Escherichia coli (ETEC) and Cholera (79), and its potential application for VLP-based candidates formulation. Although α-GalCer function was not directly evaluated on this chapter, its known that αGalCer-activated iNKT cells can provide non-cognate B cell help for the generation of B cell memory and long-lived antibody responses directed against protein antigens (150, 151). Moreover, the activation of NK T cells by α-GalCer rapidly induces *in vivo* DCs maturation promoting both $CD4^+$ and $CD8^+$ T cell immunity to a co-administered protein (152). However, we previously shown only a mild T cell response induced by NoV1/α-GalCer in human NALT (Chapter 5). Therefore, further studies are needed to determine which other populations, such as DC and/or NKT cells and follicular helper T cells are involved in α-GalCer mucosal adjuvanticity.

Collectively, this chapter also confirm the capacity of human NALTs as induction sites for virus-specific adaptive immune responses induced by enteric vaccines and new mucosal adjuvants, and at the same time highlight the potential impact of immunological imprinting on mucosal antibody immune responses to both rotavirus vaccine and VLP-based norovirus antigens and their potential implication for future vaccine trials.

CHAPTER VII

General Discussion

CHAPTER VII

General Discussion

Human rotavirus and noroviruses (NoV) are the leading cause of acute gastroenteritis (AGE) in children under five years of age and a major public health burden in the human population causing globally over 0.4 million deaths per year due to diarrhoeal diseases. Two antigenically distinct oral live-attenuated rotavirus vaccines have been licensed and used widely over the past 15 years. This study focused on Rotarix®, or RV1 (GlaxoSmithKline), a monovalent rotavirus vaccine licensed in Europe and Latin America in 2006 and in 2008 in the United States. In the UK, RV1 was introduced into the national childhood immunisation schedule in July 2013 and currently is commercially available worldwide in over 100 countries. Despite such progress, the lack of absolute correlates of protection and considerable variations in rotavirus vaccine efficacies among different socioeconomic settings remains a major concern to address. On the other hand, while research efforts to develop a safe and efficient NoV vaccine are still in progress, the immune correlates of protection remain incompletely understood. In this PhD project, I studied mucosal immune responses in human NALT to RV1 vaccine and a candidate NoV vaccine. The results provide important insights into mucosal immunity to enteric vaccines and to our current understanding of the immune response against human rotavirus and norovirus.

7.1 Vaccine-Induced Mucosal Immune Response and Their Associated Mechanisms of Protection

The present study provided a comprehensive evaluation of the mucosal immunity in children and adults to both rotavirus vaccine and norovirus antigens. We used human tonsillar tissues as an *ex vivo* cell culture system modelling nasopharynx-associated lymphoid tissue (NALT) to describe the immunogenicity of two different oral enteric vaccines/immunogens: a live-attenuated monovalent rotavirus vaccine (RV1) and a VLP-based GII.4 norovirus potential vaccine candidate (NoV1). Tonsils are organised mucosal lymphoid tissues and known induction sites for immune responses against many pathogens, including Poliovirus and Influenza (39, 40). Freshly isolated tonsillar MNCs contain essential cellular components necessary to mount a protective antigen-specific adaptive response, such

as $CD3^+$ T cells (34-45%) and high percentages of $CD19^+$ B cells (up to 75%) (37). Human tonsillar MNC can be isolated at high yields ($1x10^8$-$2x10^9$ cells per pair of tonsils) functioning also as an important source of NK cells and antigen presenting cells, i.e., DCs (153, 154). These components are essential for the development of adaptive immune responses to LAV (39).

7.1.1 Mucosal immune response induced by live-attenuated rotavirus vaccine in human NALT

We have shown that RV1 vaccine (Rotarix®, GSK) promotes a robust mucosal rotavirus-specific antibody production in NALT from children and adults. Several studies have provided evidence of protective antibodies induced by natural rotavirus infection (116, 155) and oral rotavirus vaccines (55, 118, 156, 157) highlighting the importance of rotavirus-specific antibody response against disease severity. Most of these serological studies have focused on rotavirus-specific IgA and IgG antibodies yet with mixed results. Therefore, studies on the mucosal antibody response may provide valuable insights on the protective role against rotavirus illness (128). The presence of rotavirus-specific IgA and IgG antibodies in the gut (measured as copro-antibodies) have shown to be associated with disease protection in animal models (158-160) and human studies (109, 161, 162). By using tonsils of children and adults as a mucosal model, we evidenced that mucosal B cell antibody responses to RV1 vaccine were characterized by an increased production of both rotavirus-specific IgG and IgA antibodies in tonsillar cell culture supernatants at day 7 and day 14 following RV1-stimulation. These results confirm the high mucosal efficacy and immunogenicity of Rotarix in a high-income country cohort (148). Contrary to the predominant intestinal IgA response to rotavirus, we observed a higher ratio of rotavirus-specific IgG/IgA in NALT from children and adults following RV1-stimulaton. This particular difference may be related to the general predominance of IgG (55–72%) over IgA (13–18%) immunoglobulin-producing cells, i.e., plasmablast or PCs, in human NALT tissues (163, 164). Previous studies using a similar tissue culture strategy, have described a predominant virus-specific IgG antibody response in human tonsillar MNCs following stimulation with live-attenuated vaccines such as LAIV and MMR (39). A recent study has suggested a protective neutralizing role of rotavirus-specific IgG antibodies, after IgG-deficient mice shown a significant deficit in intracellular antibody-mediated protection against rotavirus (60). Moreover, intracellular rotavirus neutralization may be mediated by

VP6-specific IgG more efficiently than VP6-specific IgA antibodies (60). Although rotavirus-neutralization assays were not included in this study, the significant rotavirus-specific IgG responses evidenced in NALT from both children and adults strongly support the role of IgG antibodies as an essential component of mucosal immune responses against rotavirus.

We also showed that rotavirus vaccine (RV1) elicited a marked T cell immune response in human NALT. Human tonsillar T cells are composed of predominantly $CD4^+$ subsets (>80%) and $CD8^+$ T cells (37). We found increased frequencies of IFN-γ-producing cells and proliferative responses from both $CD3^+CD4^+$ and $CD3^+CD8^+$ subsets in RV1-stimulated tonsillar MNCs. Although several studies using human PBMCs have shown cell-mediated responses following rotavirus stimulation (62, 136, 137), to our knowledge this is the first *ex vivo* study supporting mucosal antigen-specific T cells responses to a live-attenuated rotavirus vaccine in children and adults. Natural rotavirus infection is generally a poor inducer of circulating T cells that secrete IFN-γ, however higher frequencies of rotavirus-specific IFN-γ-secreting $CD4^+$ and $CD8^+$ T cells have been detected in infected adults as compared to both healthy adults and children with acute rotavirus diarrhoea (62, 136). $CD4^+$ T cells have proven to be essential for plasmablast differentiation and for the magnitude and affinity of the antibody response to LAV (39). Additionally, $CD4^+$ T cells are also important for the development of rotavirus-specific intestinal IgA response in mice (137). We showed that T cell responses in tonsillar MNCs were not homogenous with significant variations. Overall, our data suggest the presence of both IFN-γ-producing and proliferative rotavirus-specific T cells (both $CD8^+$ and $CD4^+$ T cells) and the activation of local immunity by RV1 stimulation. Further, using $CD45RO^+$ cell depleted tonsillar MNC, we found that RV1 induced a significant native T cell response, demonstrated by the increase in frequencies of IFN-γ producing and proliferative T cell responses from both children and adults NALTs. Therefore, our findings support the role of tonsils as a mucosal induction site for rotavirus vaccines.

7.1.2 Mucosal immune response induced by a Norovirus VLP vaccine candidate in human NALT

Clinical trials on Norovirus vaccines have been performed using VP1-based VLPs made from the most commonly circulating human NoV strains (71, 73, 165). Most clinical studies have been performed in

healthy adults, which may not represent the immunological behaviour of infants and young children, who are exposed most to the infection/disease, and thus, with a higher antigenic diversity among strains (165). Moreover, the lack of mucosal immune correlates of protection in both adults and children remains a significant challenge to guarantee the success of NoV vaccines. We therefore studied and provided the first data on mucosal immunity to norovirus GII.4 VLPs (referred to as NoV1) using NALT from children and adults.

We showed that NoV1 vaccine candidate elicits a marked production of GII.4 NoV-specific IgG antibodies 7-and-14 days after tonsillar MNCs stimulation. VLP-based vaccines alone have been shown to be more efficacious than common subunit vaccines (78). However, studies with adult volunteers have described higher NoV-specific IgG antibody responses in sera after challenge with live wild-type Norwalk virus than oral vaccination with Norwalk VLPs, suggesting that mucosal adjuvants may improve the immunogenicity of VLP-based formulations against norovirus (138, 166).

Indeed, we provided evidence that NoV1 immunogenicity was potentiated after VLP combination with the adjuvant α-GalCer, with an overall NoV-specific IgG response rate of 92% (100% in adults and 80% in children) as compared to NoV1 vaccine alone (65% overall; 70% in adults and 60 % children). These findings were consistent with data from an oral immunization experiment in mice using VLPs, where we observed that only vaccinated groups who received GII.4 NoV VLPs (NoV1) adjuvanted with α-GalCer were able to develop both mucosal and systemic NoV-specific antibody responses. To date, most licensed VLP-based vaccines, including NoV vaccine candidates, have incorporated adjuvants in their formulations. Takeda's bivalent NoV vaccine candidate (TAK-214), as an intramuscular injection of purified GI.1 and GII.4 (2006a, Yerseke; 2006b, Den Haag; and 2002, Houston) VP1-based VLPs using $Al(OH)_3$ as adjuvant, have progressed into an advanced stage of development showing a 62% efficacy against moderate/severe NoV-associated AGE in healthy US adults (76). However, while several adjuvants are licensed for use in parenteral vaccines, there are currently no adjuvants included in clinically applied oral vaccines (73, 76-78, 167). Only experimental studies performed in mice have described the mucosal adjuvanticity of α-GalCer when orally administered with whole-cell killed vaccines against Enterotoxigenic Escherichia coli (ETEC) (168)

and Cholera (79), showing a significant increase in both mucosal and systemic antigen-specific IgA and IgG antibody production. Our results provided supporting evidence on the potential role of α-GalCer as a human mucosal adjuvant for VLP delivery.

Adjuvants can also help to reduce vaccine dosage and promote a stronger response among low-responders individuals, such as neonates and the elderly (78, 167). Notably, while the use of NoV1 alone (0.1 μg/ml) elicited GII.4 NoV-specific mucosal B cell antibody response in tonsillar MNCs from children and adults, we observed that higher VLP concentrations (0.5-2.5 μg/ml) did not improve this response (Appendix C). Similar results have been described using two-times or higher oral dosage of Norwalk VLPs in humans, suggesting that mucosal antigen uptake and processing sites could be saturated at higher dose of VLP particles (138). Using a low dose NoV VLP (0.1 μg/ml) adjuvanted with α-GalCer we demonstrated a significantly increased GII.4-specific IgG response in both adults and children. Therefore, our study supports the use of α-GalCer adjuvant and NoV VLP as an orally delivered vaccine formulation in subsequent human challenges studies and for potential vaccine dose-sparing evaluation making vaccine production costs more affordable.

7.2 Characterization of Pre-Existing Immunity to Rotavirus and Norovirus in Children and Adults

We further described the serological levels of pre-existing antibodies to rotavirus and norovirus in a cohort of patients referred to adenotonsillectomy from 2017 to 2021. Overall, we observed an heterogenous distribution of both Rotavirus and Norovirus-specific antibody levels among patients, which significantly increased with age. As described for influenza virus, immune system imprinting by natural infection and the accumulation of antigen-specific antibody responses through life involves complex individual antibody profiles reflecting both recent and past exposures (120).

7.2.1 Pre-existing norovirus-specific immunity and its relationship with mucosal immune response

Using VP1-based VLP from a GII.4 2012-Sydney strain (GII.4-SYD), we showed that pre-existing serum GII.4 NoV-specific IgG antibody levels significantly increase after the first few years in life.

These findings are consistent with the increased prevalence of NoV infection and NoV-specific antibodies described in children (124). Moreover, by analysing a wider age range (1.5 - 43 years), we showed that GII.4-2012 NoV-specific IgG antibodies are also present in adolescent and adults. In agreement with a previous report performed in samples from adults for antibodies to GII.4-SYD and GII.4-99 strains (169), our results confirmed that GII.4-SYD NoV-specific antibodies were present in all subjects analysed in this study (N=50). Additionally, we found that GII.4-SYD NoV-specific antibodies positively correlates with patients' age, suggesting that NoV previous exposure history accumulates throughout the years. These findings are consistent with described global prevalence of GII.4 NoV strains (26, 121, 122, 124, 170). Since 2012 pandemic, GII.4-SYD has emerged as the primary norovirus strain in most countries (123, 171). In addition, a novel NoV lineage (GII.P16-GII.4 Sydney 2012; referred as GII.4-2015) containing GII.4-SYD capsid has been detected in Asia and Germany, while parallelly circulating in the UK and USA since 2014 (172). Although a recent study suggests that antigenic variation in GII.4-2015 capsid may impact on antibody blocking activities (26), we cannot fully exclude the presence of antibody levels to this novel strain using our VP1-based VLP approach.

While the serological diversity was not directly evaluated in the present study, previous reports have demonstrated the generation of both homotypic and heterotypic immunity in adults' sera following GII.4 infection and vaccination (173, 174). Particularly, homotypic antibody responses to GII.4 strains seem to be stronger and long-lasting as comparted to heterotypic counterpart (173-175), suggesting that previous exposure history to a dominant circulating genotype (e.g., natural infection to GII.4-SYD) may have a significant impact on vaccine-induced antibody response. Indeed, we showed that pre-existing serum IgG levels to GII.4-SYD positively correlated with homotypic NoV-specific IgG antibody response in human NALT following stimulation with NoV1 vaccine candidate. Notably, we found that pre-existing NoV-specific immunity also correlates with NoV1-induced mucosal IFN-γ responses mediated by both $CD4^+$ and $CD8^+$ subsets in tonsillar MNCs. Although little information is available regarding the role of T cells during NoV infection, human challenge studies describing both GI. I and GII NoV-induced responses have shown increased $CD4^+$ T cell responses characterized by a significant

IFN-γ production (176, 177). Similarly, NoV VLPs immunization studies in adults have reported an increased IFN-γ response by NoV-specific T cells (138). Recent reports have described an increased magnitude of T cell response to NoV GII.4-VLPs in children and adults, however no correlation between cell-mediated responses and previous NoV immunity (measured by NoV-specific IgG seroconversion) was observed (124, 169). Nevertheless, all these studies have been performed in human PBMCs and might not represent the mucosal immune environment associated with enteric virus-specific immune responses.

Current advances using human intestinal enteroid (HIE) cultures have shown an upregulation of IFN signalling during NoV infection and a strain-specific sensitivity to different host interferon pathways, as both type I and III responses were not enough to control GII.4 NoV infection (178). GII.4 SYD strain has shown major antigenic differences with previous circulating outbreaks strains, which are associated with GII.4 escape from herd immunity (123, 171), however conserved T cell epitopes among different strains have been described (110, 179, 180). Interestingly, we also observed a significant relationship between pre-existing NoV Immunity and T cell-mediated IFN-γ response induced by NoV1 vaccine adjuvant with α-Galcer. Therefore, further studies are needed to evaluate the role of mucosal T cell mediated IFN response against NoV infection. Although a larger sample size is needed to support our findings, the present study provides novel evidence which correlates both T cell and B cell-mediated mucosal immunity to NoV with pre-existing homotypic immunity in children and adults, suggesting a protective role of both mucosal IFN-γ and NoV-specific IgG antibodies against Norovirus. Moreover, these findings support the potential for mucosal delivery of non-replicating NoV VLPs for a human NoV vaccination, although complementary functional assays of vaccine-induced mucosal T cell and B-cell mediated responses against NoV infection requires further investigation.

7.2.2 Pre-exiting rotavirus-specific immunity and its relationship with mucosal immune response

We showed that pre-existing serum rotavirus-specific IgG antibody titres were detected in all the individuals studied, and that significantly increased with age. Our ELISA approach used antigens derived from whole SA11 rotavirus particles, a prototype strain of group A rotaviruses which has been widely used for serological detection of rotavirus-specific antibodies (97). In this regard, the use of

whole purified virus may increase the range of antigenic epitopes likely recognized by patients` sera. In the same way, cell-grown animal strains have been used in human rotavirus vaccine studies (181), which in general are based on a Jennerian approach defined by the presence of a common rotavirus group antigen (VP6) shared between animal and human rotaviruses. Rotavirus VP6 is highly conserved and immunogenic, and most rotavirus-specific antibodies are likely directed to this protein (182). Therefore, the pre-existing rotavirus-specific antibodies detected among the patients in our study are likely a combination of both homotypic and heterotypic response (i.e., polygenic and cross-reactive when compared to RV1 vaccine strain). While serum rotavirus-specific IgA has commonly been used for determination of rotavirus infection and vaccine-induced antibody responses in clinical trials, others have recognized serum rotavirus-specific IgG antibodies as the most reliable marker for seroconversion and as a proxy for protection against severe disease in children (183). Moreover, maternal rotavirus-specific IgG antibodies was the most important predictor of post-vaccination RV-IgA among infants with neonatal infection (148). Indeed, we showed a strong positive correlation between pre-existing IgG levels and mucosal antibody response following RV1-stimulation in both children and adults. Thus, in line with the natural history of rotaviruses, our findings indicate that increasing pre-existing immunity levels may be associated with multiple infections throughout life, suggesting that serum rotavirus-specific IgG levels as a more accurate and long-term indicator of pre-existing immunity as compared to acute infection markers such as described for rotavirus-specific IgA and IgM (183).

High levels of pre-existing serum IgG antibodies against rotavirus have shown inhibitory effects on RV1 immunogenicity among infants, while may contribute to decreased vaccine efficacy in low-income countries (93). A possible hypothesis is that neutralization of live-attenuated vaccines by pre-existing antibodies could consequently decrease the amount of viral antigens below the threshold for immune detection and recognition (91). Interestingly, in this study, while the mucosal rotavirus-specific antibody response induced by RV1 was positively correlated with pre-existing serum antibody titres, by contrast, the relationship between RV1-induced cellular responses in tonsillar MNCs and the pre-existing immunity appeared rather different. Overall, there were no statistically significant correlations between the several T cell response indicators and the pre-existing serum antibody titres. However, in

contrast to the markedly positive correlation observed in the antibody responses, a trend of inverse correlations was noted between the pre-existing immunity and both $CD4^+$ and $CD8^+$ T cell-mediated mucosal IFN-γ responses. As the sample size (number of patients) is small and a more variable T cell responses detected, a potential negative association cannot be ruled out, and further studies with large sample sizes are warranted to define this relationship. Weak correlations between seroconversion and cell-mediated IFN-γ response to rotavirus have been described in children under 5 years, with high individual variations (44). Of particular interest, detailed analysis of a small number of six children (3-16 years, median 4.5) revealed a strong negative correlation (Pearson r = -0.76, p=0.038) between the pre-existing immunity and IFN-γ producing CD4+T cell response induced by RV1. Specifically, this group shown a marked low/non-response of IFN-γ-producing T cells following tonsillar MNC stimulation with RV1 as compared to unstimulated control (Fold change $\leq$ 1) and therefore was analysed separately. Interestingly, a similar inverse relationship between the pre-existing immunity and IFN-γ producing CD8+T cell response induced by RV1 (Pearson r = -0.75, p=0.044) was also shown by analysing the same group of children. Further analysis from this group also revealed a low mucosal rotavirus-specific IgG response in RV1-stimulated Tonsillar MNCs. These findings may suggest a possible novel hypothesis that pre-existing immunity (antibody levels) due to previous exposure history may play an important role in affecting the vaccine-induced mucosal T cell responses which could be a crucial immune correlate of vaccine-induced protection, especially in the highly susceptible young patient groups. However, a more robust analysis with larger sample size needs to be performed to support this notion.

We have shown that RV1-stimulation induce the expression of the gut homing receptor α4β7 in human tonsillar $CD4^+$ and $CD8^+$ T cells. Reports using children PBMCs after acute rotavirus infection (142) or vaccination with a live-attenuated precursor of RV1 vaccine (RIX-4414) (63) have described the presence of circulating rotavirus-specific memory $CD4^+$ T cells expressing α4β7, yet little is known about the immune protective role of this subset. To date only studies with memory B cells expressing α4β7 have shown their importance for clearance and protection against rotavirus infection (143, 184). α4β7 interacts with MAdCAM-1 expressed on venules within different gastrointestinal tissues

facilitating the homing of $\alpha4\beta7^+$ cells to the gut (185). However, only a weak correlation between circulating rotavirus-specific $\alpha4\beta7^+$ memory B cells and disease protection (measured as rotavirus-specific IgA seroconversion) have been described in a RIX4414 vaccine trial using both vaccinees and placebo recipients (162). Here we showed that increased frequencies of RV1-induced tonsillar $\alpha4\beta7^+CD4^+$T cells positively correlate with pre-existing immunity to rotavirus (i.e., rotavirus-specific IgG levels in patient`s sera; two-tailed Pearson test: $r = 0.46$, $p<0.047$). As we showed that human NALT tissues are good induction sites for rotavirus vaccine-induced T and B cell immune responses, they may constitute an important reservoir of activated memory and effector T cells capable of migrating to other tissues via efferent lymph and blood. In fact, a previous study has described the induction of both local and systemic B-cell responses, with circulating specific memory B cell, after the direct immunization of the palatine and nasopharyngeal tonsils in adult volunteers (186). Another study exploiting latent Epstein-Barr Virus (EBV) infection of memory B cells have suggested that B-cell trafficking from Waldeyer`s ring may migrate mainly to peripheral blood and to a less extent into systemic lymphoid organs, such as mesenteric lymph nodes (187). In addition, a study using class II tetramers loaded with rotavirus peptides have suggest that human blood rotavirus-specific $CD4^+$ T cells expressing α4β7 homing receptor may be primed locally at the intestine and therefore represent their intestinal counterparts (63). The findings in this study suggest a local activation of mucosal T cells in NALT from children and adults expressing the α4β7 homing receptor following RV1-stimulation, therefore a potential source of effector RV-specific T cells migrating to intestinal sites against RV infection. Further detailed studies with larger sample size will increase our understanding on the importance of these RV vaccine-induced specific T cell population with intestinal homing potential.

Closing Remarks

This study has several important implications for the testing of present and new mucosal vaccines. We provided evidence that human NALT may be an important immune induction sites for enteric mucosal vaccines, and that human NALT immune tissue could be used to study both vaccine-induced responses and underlying immune mechanisms of protection by mucosal vaccines. Following *ex vivo* stimulation, we demonstrated that either a live attenuated rotavirus vaccine (RV1) or a non-replicating NoV VLP-

based vaccine candidate (NoV1) elicited virus-specific mucosal B cell antibody responses in NALT of children and adults. Moreover, we showed a positive relationship between the virus-specific mucosal antibody responses induced by these mucosal vaccines and patients' pre-existing immunity to either rotavirus or norovirus, respectively. We first evidenced that both pre-existing rotavirus-specific and GII.4 NoV-specific IgG antibody titres in sera increase with age. Secondly, the magnitude of either RV1 or NoV1 induced mucosal antibody response in human NALT correlated with their respective virus-specific IgG levels in sera, suggesting a role of natural infections on the accumulation of antigen-specific antibodies through life and the potential impact of immunological imprinting on the immune response induced by mucosal vaccines. We also show that the rotavirus vaccine elicited marked T cell responses in NALT of children and adults, with increased frequencies of both CD4+ and CD8+ IFN-γ-producing T cells, T cell proliferative responses and α4β7-expressing tonsillar T cells.

Although no significant correlation was found between mucosal T cell responses and pre-existing antibody titres, there was a trend of inverse correlation particularly in those individuals who demonstrated low/no mucosal T cell response following rotavirus vaccine stimulation. This finding, if confirmed by further studies, would suggest pre-existing antibodies affect mucosal T cell responses induced by enteric vaccines, which may be an important correlate of vaccine-induced protection. findings in this study.

However, these findings are subject to some limitations and cautious interpretation of vaccine-induced immune responses must be considered. First, HBGA expression patterns were not evaluated between recruited individuals and may shape subsequent immune susceptibility to both rotavirus and norovirus and vaccines efficacy. Second, we cannot discard the presence of an asymptomatic or symptomatic infection when samples were collected. Thus, future studies will need to examine patients' profiles, including their vaccination history and a wide range of related illness (mild to severe). Lastly, given tonsils are an accessible source of human tissue containing key cell types involved in adaptive immunity, future studies with a larger cohort including patients from LMIC would help to investigate the role of immunological imprinting on patients from high viral prevalence areas and the potential impact of pre-existing immunity on vaccine-induced immune response and efficacies.

REFERENCES

1. Elliott EJ. Acute gastroenteritis in children. BMJ. 2007;334(7583):35-40.

2. Troeger C, Blacker BF, Khalil IA, Rao PC, Cao S, Zimsen SRM, et al. Estimates of the global, regional, and national morbidity, mortality, and aetiologies of diarrhoea in 195 countries: a systematic analysis for the Global Burden of Disease Study 2016. The Lancet Infectious Diseases. 2018;18(11):1211-28.

3. Troeger C, Khalil IA, Rao PC, Cao S, Blacker BF, Ahmed T, et al. Rotavirus Vaccination and the Global Burden of Rotavirus Diarrhea Among Children Younger Than 5 Years. JAMA Pediatr. 2018;172(10):958-65.

4. Clark A, Black R, Tate J, Roose A, Kotloff K, Lam D, et al. Estimating global, regional and national rotavirus deaths in children aged <5 years: Current approaches, new analyses and proposed improvements. PLoS One. 2017;12(9):e0183392.

5. Tam CC, Rodrigues LC, Viviani L, Dodds JP, Evans MR, Hunter PR, et al. Longitudinal study of infectious intestinal disease in the UK (IID2 study): incidence in the community and presenting to general practice. Gut. 2012;61(1):69-77.

6. Harris JP, Iturriza-Gomara M, O'Brien SJ. Re-assessing the total burden of norovirus circulating in the United Kingdom population. Vaccine. 2017;35(6):853-5.

7. Pires SM, Fischer-Walker CL, Lanata CF, Devleesschauwer B, Hall AJ, Kirk MD, et al. Aetiology-Specific Estimates of the Global and Regional Incidence and Mortality of Diarrhoeal Diseases Commonly Transmitted through Food. PLoS One. 2015;10(12):e0142927.

8. Lopman BA, Steele D, Kirkwood CD, Parashar UD. The Vast and Varied Global Burden of Norovirus: Prospects for Prevention and Control. PLoS Med. 2016;13(4):e1001999.

9. Dolin R, Blacklow NR, DuPont H, Formal S, Buscho RF, Kasel JA, et al. Transmission of acute infectious nonbacterial gastroenteritis to volunteers by oral administration of stool filtrates. J Infect Dis. 1971;123(3):307-12.

10. Bishop RF, Davidson GP, Holmes IH, Ruck BJ. Virus particles in epithelial cells of duodenal mucosa from children with acute non-bacterial gastroenteritis. Lancet. 1973;2(7841):1281-3.

11. Flewett TH, Bryden AS, Davies H. Letter: Virus particles in gastroenteritis. Lancet. 1973;2(7844):1497.

12. Bishop RF, Kirkwood CD. Enteric Viruses. Encyclopedia of Virology. 2008:116-23.

13. Jayaram H, Estes MK, Prasad BV. Emerging themes in rotavirus cell entry, genome organization, transcription and replication. Virus Res. 2004;101(1):67-81.

14. Caddy S, Papa G, Borodavka A, Desselberger U. Rotavirus research: 2014-2020. Virus Res. 2021;304:198499.

15. Crawford SE, Ramani S, Tate JE, Parashar UD, Svensson L, Hagbom M, et al. Rotavirus infection. Nat Rev Dis Primers. 2017;3:17083.

16. Matthijnssens J, Ciarlet M, Rahman M, Attoui H, Banyai K, Estes MK, et al. Recommendations for the classification of group A rotaviruses using all 11 genomic RNA segments. Arch Virol. 2008;153(8):1621-9.

17. Matthijnssens J, Ciarlet M, Heiman E, Arijs I, Delbeke T, McDonald SM, et al. Full genome-based classification of rotaviruses reveals a common origin between human Wa-Like and porcine rotavirus strains and human DS-1-like and bovine rotavirus strains. J Virol. 2008;82(7):3204-19.

18. Doro R, Laszlo B, Martella V, Leshem E, Gentsch J, Parashar U, et al. Review of global rotavirus strain prevalence data from six years post vaccine licensure surveillance: is there evidence of strain selection from vaccine pressure? Infect Genet Evol. 2014;28:446-61.

19. Rasebotsa S, Mwangi PN, Mogotsi MT, Sabiu S, Magagula NB, Rakau K, et al. Whole genome and in-silico analyses of G1P[8] rotavirus strains from pre- and post-vaccination periods in Rwanda. Sci Rep. 2020;10(1):13460.

20. Alfieri AA, Leite JP, Nakagomi O, Kaga E, Woods PA, Glass RI, et al. Characterization of human rotavirus genotype P[8]G5 from Brazil by probe-hybridization and sequence. Arch Virol. 1996;141(12):2353-64.

21. Cunliffe NA, Ngwira BM, Dove W, Thindwa BD, Turner AM, Broadhead RL, et al. Epidemiology of rotavirus infection in children in Blantyre, Malawi, 1997-2007. J Infect Dis. 2010;202 Suppl:S168-74.

22. Kapikian AZ, Wyatt RG, Dolin R, Thornhill TS, Kalica AR, Chanock RM. Visualization by immune electron microscopy of a 27-nm particle associated with acute infectious nonbacterial gastroenteritis. J Virol. 1972;10(5):1075-81.

23. Ludwig-Begall LF, Mauroy A, Thiry E. Noroviruses-The State of the Art, Nearly Fifty Years after Their Initial Discovery. Viruses. 2021;13(8).

24. Chhabra P, de Graaf M, Parra GI, Chan MC, Green K, Martella V, et al. Updated classification of norovirus genogroups and genotypes. J Gen Virol. 2019;100(10):1393-406.

25. de Graaf M, van Beek J, Koopmans MP. Human norovirus transmission and evolution in a changing world. Nat Rev Microbiol. 2016;14(7):421-33.

26. Ruis C, Roy S, Brown JR, Allen DJ, Goldstein RA, Breuer J. The emerging GII.P16-GII.4 Sydney 2012 norovirus lineage is circulating worldwide, arose by late-2014 and contains polymerase changes that may increase virus transmission. PLoS One. 2017;12(6):e0179572.

27. Estes MK, Ettayebi K, Tenge VR, Murakami K, Karandikar U, Lin SC, et al. Human Norovirus Cultivation in Nontransformed Stem Cell-Derived Human Intestinal Enteroid Cultures: Success and Challenges. Viruses. 2019;11(7).

28. Jones MK, Watanabe M, Zhu S, Graves CL, Keyes LR, Grau KR, et al. Enteric bacteria promote human and mouse norovirus infection of B cells. Science. 2014;346(6210):755-9.

29. Jones MK, Grau KR, Costantini V, Kolawole AO, de Graaf M, Freiden P, et al. Human norovirus culture in B cells. Nat Protoc. 2015;10(12):1939-47.

30. Ettayebi K, Crawford SE, Murakami K, Broughman JR, Karandikar U, Tenge VR, et al. Replication of human noroviruses in stem cell-derived human enteroids. Science. 2016;353(6306):1387-93.

31. McGhee JR, Fujihashi K. Inside the mucosal immune system. PLoS Biol. 2012;10(9):e1001397.

32. Brandtzaeg P. Mucosal immunity: induction, dissemination, and effector functions. Scand J Immunol. 2009;70(6):505-15.

33. Brandtzaeg P, Kiyono H, Pabst R, Russell MW. Terminology: nomenclature of mucosa-associated lymphoid tissue. Mucosal Immunol. 2008;1(1):31-7.

34. Silva-Sanchez A, Randall TD. Anatomical Uniqueness of the Mucosal Immune System (GALT, NALT, iBALT) for the Induction and Regulation of Mucosal Immunity and Tolerance. Mucosal Vaccines2020. p. 21-54.

35. Kiyono H, Fukuyama S. NALT- versus Peyer's-patch-mediated mucosal immunity. Nat Rev Immunol. 2004;4(9):699-710.

36. Holmgren J, Czerkinsky C. Mucosal immunity and vaccines. Nat Med. 2005;11(4 Suppl):S45-53.

37. Boyaka PN, Wright PF, Marinaro M, Kiyono H, Johnson JE, Gonzales RA, et al. Human nasopharyngeal-associated lymphoreticular tissues. Functional analysis of subepithelial and intraepithelial B and T cells from adenoids and tonsils. Am J Pathol. 2000;157(6):2023-35.

38. Brandtzaeg P. Immune functions of nasopharyngeal lymphoid tissue. Adv Otorhinolaryngol. 2011;72:20-4.

39. Wagar LE, Salahudeen A, Constantz CM, Wendel BS, Lyons MM, Mallajosyula V, et al. Modeling human adaptive immune responses with tonsil organoids. Nat Med. 2021;27(1):125-35.

40. Shen L, Chen CY, Huang D, Wang R, Zhang M, Qian L, et al. Pathogenic Events in a Nonhuman Primate Model of Oral Poliovirus Infection Leading to Paralytic Poliomyelitis. J Virol. 2017;91(14).

41. Ogra PL. Effect of tonsillectomy and adenoidectomy on nasopharyngeal antibody response to poliovirus. N Engl J Med. 1971;284(2):59-64.

42. Lycke N. Recent progress in mucosal vaccine development: potential and limitations. Nat Rev Immunol. 2012;12(8):592-605.

43. Kim SH, Jang YS. The development of mucosal vaccines for both mucosal and systemic immune induction and the roles played by adjuvants. Clin Exp Vaccine Res. 2017;6(1):15-21.

44. Clarke E, Desselberger U. Correlates of protection against human rotavirus disease and the factors influencing protection in low-income settings. Mucosal Immunol. 2015;8(1):1-17.

45. Bandyopadhyay AS, Garon J, Seib K, Orenstein WA. Polio vaccination: past, present and future. Future Microbiol. 2015;10(5):791-808.

46. The Global Polio Eradication Initiative. Global Polio Eradication Initiative, Polio today http://www.polioeradication.org/. Accessed 21 Dec 2021 [cited 2021 26.12.21]. Available from: https://polioeradication.org/polio-today/history-of-polio/.

47. Babji S, Manickavasagam P, Chen YH, Jeyavelu N, Jose NV, Praharaj I, et al. Immune predictors of oral poliovirus vaccine immunogenicity among infants in South India. NPJ Vaccines. 2020;5(1):27.

48. Combined immunization of infants with oral and inactivated poliovirus vaccines: results of a randomized trial in The Gambia, Oman, and Thailand. WHO Collaborative Study Group on Oral and Inactivated Poliovirus Vaccines. J Infect Dis. 1997;175 Suppl 1:S215-27.

49. Vesikari T. Rotavirus vaccination: a concise review. Clin Microbiol Infect. 2012;18 Suppl 5:57-63.

50. Bernstein DI, Sack DA, Rothstein E, Reisinger K, Smith VE, O'Sullivan D, et al. Efficacy of live, attenuated, human rotavirus vaccine 89–12 in infants: a randomised placebo-controlled trial. The Lancet. 1999;354(9175):287-90.

51. Madhi SA, Cunliffe NA, Steele D, Witte D, Kirsten M, Louw C, et al. Effect of human rotavirus vaccine on severe diarrhea in African infants. N Engl J Med. 2010;362(4):289-98.

52. Patriarca PA, Wright PF, John TJ. Factors affecting the immunogenicity of oral poliovirus vaccine in developing countries: review. Rev Infect Dis. 1991;13(5):926-39.

53. Parker EP, Ramani S, Lopman BA, Church JA, Iturriza-Gomara M, Prendergast AJ, et al. Causes of impaired oral vaccine efficacy in developing countries. Future Microbiol. 2018;13:97-118.

54. O'Ryan ML, Matson DO, Estes MK, Pickering LK. Anti-rotavirus G type-specific and isotype-specific antibodies in children with natural rotavirus infections. J Infect Dis. 1994;169(3):504-11.

55. Patel M, Glass RI, Jiang B, Santosham M, Lopman B, Parashar U. A systematic review of anti-rotavirus serum IgA antibody titer as a potential correlate of rotavirus vaccine efficacy. J Infect Dis. 2013;208(2):284-94.

56. Jiang V, Jiang B, Tate J, Parashar UD, Patel MM. Performance of rotavirus vaccines in developed and developing countries. Hum Vaccin. 2010;6(7):532-42.

57. Angel J, Franco MA, Greenberg HB. Rotavirus immune responses and correlates of protection. Curr Opin Virol. 2012;2(4):419-25.

58. Nair N, Feng N, Blum LK, Sanyal M, Ding S, Jiang B, et al. VP4- and VP7-specific antibodies mediate heterotypic immunity to rotavirus in humans. Sci Transl Med. 2017;9(395).

59. Svensson L, Sheshberadaran H, Vesikari T, Norrby E, Wadell G. Immune response to rotavirus polypeptides after vaccination with heterologous rotavirus vaccines (RIT 4237, RRV-1). J Gen Virol. 1987;68 (Pt 7):1993-9.

60. Caddy SL, Vaysburd M, Wing M, Foss S, Andersen JT, O'Connell K, et al. Intracellular neutralisation of rotavirus by VP6-specific IgG. PLoS Pathog. 2020;16(8):e1008732.

61. Herrera D, Vasquez C, Corthesy B, Franco MA, Angel J. Rotavirus specific plasma secretory immunoglobulin in children with acute gastroenteritis and children vaccinated with an attenuated human rotavirus vaccine. Hum Vaccin Immunother. 2013;9(11):2409-17.

62. Jaimes MC, Rojas OL, Gonzalez AM, Cajiao I, Charpilienne A, Pothier P, et al. Frequencies of virus-specific CD4(+) and CD8(+) T lymphocytes secreting gamma interferon after acute natural rotavirus infection in children and adults. J Virol. 2002;76(10):4741-9.

63. Parra M, Herrera D, Calvo-Calle JM, Stern LJ, Parra-Lopez CA, Butcher E, et al. Circulating human rotavirus specific CD4 T cells identified with a class II tetramer express the intestinal homing receptors alpha4beta7 and CCR9. Virology. 2014;452-453:191-201.

64. Reeck A, Kavanagh O, Estes MK, Opekun AR, Gilger MA, Graham DY, et al. Serological correlate of protection against norovirus-induced gastroenteritis. J Infect Dis. 2010;202(8):1212-8.

65. Atmar RL, Bernstein DI, Harro CD, Al-Ibrahim MS, Chen WH, Ferreira J, et al. Norovirus vaccine against experimental human Norwalk Virus illness. N Engl J Med. 2011;365(23):2178-87.

66. Atmar RL, Ettayebi K, Ayyar BV, Neill FH, Braun RP, Ramani S, et al. Comparison of Microneutralization and Histo-Blood Group Antigen-Blocking Assays for Functional Norovirus Antibody Detection. J Infect Dis. 2020;221(5):739-43.

67. Costantini VP, Cooper EM, Hardaker HL, Lee LE, DeBess EE, Cieslak PR, et al. Humoral and Mucosal Immune Responses to Human Norovirus in the Elderly. J Infect Dis. 2020;221(11):1864-74.

68. Blazevic V, Malm M, Vesikari T. Induction of homologous and cross-reactive GII.4-specific blocking antibodies in children after GII.4 New Orleans norovirus infection. J Med Virol. 2015;87(10):1656-61.

69. O'Ryan ML, Lucero Y, Prado V, Santolaya ME, Rabello M, Solis Y, et al. Symptomatic and asymptomatic rotavirus and norovirus infections during infancy in a Chilean birth cohort. Pediatr Infect Dis J. 2009;28(10):879-84.

70. Lucero Y, Vidal R, O'Ryan GM. Norovirus vaccines under development. Vaccine. 2018;36(36):5435-41.

71. Esposito S, Principi N. Norovirus Vaccine: Priorities for Future Research and Development. Front Immunol. 2020;11:1383.

72. Schiller J, Lowy D. Explanations for the high potency of HPV prophylactic vaccines. Vaccine. 2018;36(32 Pt A):4768-73.

73. Zhang M, Fu M, Hu Q. Advances in Human Norovirus Vaccine Research. Vaccines (Basel). 2021;9(7).

74. Ramirez K, Wahid R, Richardson C, Bargatze RF, El-Kamary SS, Sztein MB, et al. Intranasal vaccination with an adjuvanted Norwalk virus-like particle vaccine elicits antigen-specific B memory responses in human adult volunteers. Clin Immunol. 2012;144(2):98-108.

75. Ball JP, Springer MJ, Ni Y, Finger-Baker I, Martinez J, Hahn J, et al. Intranasal delivery of a bivalent norovirus vaccine formulated in an in situ gelling dry powder. PLoS One. 2017;12(5):e0177310.

76. Sherwood J, Mendelman PM, Lloyd E, Liu M, Boslego J, Borkowski A, et al. Efficacy of an intramuscular bivalent norovirus GI.1/GII.4 virus-like particle vaccine candidate in healthy US adults. Vaccine. 2020;38(41):6442-9.

77. Ramani S, Neill FH, Ferreira J, Treanor JJ, Frey SE, Topham DJ, et al. B-Cell Responses to Intramuscular Administration of a Bivalent Virus-Like Particle Human Norovirus Vaccine. Clin Vaccine Immunol. 2017;24(5).

78. Cimica V, Galarza JM. Adjuvant formulations for virus-like particle (VLP) based vaccines. Clin Immunol. 2017;183:99-108.

79. Davitt CJH, Longet S, Albutti A, Aversa V, Nordqvist S, Hackett B, et al. Alpha-galactosylceramide enhances mucosal immunity to oral whole-cell cholera vaccines. Mucosal Immunol. 2019;12(4):1055-64.

80. Lavelle EC, Ward RW. Mucosal vaccines - fortifying the frontiers. Nat Rev Immunol. 2021.

81. Hallander HO, Paniagua M, Espinoza F, Askelof P, Corrales E, Ringman M, et al. Calibrated serological techniques demonstrate significant different serum response rates to an oral killed cholera vaccine between Swedish and Nicaraguan children. Vaccine. 2002;21(1-2):138-45.

82. Bruni L, Diaz M, Barrionuevo-Rosas L, Herrero R, Bray F, Bosch FX, et al. Global estimates of human papillomavirus vaccination coverage by region and income level: a pooled analysis. The Lancet Global Health. 2016;4(7):e453-e63.

83. Kambhampati A, Payne DC, Costantini V, Lopman BA. Host Genetic Susceptibility to Enteric Viruses: A Systematic Review and Metaanalysis. Clin Infect Dis. 2016;62(1):11-8.

84. Loureiro Tonini MA, Pires Goncalves Barreira DM, Bueno de Freitas Santolin L, Bondi Volpini LP, Gagliardi Leite JP, Le Moullac-Vaidye B, et al. FUT2, Secretor Status and FUT3 Polymorphisms of Children with Acute Diarrhea Infected with Rotavirus and Norovirus in Brazil. Viruses. 2020;12(10).

85. Pollock L, Bennett A, Jere KC, Dube Q, Mandolo J, Bar-Zeev N, et al. Nonsecretor Histo-blood Group Antigen Phenotype Is Associated With Reduced Risk of Clinical Rotavirus Vaccine Failure in Malawian Infants. Clin Infect Dis. 2019;69(8):1313-9.

86. Lynn DJ, Benson SC, Lynn MA, Pulendran B. Modulation of immune responses to vaccination by the microbiota: implications and potential mechanisms. Nat Rev Immunol. 2021.

87. Harris V, Ali A, Fuentes S, Korpela K, Kazi M, Tate J, et al. Rotavirus vaccine response correlates with the infant gut microbiota composition in Pakistan. Gut Microbes. 2018;9(2):93-101.

88. Harris VC, Armah G, Fuentes S, Korpela KE, Parashar U, Victor JC, et al. Significant Correlation Between the Infant Gut Microbiome and Rotavirus Vaccine Response in Rural Ghana. J Infect Dis. 2017;215(1):34-41.

89. Ryder RW, Singh N, Reeves WC, Kapikian AZ, Greenberg HB, Sack RB. Evidence of immunity induced by naturally acquired rotavirus and Norwalk virus infection on two remote Panamanian islands. J Infect Dis. 1985;151(1):99-105.

90. Johnson PC, Mathewson JJ, DuPont HL, Greenberg HB. Multiple-challenge study of host susceptibility to Norwalk gastroenteritis in US adults. J Infect Dis. 1990;161(1):18-21.

91. Moon SS, Wang Y, Shane AL, Nguyen T, Ray P, Dennehy P, et al. Inhibitory effect of breast milk on infectivity of live oral rotavirus vaccines. Pediatr Infect Dis J. 2010;29(10):919-23.

92. Lee B. Update on rotavirus vaccine underperformance in low- to middle-income countries and next-generation vaccines. Hum Vaccin Immunother. 2021;17(6):1787-802.

93. Moon SS, Groome MJ, Velasquez DE, Parashar UD, Jones S, Koen A, et al. Prevaccination Rotavirus Serum IgG and IgA Are Associated With Lower Immunogenicity of Live, Oral Human Rotavirus Vaccine in South African Infants. Clin Infect Dis. 2016;62(2):157-65.

94. Siegrist C. Mechanisms by which maternal antibodies influence infant vaccine responses: review of hypotheses and definition of main determinants. Vaccine. 2003;21(24):3406-12.

95. Donaldson B, Lateef Z, Walker GF, Young SL, Ward VK. Virus-like particle vaccines: immunology and formulation for clinical translation. Expert Rev Vaccines. 2018;17(9):833-49.

96. Malm M, Vesikari T, Blazevic V. Simultaneous Immunization with Multivalent Norovirus VLPs Induces Better Protective Immune Responses to Norovirus Than Sequential Immunization. Viruses. 2019;11(11).

97. McLean B, Sonza S, Holmes IH. Measurement of immunoglobulin A, G, and M class rotavirus antibodies in serum and mucosal secretions. J Clin Microbiol. 1980;12(3):314-9.

98. Allen DJ, Noad R, Samuel D, Gray JJ, Roy P, Iturriza-Gomara M. Characterisation of a GII-4 norovirus variant-specific surface-exposed site involved in antibody binding. Virol J. 2009;6:150.

99. Zhang Q, Bernatoniene J, Bagrade L, Pollard AJ, Mitchell TJ, Paton JC, et al. Serum and mucosal antibody responses to pneumococcal protein antigens in children: relationships with carriage status. Eur J Immunol. 2006;36(1):46-57.

100. Jiang X, Wang M, Graham DY, Estes MK. Expression, self-assembly, and antigenicity of the Norwalk virus capsid protein. J Virol. 1992;66(11):6527-32.

101. Tian P, Brandl M, Mandrell R. Porcine gastric mucin binds to recombinant norovirus particles and competitively inhibits their binding to histo-blood group antigens and Caco-2 cells. Lett Appl Microbiol. 2005;41(4):315-20.

102. Kou B, Crawford SE, Ajami NJ, Czako R, Neill FH, Tanaka TN, et al. Characterization of cross-reactive norovirus-specific monoclonal antibodies. Clin Vaccine Immunol. 2015;22(2):160-7.

103. Studentsov YY, Schiffman M, Strickler HD, Ho GY, Pang YY, Schiller J, et al. Enhanced enzyme-linked immunosorbent assay for detection of antibodies to virus-like particles of human papillomavirus. J Clin Microbiol. 2002;40(5):1755-60.

104. Blazevic V, Lappalainen S, Nurminen K, Huhti L, Vesikari T. Norovirus VLPs and rotavirus VP6 protein as combined vaccine for childhood gastroenteritis. Vaccine. 2011;29(45):8126-33.

105. Tamminen K, Huhti L, Vesikari T, Blazevic V. Pre-existing immunity to norovirus GII-4 virus-like particles does not impair de novo immune responses to norovirus GII-12 genotype. Viral Immunol. 2013;26(2):167-70.

106. Heinimaki S, Malm M, Vesikari T, Blazevic V. Parenterally Administered Norovirus GII.4 Virus-Like Particle Vaccine Formulated with Aluminum Hydroxide or Monophosphoryl Lipid A Adjuvants Induces Systemic but Not Mucosal Immune Responses in Mice. J Immunol Res. 2018;2018:3487095.

107. Bishop RF, Cipriani E, Lund JS, Barnes GL, Hosking CS. Estimation of rotavirus immunoglobulin G antibodies in human serum samples by enzyme-linked immunosorbent assay: expression of results as units derived from a standard curve. J Clin Microbiol. 1984;19(4):447-52.

108. Guarino A, Canani RB, Russo S, Albano F, Canani MB, Ruggeri FM, et al. Oral immunoglobulins for treatment of acute rotaviral gastroenteritis. Pediatrics. 1994;93(1):12-6.

109. Losonsky GA, Johnson JP, Winkelstein JA, Yolken RH. Oral administration of human serum immunoglobulin in immunodeficient patients with viral gastroenteritis. A pharmacokinetic and functional analysis. J Clin Invest. 1985;76(6):2362-7.

110. van Loben Sels JM, Green KY. The Antigenic Topology of Norovirus as Defined by B and T Cell Epitope Mapping: Implications for Universal Vaccines and Therapeutics. Viruses. 2019;11(5).

111. Tsang JS, Dobano C, VanDamme P, Moncunill G, Marchant A, Othman RB, et al. Improving Vaccine-Induced Immunity: Can Baseline Predict Outcome? Trends Immunol. 2020;41(6):457-65.

112. Mok DZL, Chan KR. The Effects of Pre-Existing Antibodies on Live-Attenuated Viral Vaccines. Viruses. 2020;12(5).

113. Jegerlehner A, Wiesel M, Dietmeier K, Zabel F, Gatto D, Saudan P, et al. Carrier induced epitopic suppression of antibody responses induced by virus-like particles is a dynamic phenomenon caused by carrier-specific antibodies. Vaccine. 2010;28(33):5503-12.

114. Grimwood K, Lund JC, Coulson BS, Hudson IL, Bishop RF, Barnes GL. Comparison of serum and mucosal antibody responses following severe acute rotavirus gastroenteritis in young children. J Clin Microbiol. 1988;26(4):732-8.

115. Awachat PS, Kelkar SD. Unexpected detection of simian SA11-human reassortant strains of rotavirus G3P[8] genotype from diarrhea epidemic among tribal children of Western India. J Med Virol. 2005;77(1):128-35.

116. Velazquez FR, Matson DO, Guerrero ML, Shults J, Calva JJ, Morrow AL, et al. Serum antibody as a marker of protection against natural rotavirus infection and disease. J Infect Dis. 2000;182(6):1602-9.

117. Ward RL, Clemens JD, Knowlton DR, Rao MR, van Loon FP, Huda N, et al. Evidence that protection against rotavirus diarrhea after natural infection is not dependent on serotype-specific neutralizing antibody. J Infect Dis. 1992;166(6):1251-7.

118. Yuan L, Ishida S, Honma S, Patton JT, Hodgins DC, Kapikian AZ, et al. Homotypic and heterotypic serum isotype-specific antibody responses to rotavirus nonstructural protein 4 and viral protein (VP) 4, VP6, and VP7 in infants who received selected live oral rotavirus vaccines. J Infect Dis. 2004;189(10):1833-45.

119. Velazquez FR, Matson DO, Calva JJ, Guerrero L, Morrow AL, Carter-Campbell S, et al. Rotavirus infection in infants as protection against subsequent infections. N Engl J Med. 1996;335(14):1022-8.

120. Yang B, Lessler J, Zhu H, Jiang CQ, Read JM, Hay JA, et al. Life course exposures continually shape antibody profiles and risk of seroconversion to influenza. PLoS Pathog. 2020;16(7):e1008635.

121. Siebenga JJ, Vennema H, Zheng DP, Vinje J, Lee BE, Pang XL, et al. Norovirus illness is a global problem: emergence and spread of norovirus GII.4 variants, 2001-2007. J Infect Dis. 2009;200(5):802-12.

122. Huhti L, Blazevic V, Puustinen L, Hemming M, Salminen M, Vesikari T. Genetic analyses of norovirus GII.4 variants in Finnish children from 1998 to 2013. Infect Genet Evol. 2014;26:65-71.

123. Debbink K, Lindesmith LC, Donaldson EF, Costantini V, Beltramello M, Corti D, et al. Emergence of new pandemic GII.4 Sydney norovirus strain correlates with escape from herd immunity. J Infect Dis. 2013;208(11):1877-87.

124. Malm M, Hyoty H, Knip M, Vesikari T, Blazevic V. Development of T cell immunity to norovirus and rotavirus in children under five years of age. Sci Rep. 2019;9(1):3199.

125. Seder RA, Darrah PA, Roederer M. T-cell quality in memory and protection: implications for vaccine design. Nat Rev Immunol. 2008;8(4):247-58.

126. McNeal MM, Rae MN, Ward RL. Evidence that resolution of rotavirus infection in mice is due to both CD4 and CD8 cell-dependent activities. J Virol. 1997;71(11):8735-42.

127. Tomov VT, Osborne LC, Dolfi DV, Sonnenberg GF, Monticelli LA, Mansfield K, et al. Persistent enteric murine norovirus infection is associated with functionally suboptimal virus-specific CD8 T cell responses. J Virol. 2013;87(12):7015-31.

128. Desselberger U, Huppertz HI. Immune responses to rotavirus infection and vaccination and associated correlates of protection. J Infect Dis. 2011;203(2):188-95.

129. Jiri Mestecky RSB, Hiroshi Kiyono, Jerry R. McGhee The Mucosal Immune System. Inductive and effector sites of the mucosal immune system. In: Wilkins PWKHLW, editor. Fundamental immunology. Fundamental immunology: Wolters Kluwer Health/Lippincott Williams & Wilkins; 2013.

130. Kawamata N, Xu B, Nishijima H, Aoyama K, Kusumoto M, Takeuchi T, et al. Expression of endothelia and lymphocyte adhesion molecules in bronchus-associated lymphoid tissue (BALT) in adult human lung. Respir Res. 2009;10:97.

131. Mavigner M, Cazabat M, Dubois M, L'Faqihi FE, Requena M, Pasquier C, et al. Altered CD4+ T cell homing to the gut impairs mucosal immune reconstitution in treated HIV-infected individuals. J Clin Invest. 2012;122(1):62-9.

132. Hiromichi Ishikawa YK, Hiromasa Hamada, Hiroshi Kiyono, . Chapter 21 - Development and Function of Organized Gut-Associated Lymphoid Tissues In: Jiri Mestecky MEL, Jerry R. McGhee, John Bienenstock, Lloyd Mayer, Warren Strober,, editor. Mucosal Immunology Third Edition: Academic Press,; 2005. p. 385-405.

133. Malm M, Tamminen K, Vesikari T, Blazevic V. Type-specific and cross-reactive antibodies and T cell responses in norovirus VLP immunized mice are targeted both to conserved and variable domains of capsid VP1 protein. Mol Immunol. 2016;78:27-37.

134. Dey A, Molodecky NA, Verma H, Sharma P, Yang JS, Saletti G, et al. Human Circulating Antibody-Producing B Cell as a Predictive Measure of Mucosal Immunity to Poliovirus. PLoS One. 2016;11(1):e0146010.

135. Kim L, Liebowitz D, Lin K, Kasparek K, Pasetti MF, Garg SJ, et al. Safety and immunogenicity of an oral tablet norovirus vaccine, a phase I randomized, placebo-controlled trial. JCI Insight. 2018;3(13).

136. Parra M, Herrera D, Jacome MF, Mesa MC, Rodriguez LS, Guzman C, et al. Circulating rotavirus-specific T cells have a poor functional profile. Virology. 2014;468-470:340-50.

137. Franco MA, Greenberg HB. Immunity to rotavirus in T cell deficient mice. Virology. 1997;238(2):169-79.

138. Tacket CO, Sztein MB, Losonsky GA, Wasserman SS, Estes MK. Humoral, mucosal, and cellular immune responses to oral Norwalk virus-like particles in volunteers. Clin Immunol. 2003;108(3):241-7.

139. Laban NM, Goodier MR, Bosomprah S, Simuyandi M, Chisenga C, Chilyabanyama ON, et al. T-Cell Responses after Rotavirus Infection or Vaccination in Children: A Systematic Review. Viruses. 2022;14(3).

140. Groome MJ, Koen A, Fix A, Page N, Jose L, Madhi SA, et al. Safety and immunogenicity of a parenteral P2-VP8-P[8] subunit rotavirus vaccine in toddlers and infants in South Africa: a randomised, double-blind, placebo-controlled trial. Lancet Infect Dis. 2017;17(8):843-53.

141. Resch TK, Wang Y, Moon SS, Joyce J, Li S, Prausnitz M, et al. Inactivated rotavirus vaccine by parenteral administration induces mucosal immunity in mice. Sci Rep. 2018;8(1):561.

142. Rott LS, Rose JR, Bass D, Williams MB, Greenberg HB, Butcher EC. Expression of mucosal homing receptor alpha4beta7 by circulating CD4+ cells with memory for intestinal rotavirus. J Clin Invest. 1997;100(5):1204-8.

143. Rose JR, Williams MB, Rott LS, Butcher EC, Greenberg HB. Expression of the mucosal homing receptor alpha4beta7 correlates with the ability of CD8+ memory T cells to clear rotavirus infection. J Virol. 1998;72(1):726-30.

144. El-Kamary SS, Pasetti MF, Mendelman PM, Frey SE, Bernstein DI, Treanor JJ, et al. Adjuvanted intranasal Norwalk virus-like particle vaccine elicits antibodies and antibody-secreting cells that express homing receptors for mucosal and peripheral lymphoid tissues. J Infect Dis. 2010;202(11):1649-58.

145. Sundararajan A, Sangster MY, Frey S, Atmar RL, Chen WH, Ferreira J, et al. Robust mucosal-homing antibody-secreting B cell responses induced by intramuscular administration of adjuvanted bivalent human norovirus-like particle vaccine. Vaccine. 2015;33(4):568-76.

146. Lettau M, Wiedemann A, Schrezenmeier EV, Giesecke-Thiel C, Dorner T. Human CD27+ memory B cells colonize a superficial follicular zone in the palatine tonsils with similarities to the spleen. A multicolor immunofluorescence study of lymphoid tissue. PLoS One. 2020;15(3):e0229778.

147. Zhang Q, Choo S, Everard J, Jennings R, Finn A. Mucosal immune responses to meningococcal group C conjugate and group A and C polysaccharide vaccines in adolescents. Infect Immun. 2000;68(5):2692-7.

148. Parker EPK, Bronowski C, Sindhu KNC, Babji S, Benny B, Carmona-Vicente N, et al. Impact of maternal antibodies and microbiota development on the immunogenicity of oral rotavirus vaccine in African, Indian, and European infants. Nat Commun. 2021;12(1):7288.

149. Ko SY, Ko HJ, Chang WS, Park SH, Kweon MN, Kang CY. alpha-Galactosylceramide can act as a nasal vaccine adjuvant inducing protective immune responses against viral infection and tumor. J Immunol. 2005;175(5):3309-17.

150. Tonti E, Galli G, Malzone C, Abrignani S, Casorati G, Dellabona P. NKT-cell help to B lymphocytes can occur independently of cognate interaction. Blood. 2009;113(2):370-6.

151. Doherty DG, Melo AM, Moreno-Olivera A, Solomos AC. Activation and Regulation of B Cell Responses by Invariant Natural Killer T Cells. Front Immunol. 2018;9:1360.

152. Fujii S, Shimizu K, Smith C, Bonifaz L, Steinman RM. Activation of natural killer T cells by alpha-galactosylceramide rapidly induces the full maturation of dendritic cells in vivo and thereby acts as an adjuvant for combined CD4 and CD8 T cell immunity to a coadministered protein. J Exp Med. 2003;198(2):267-79.

153. Johnston A, Sigurdardottir SL, Ryon JJ. Isolation of mononuclear cells from tonsillar tissue. Curr Protoc Immunol. 2009;Chapter 7:Unit 7 8.

154. Strowig T, Brilot F, Arrey F, Bougras G, Thomas D, Muller WA, et al. Tonsilar NK cells restrict B cell transformation by the Epstein-Barr virus via IFN-gamma. PLoS Pathog. 2008;4(2):e27.

155. Chiba S, Yokoyama T, Nakata S, Morita Y, Urasawa T, Taniguchi K, et al. Protective effect of naturally acquired homotypic and heterotypic rotavirus antibodies. Lancet. 1986;2(8504):417-21.

156. Kawamura N, Tokoeda Y, Oshima M, Okahata H, Tsutsumi H, Van Doorn LJ, et al. Efficacy, safety and immunogenicity of RIX4414 in Japanese infants during the first two years of life. Vaccine. 2011;29(37):6335-41.

157. Li RC, Huang T, Li Y, Wang LH, Tao J, Fu B, et al. Immunogenicity and reactogenicity of the human rotavirus vaccine, RIX4414 oral suspension, when co-administered with routine childhood vaccines in Chinese infants. Hum Vaccin Immunother. 2016;12(3):785-93.

158. Van Zaane D, Ijzerman J, De Leeuw PW. Intestinal antibody response after vaccination and infection with rotavirus of calves fed colostrum with or without rotavirus antibody. Vet Immunol Immunopathol. 1986;11(1):45-63.

159. Azevedo MS, Yuan L, Iosef C, Chang KO, Kim Y, Nguyen TV, et al. Magnitude of serum and intestinal antibody responses induced by sequential replicating and nonreplicating rotavirus vaccines in gnotobiotic pigs and correlation with protection. Clin Diagn Lab Immunol. 2004;11(1):12-20.

160. Westerman LE, McClure HM, Jiang B, Almond JW, Glass RI. Serum IgG mediates mucosal immunity against rotavirus infection. Proc Natl Acad Sci U S A. 2005;102(20):7268-73.

161. Matson DO, O'Ryan ML, Herrera I, Pickering LK, Estes MK. Fecal antibody responses to symptomatic and asymptomatic rotavirus infections. J Infect Dis. 1993;167(3):577-83.

162. Rojas OL, Caicedo L, Guzman C, Rodriguez LS, Castaneda J, Uribe L, et al. Evaluation of circulating intestinally committed memory B cells in children vaccinated with attenuated human rotavirus vaccine. Viral Immunol. 2007;20(2):300-11.

163. Korsrud FR, Brandtzaeg P. Immune systems of human nasopharyngeal and palatine tonsils: histomorphometry of lymphoid components and quantification of immunoglobulin-producing cells in health and disease. Clin Exp Immunol. 1980;39(2):361-70.

164. Brandtzaeg P, Surjan L, Jr., Berdal P. Immunoglobulin systems of human tonsils. I. Control subjects of various ages: quantification of Ig-producing cells, tonsillar morphometry and serum Ig concentrations. Clin Exp Immunol. 1978;31(3):367-81.

165. Zweigart MR, Becker-Dreps S, Bucardo F, Gonzalez F, Baric RS, Lindesmith LC. Serological Humoral Immunity Following Natural Infection of Children with High Burden Gastrointestinal Viruses. Viruses. 2021;13(10).

166. Ball JM, Graham DY, Opekun AR, Gilger MA, Guerrero RA, Estes MK. Recombinant Norwalk virus-like particles given orally to volunteers: phase I study. Gastroenterology. 1999;117(1):40-8.

167. Davitt CJ, Lavelle EC. Delivery strategies to enhance oral vaccination against enteric infections. Adv Drug Deliv Rev. 2015;91:52-69.

168. Davitt CJ, McNeela EA, Longet S, Tobias J, Aversa V, McEntee CP, et al. A novel adjuvanted capsule based strategy for oral vaccination against infectious diarrhoeal pathogens. J Control Release. 2016;233:162-73.

169. Malm M, Tamminen K, Vesikari T, Blazevic V. Norovirus-Specific Memory T Cell Responses in Adult Human Donors. Front Microbiol. 2016;7:1570.

170. Malm M, Uusi-Kerttula H, Vesikari T, Blazevic V. High serum levels of norovirus genotype-specific blocking antibodies correlate with protection from infection in children. J Infect Dis. 2014;210(11):1755-62.

171. Ruis C, Lindesmith LC, Mallory ML, Brewer-Jensen PD, Bryant JM, Costantini V, et al. Preadaptation of pandemic GII.4 noroviruses in unsampled virus reservoirs years before emergence. Virus Evol. 2020;6(2):veaa067.

172. Lindesmith LC, Brewer-Jensen PD, Mallory ML, Debbink K, Swann EW, Vinje J, et al. Antigenic Characterization of a Novel Recombinant GII.P16-GII.4 Sydney Norovirus Strain With Minor Sequence Variation Leading to Antibody Escape. J Infect Dis. 2018;217(7):1145-52.

173. Lindesmith LC, Ferris MT, Mullan CW, Ferreira J, Debbink K, Swanstrom J, et al. Broad blockade antibody responses in human volunteers after immunization with a multivalent norovirus VLP candidate vaccine: immunological analyses from a phase I clinical trial. PLoS Med. 2015;12(3):e1001807.

174. Lindesmith LC, McDaniel JR, Changela A, Verardi R, Kerr SA, Costantini V, et al. Sera Antibody Repertoire Analyses Reveal Mechanisms of Broad and Pandemic Strain Neutralizing Responses after Human Norovirus Vaccination. Immunity. 2019;50(6):1530-41 e8.

175. Bernstein DI, Atmar RL, Lyon GM, Treanor JJ, Chen WH, Jiang X, et al. Norovirus vaccine against experimental human GII.4 virus illness: a challenge study in healthy adults. J Infect Dis. 2015;211(6):870-8.

176. Lindesmith L, Moe C, Lependu J, Frelinger JA, Treanor J, Baric RS. Cellular and humoral immunity following Snow Mountain virus challenge. J Virol. 2005;79(5):2900-9.

177. Lindesmith LC, Donaldson E, Leon J, Moe CL, Frelinger JA, Johnston RE, et al. Heterotypic humoral and cellular immune responses following Norwalk virus infection. J Virol. 2010;84(4):1800-15.

178. Lin SC, Qu L, Ettayebi K, Crawford SE, Blutt SE, Robertson MJ, et al. Human norovirus exhibits strain-specific sensitivity to host interferon pathways in human intestinal enteroids. Proc Natl Acad Sci U S A. 2020;117(38):23782-93.

179. Pattekar A, Mayer LS, Lau CW, Liu C, Palko O, Bewtra M, et al. Norovirus-Specific CD8(+) T Cell Responses in Human Blood and Tissues. Cell Mol Gastroenterol Hepatol. 2021;11(5):1267-89.

180. LoBue AD, Lindesmith LC, Baric RS. Identification of cross-reactive norovirus CD4+ T cell epitopes. J Virol. 2010;84(17):8530-8.

181. Kapikian AZ, Flores J, Hoshino Y, Midthun K, Gorziglia M, Green KY, et al. Prospects for development of a rotavirus vaccine against rotavirus diarrhea in infants and young children. Rev Infect Dis. 1989;11 Suppl 3:S539-46.

182. Svensson L, Sheshberadaran H, Vene S, Norrby E, Grandien M, Wadell G. Serum antibody responses to individual viral polypeptides in human rotavirus infections. J Gen Virol. 1987;68 (Pt 3):643-51.

183. Xu J, Dennehy P, Keyserling H, Westerman LE, Wang Y, Holman RC, et al. Serum antibody responses in children with rotavirus diarrhea can serve as proxy for protection. Clin Diagn Lab Immunol. 2005;12(2):273-9.

184. Gonzalez AM, Jaimes MC, Cajiao I, Rojas OL, Cohen J, Pothier P, et al. Rotavirus-specific B cells induced by recent infection in adults and children predominantly express the intestinal homing receptor alpha4beta7. Virology. 2003;305(1):93-105.

185. Berlin C, Berg EL, Briskin MJ, Andrew DP, Kilshaw PJ, Holzmann B, et al. Alpha 4 beta 7 integrin mediates lymphocyte binding to the mucosal vascular addressin MAdCAM-1. Cell. 1993;74(1):185-95.

186. Quiding-Jarbrink M, Granstrom G, Nordstrom I, Holmgren J, Czerkinsky C. Induction of compartmentalized B-cell responses in human tonsils. Infect Immun. 1995;63(3):853-7.

187. Laichalk LL, Hochberg D, Babcock GJ, Freeman RB, Thorley-Lawson DA. The dispersal of mucosal memory B cells: evidence from persistent EBV infection. Immunity. 2002;16(5):745-54.

APPENDIX

Appendix A. Gel analysis for purified Norovirus VLPs

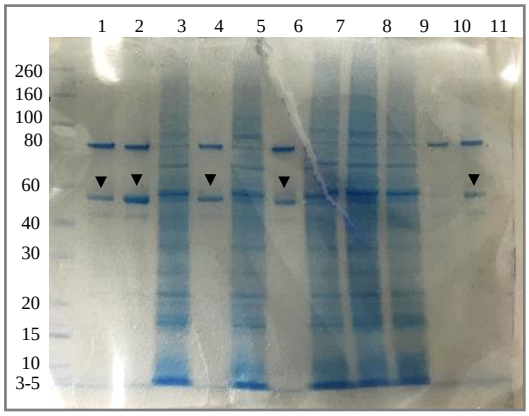

Figure A1. Analysis of NoV VP1 Protein by SDS PAGE. NuPAGE 12% Bis-Tris protein gels (Invitrogen) were stained using SimplyBlue Safe Stain and run for 50 minutes at 200V for the visualization of purified fractions. A ~58kDa band (Black arrows) was observed in lanes 1, 2, 4, 6 and 11, which is equivalent to VP1 molecular weight from norovirus GII.4 strain. All VP1-containing fractions were pooled and quantified using a Qubit Protein Assay Kit (Thermo Fisher Scientific) according to manufacturer's instruction. Two different VLP batches were produced and a total amount of ~ 3,2 mg of human NoV VLPs were successfully recovered.

Appendix B. Analysis of CD45RO-depleted cells by Flow cytometry

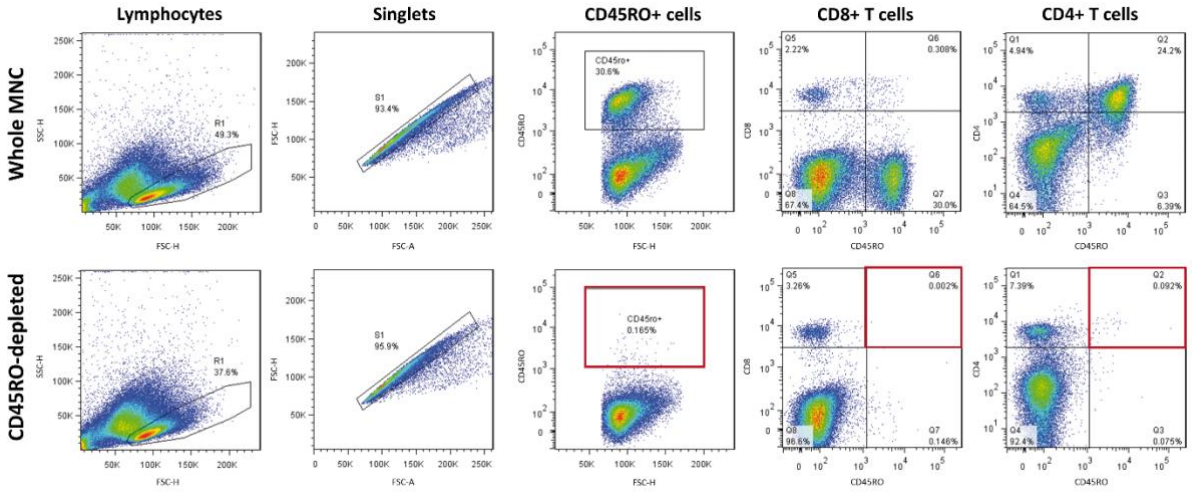

Figure B1. FACS analysis of CD45RO-depletion in Human NALTs. CD45RO-depleted and whole tonsillar MNCs were harvested 24 hours after processing and stained with Pacific Blue anti-human CD45RO, PerCP anti-human CD8 and APC-Cy7 anti-human CD4 antibodies and analysed by flow cytometry. Lymphocytes from CD45RO-depleted (lower dot plots) and whole tonsillar MNCs (upper dot plots) were gated based on cell size (FSC-H) and granularity (SSC-H), respectively. Doublets were excluded from the analysis by singlets selection. Percentage of $CD45RO^{+}$ cells were shown from tonsillar MNCs, CD8+ and CD4+ T cells, respectively. Red squares indicate a purity over 99% of CD45RO-depleted cells by MACS.

Appendix C. Dose-Response to Enteric Vaccines in Human NALTs

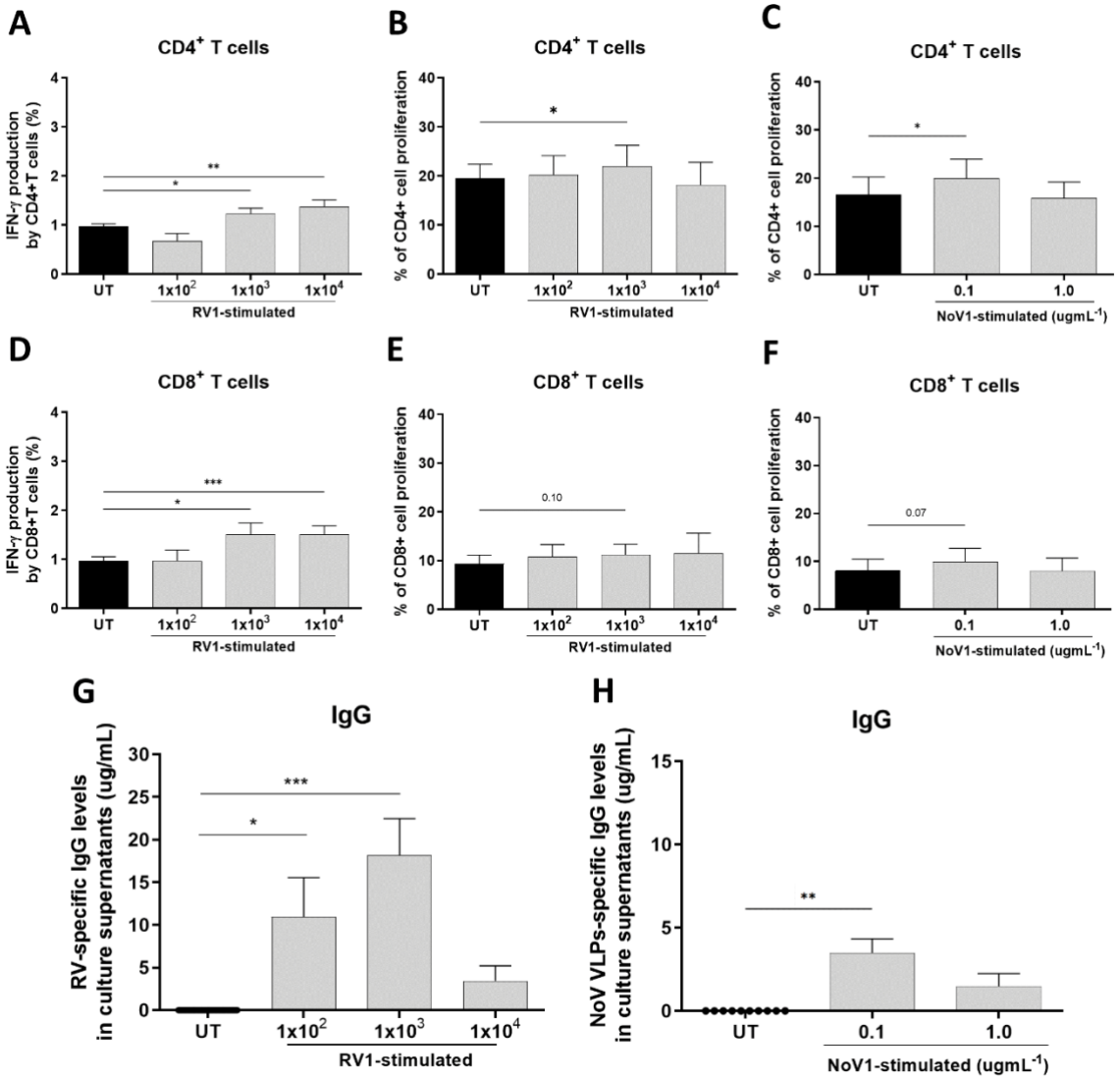

Figure C1. Evaluation of Enteric Vaccine doses in human NALTs. Human tonsillar MNCs were stimulated with 1x 10^2, 10^3 and 10^4 CCID50 mL^{-1} of Rotarix vaccine (RV1), 0.1 and 1.0 μg/mL of norovirus VLP-based vaccine candidate (NoV1) or left with media alone as an unstimulated control (UT). IFN-γ levels for $CD4^+$ (A) and $CD8^+$ (D) T cells were analysed at day 3 following RV1-stimulation by flow cytometry. Additionally, percentage of T cell proliferation were analysed after 5 days from RV1 (B, E) or NoV1 (C, F) vaccine stimulation, respectively. Cell culture supernatants were analysed at day 14 following vaccine stimulation by ELISA for either rotavirus (G) or norovirus specific IgG antibodies (H) detection. Data were presented as means plus SEM. Statistical analysis was performed by GraphPad paired t-test * P <0.05, *** P<0.001. A decreased IgG production was observed after 14 days at the highest RV1 and NoV1 doses, which correlated with a decrease in cell viability observed after longer stimulation period (i.e., day 5, day 7 and day 14) (data not shown). Finally, an RV1 dose of $1x10^3$ CCID50 mL^{-1} and 0.1 μg/mL of NoV1 was selected for further experiments considering cell viability and consistent response among subjects.

Appendix D. Gating strategy for T cell analysis in Human tonsillar MNCs

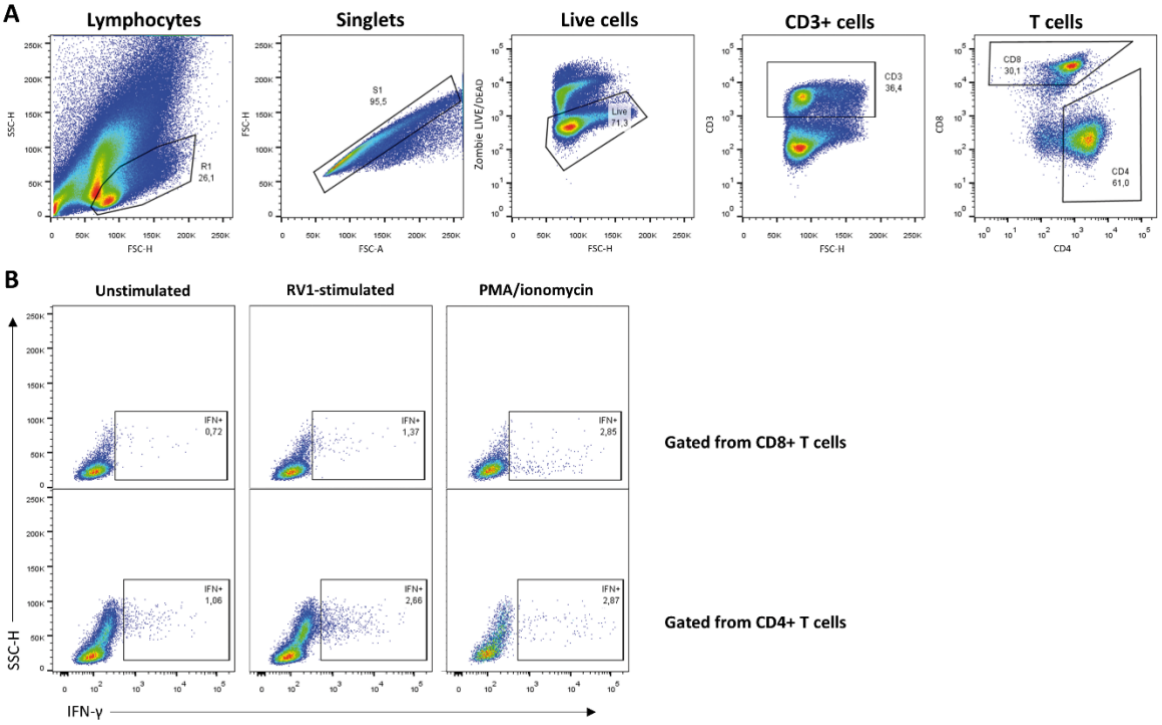

Figure D1. FACS analysis of IFN-γ production in human tonsillar T cells. Tonsillar mononuclear cells were harvested after 3 days of stimulation and stained for Flow cytometry analysis. Representatives dot plots shows the gating strategies used for T cells selection (A) and IFN-γ production (B) analyses from human tonsillar MNCs. As shown in the upper panel (A), lymphocytes (R1) were selected using forward (FSC-H) and side scatter (SSC-H). Doublets and dead cells were excluded from the analysis by singlets selection (S1) and zombie live/Dead staining (live), respectively. T cells were gated on CD3+ population and both CD4+ and CD8+ T cells were selected. Lower panels (B) show representative dot plots for IFN-γ production in CD8+ and CD4+ tonsillar T cells following stimulation with either 10^3 CCID50 mL^{-1} of Rotarix vaccine (RV1) or PMA/ionomycin cocktail. (Biolegend) as a cell activation control. Human tonsillar MNCs were left with media alone as an unstimulated control. FACS Data was analysed by using FlowJo X v10.0.7 software.

Appendix D. Gating strategy for T cell analysis in Human tonsillar MNCs

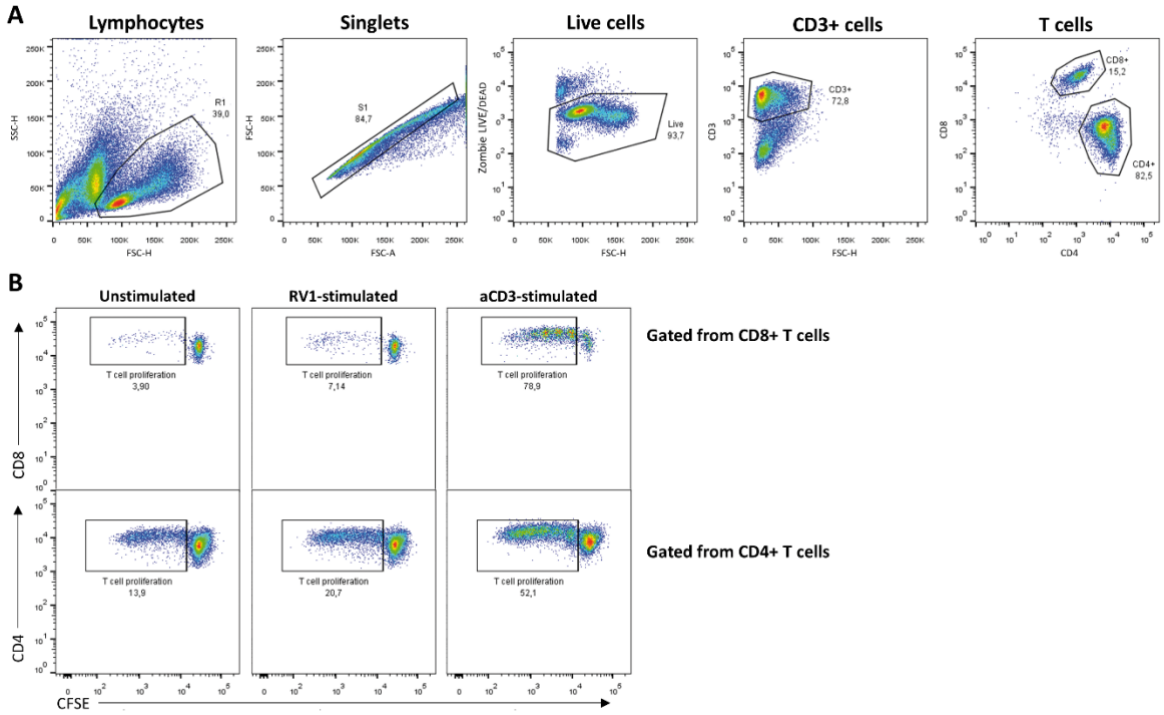

Figure D2. Gating strategy used for CFSE-labelled T cell proliferation analysis. Human tonsillar MNCs were labelled with CFSE and analysed after 5 days of stimulation by Flow cytometry. Representatives dot plots shows the gating strategies used for T cells selection (A) and cell proliferation (B) analyses from human tonsillar MNCs. As shown in the upper panel (A), lymphocytes were first selected based on their forward (FSC-H) and side scatter (SSC-H) properties (R1). Doublets and dead cells were excluded by singlets selection (S1) and zombie live/Dead staining (live), respectively. Both CD4+ and CD8 T cells were selected from previously gated CD3+ cell population. Lower panels (B) show representative dot plots for CFSE dilution, i.e., cell proliferation, from stimulated CD8+ and CD4+ tonsillar T cells. Cells were previously stimulated with Rotarix vaccine (RV1, 10^3 CCID50 mL^{-1}) or anti-human CD3 antibody (Clone: HIT3a, Biolegend) as a T cell proliferation control or left with media alone as an unstimulated control. FACS Data was analysed by using FlowJo X v10.0.7 software.

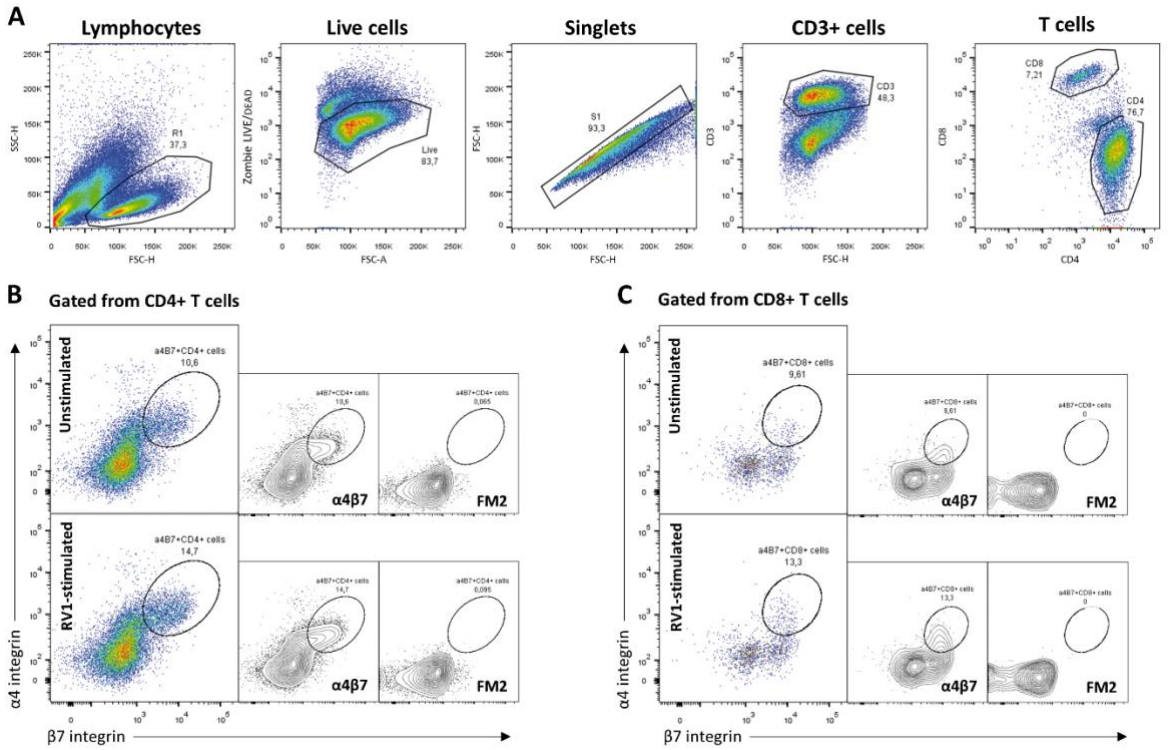

Appendix D. Gating strategy for T cell analysis in Human tonsillar MNCs

Figure D3. Flow cytometry analysis of gut homing receptors in human tonsillar T cells. Human tonsillar MNCs were stimulated with rotavirus vaccine (RV1, 1 x 10^3 CCID50 mL^{-1}) and evaluated 5 days later for gut-homing receptor expression by FACS. Representatives dot plots shows the gating strategies used for T cells selection (A) and gut-homing receptor expression (B) from human tonsillar MNCs. Upper panel (A) shows lymphocytes selection based on their forward (FSC-H) and side scatter (SSC-H) properties (R1). Doublets and dead cells were excluded from the analyses by singlets selection (S1) and zombie live/Dead staining (live), respectively. CD4+ and CD8+ tonsillar T cells were selected from CD3+ gated live cell population. Lower panels show representative dots and contour plots for α4β7 receptor expression in CD4+ (B) and CD8+ (C) tonsillar T cells. A mix of FITC anti-human CD49d, i.e., Integrin α4, and APC anti-human/mouse Integrin β7 antibodies were used for gut-homing receptor analyses by FACS. T cell antibody cocktail minus these two integrins (FM2) were used as a negative staining control. Double positive (α4+β7+) T cells populations were selected as gut-homing receptor expressing cells. Data was analysed by using FlowJo X v10.0.7 software.

Appendix E. Correlation of Serum Pre-existing immunity to GII.4 Norovirus and NoV1-induced IFN-γ production by human tonsillar T cells.

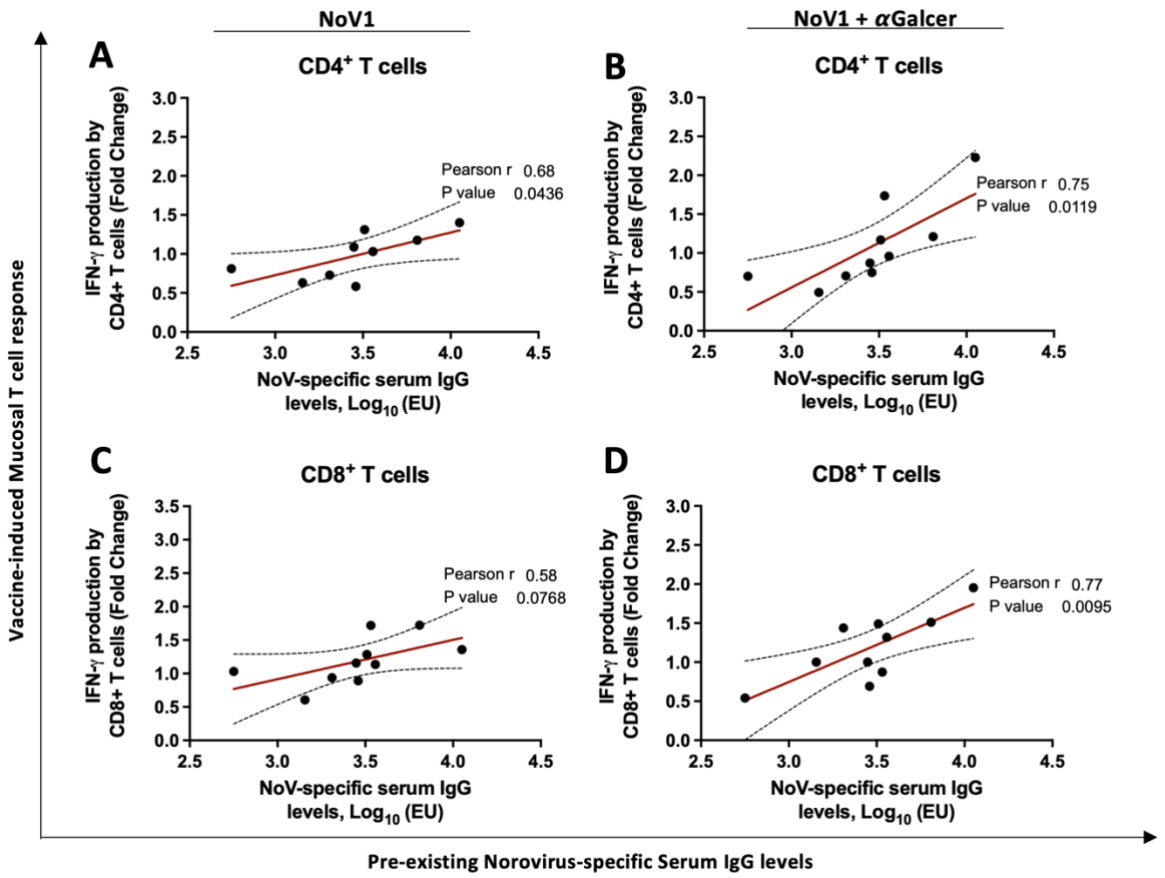

Figure E1. Correlation between Pre-existing immunity to NoV and T cell-mediated IFN-γ response induced by NoV1 vaccine alone or adjuvanted with α-Galcer. CD4+ (A, B) and CD8+ (C, D) mucosal T cell-mediated IFN-γ responses were recorded after stimulation of human tonsillar MNC with a VLP-based norovirus vaccine candidate (NoV1) alone (A, C) or adjuvanted with α-Galcer (B, D). Fold increase data from IFN-γ production by T cells were paired and correlated with patients' pre-existing immunity, i.e., NoV-specific serum IgG titres (Log10-transformed ELISA units; EU). Statistical analyses, including Pearson correlation (r) and linear regression (red line) were performed by GraphPad prism 9 software.